

การสังเคราะห์โคปพอลิโทโอฟินฟิล์ม โดยไมโครเวฟพลาสมาพอลิเมอไรเซชัน



นางสาวเพ็ญสุภา คัมภีรานนท์

ศูนย์วิทยทรัพยากร

วิทยานิพนธ์นี้เป็นส่วนหนึ่งของการศึกษาตามหลักสูตรปริญญาวิทยาศาสตรมหาบัณฑิต

สาขาวิชาปิโตรเคมีและวิทยาศาสตร์พอลิเมอร์

คณะวิทยาศาสตร์ จุฬาลงกรณ์มหาวิทยาลัย

ปีการศึกษา 2551

ลิขสิทธิ์ของจุฬาลงกรณ์มหาวิทยาลัย

SYNTHESIS OF DOPED POLYTHIOPHENE FILM BY
MICROWAVE PLASMA POLYMERIZATION



Miss Phensupa Kamphiranon

ศูนย์วิทยทรัพยากร

A Thesis Submitted in Partial Fulfillment of the Requirements
for the Degree of Master of Science Program in Petrochemistry and Polymer Science

Faculty of Science

Chulalongkorn University

Academic Year 2008

Copyright of Chulalongkorn University

511166

เพ็ญสุภา คัมภีรานนท์ : การสังเคราะห์โพลีไทโอฟินฟิล์มโดยไมโครเวฟพลาสมาพอลิเมอร์ไรเซชัน (SYNTHESIS OF DOPED POLYTHIOPHENE FILM BY MICROWAVE PLASMA POLYMERIZATION) อ.ที่ปรึกษาวิทยานิพนธ์หลัก: ผศ.ดร. วรพรรณ พันธุมนาวิน, อ.ที่ปรึกษาวิทยานิพนธ์ร่วม: ผศ.ดร. บุญโชติ เผ่าสวัสดิ์ขรรค์, 81 หน้า.

งานวิจัยนี้ได้ออกแบบและสร้างระบบไมโครเวฟพลาสมาขึ้น เพื่อใช้ในการสังเคราะห์โพลีไทโอฟินฟิล์ม ในการสังเคราะห์โพลีไทโอฟินใช้กำลังไมโครเวฟในช่วง 150-300 วัตต์ และใช้เวลาในการสังเคราะห์ 1 และ 2 นาที จากนั้นนำมาวิเคราะห์ด้วยเทคนิคสเปกโทรโฟโตเมทรี การวิเคราะห์หมู่ฟังก์ชันของโครงสร้างฟิล์มโพลีไทโอฟินด้วยเทคนิคอินฟราเรดสเปกโทรสโคปี พบว่าโพลีไทโอฟินที่สังเคราะห์ด้วยวิธีนี้ มีหมู่ฟังก์ชันสอดคล้องกับสารที่ได้จากการสังเคราะห์ทางเคมี ผลของยูวีวิสซิเบิลสเปกโทรสโคปี แสดงให้เห็นว่าฟิล์มที่ได้มีระบบคอนจูเกตที่ยาวขึ้นเมื่อใช้กำลังไมโครเวฟในการสังเคราะห์สูงขึ้น แต่เมื่อกำลังสูงมากเกินไปจะเกิดการแตกของวงไทโอฟินบางส่วน จากการวิเคราะห์พื้นผิวด้วยเทคนิคสแกนนิ่งอิเล็กตรอนไมโครสโคปี พบว่าลักษณะพื้นผิวภายในเป็นแบบเม็ดกลม นอกจากนั้นยังได้ฟิล์มเนื้อแน่นไม่มีรูพรุนภายในอีกด้วย ในการวิเคราะห์องค์ประกอบของฟิล์มด้วยเทคนิคเอนเนอร์จิสเปกโทรสโกปีเอกซเรย์สเปกโทรโฟโตเมทรี พบว่าการใช้กำลังไมโครเวฟสูงขึ้นส่งผลต่อการแตกของวงไทโอฟิน ซึ่งตรวจวัดได้ว่าปริมาณของซัลเฟอร์ที่มีอยู่ภายในฟิล์มลดลง เนื่องจากเกิดการแตกพันธะระหว่างคาร์บอนกับซัลเฟอร์ของวงไทโอฟิน ค่าการนำไฟฟ้าของฟิล์มโพลีไทโอฟินที่ยังไม่โดป (5.4×10^{-7} ถึง 1.9×10^{-6} ซีเมนส์ต่อเซนติเมตร) ที่ได้มีค่าสูงกว่าการสังเคราะห์โพลีไทโอฟินด้วยวิธีเคมีไฟฟ้า ส่วนโพลีไทโอฟินด้วยวิธีอินสิทู่ (1.4×10^{-5} ถึง 1.0×10^{-4} ซีเมนส์ต่อเซนติเมตร) มีค่าการนำไฟฟ้าในคอนเริ่มต้นต่ำกว่าการโดปด้วยวิธีทั่วไป (1.5×10^{-4} ถึง 1.9×10^{-3} ซีเมนส์ต่อเซนติเมตร) อย่างไรก็ตามค่าการนำไฟฟ้าของวัสดุที่โดปด้วยวิธีทั่วไปนั้นจะลดลงอย่างรวดเร็วภายใน 48 ชั่วโมง จนมีค่าใกล้เคียงกับคอนที่ยังไม่โดป ส่วนการโดปแบบอินสิทู่ นั้นค่าการนำไฟฟ้าจะลดลงในช่วงแรก และเมื่อเวลาผ่านไปนานขึ้นค่าการนำไฟฟ้าค่อนข้างคงที่ (นานกว่า 96 ชั่วโมง)

สาขาวิชา: ปิโตรเคมีและวิทยาศาสตร์พอลิเมอร์ ลายมือชื่อนิสิต: ...เพ็ญสุภา... คัมภีรานนท์.....

ปีการศึกษา:2551.....

ลายมือชื่ออาจารย์ที่ปรึกษาวิทยานิพนธ์หลัก:

ลายมือชื่ออาจารย์ที่ปรึกษาวิทยานิพนธ์ร่วม:

4872398523 : MAJOR PETROCHEMISTRY AND POLYMER SCIENCE
 KEY WORD: CONDUCTIVE POLYMER/POLYTHIOPHENE/PLASMA
 POLYMERIZATION

PHENSUPA KAMPHIRANON: SYNTHESIS OF DOPED
 POLYTHIOPHENE FILM BY MICROWAVE PLASMA
 POLYMERIZATION. THESIS PRINCIPAL ADVISOR: ASST
 PROF. WORAWAN BHANTUMNAVIN, Ph.D., THESIS
 COADVISOR: ASST PROF. BOONCHOAT PAOSAWATYAN
 YONG, Ph.D., 81 pp.

A microwave plasma reactor for the synthesis of polythiophene thin films has been designed and assembled. Plasma polymerization parameters were studied. Microwave power in the range of 150-300W was employed for 1-2 minutes. Polythiophene films were characterized by various spectrophotometric methods. Infrared analyses showed absorption frequencies of important functional groups mostly similarly observed in the case of chemically-synthesized materials. Fabricated polythiophene films exhibited UV-Vis spectra indicative of increased conjugative systems as the microwave power increased although at high microwave power partial fragmentation was evident. Surface analysis by Scanning Electron Microscopy revealed a uniformly fabricated globular particle morphology. In addition, these polythiophene thin films were found to be dense and pinhole-free. Results from Energy-dispersive X-ray spectroscopy analysis were suggestive of partial fragmentation of the films at high microwave powers as some degree of sulfur content was decreased. This is in good agreement with a possibility of partial cleavage of a C-S bond in the thiophene rings. Electrical conductive measurements revealed that the undoped films exhibit higher conductivity (5.4×10^{-7} to 1.9×10^{-6} S/cm) than polythiophene typically prepared from electrochemical methods. As for the doped materials, initial conductivities (1.4×10^{-5} to 1.0×10^{-4} S/cm) were lower than plasma-polymerized films which were doped with conventional method (1.5×10^{-4} to 1.9×10^{-3} S/cm). However, it was found that conductivity of the latter decreased more rapidly and reached an undoped value in a short time (48 hours). In contrary, the decaying rate of conductivity of *in situ* doped material could be sustained for a longer period of time (more than 96 hours).

Field of study: Petrochemistry and polymer science Student's signature: Phensupa.....

Academic year: 2008 Thesis Principal Advisor's signature:

Thesis Co-advisor's signature:

ACKNOWLEDGEMENTS

I would like to express my sincere appreciation and gratitude to my advisor, Assistant Professor Dr. Worawan Bhanthumnavin, my co-advisor, Assistant Professor Dr. Boonchoat Paosawatyanong for supporting me both in science and life, and encouraging me throughout the course of my study. I am sincerely grateful to the members of the thesis committee, Professor Dr. Pattarapan Prasassarakich, Assistant Professor Dr. Warinthorn Chavasiri, and Assistant Professor Dr. Yongsak Sritananant for their comments, suggestion, and time to read the thesis.

Gratefully thanks to Associate Professor Dr. Sanong Ekgasit, and Miss Duangta Tongsakul for analyze of ATR FT-IR spectroscopy, Assistant Professor Dr. Oravan Sanguanruang for use solid-state UV-Vis spectrophotometer, and Assistant Professor Dr. Voravee P. Hoven for Soxhlet extractor.

Many thanks go to Dr. Dusit Ngamrunroj and Miss Kanchaya Honglertkongsakul and Plasma lab members for the invaluable guidance, comments, and suggestions during my thesis work.

Also many thanks to Mr. Anusorn Adirekkittikun of Naretlohasupply Ltd. and Mr. Hunsa Boonhao for suggestions concerning construction.

Finally, I am profoundly grateful to my family for their patient love, perpetual encouragement, and overwhelming support.

ศูนย์วิทยทรัพยากร
จุฬาลงกรณ์มหาวิทยาลัย

CONTENTS

| | Page |
|--|------|
| ABTRACT (THAI) | iv |
| ABTRACT (ENGLISH)..... | v |
| ACKNOWLEDGEMENTS..... | vi |
| CONTENTS..... | vii |
| LIST OF TABLES..... | x |
| LIST OF FIGURES | xii |
| LIST OF ABBREVIATIONS..... | xv |
| LIST OF SYMBOLS..... | xvi |
| | |
| CHAPTER I INTRODUCTION..... | 1 |
| 1.1 Evolution of conjugated polymer..... | 1 |
| 1.2 Classification of conjugated polymers..... | 1 |
| 1.3 Structure of Conducting Polymers | 3 |
| 1.4 Conductivity and doping..... | 5 |
| 1.4.1 Chemical Doping by Charge Transfer..... | 8 |
| 1.4.2 Electrochemical Doping | 8 |
| 1.5 Mechanism of Conduction by doping..... | 9 |
| 1.6 Applications of conducting polymers | 11 |
| 1.7 Polythiophene | 12 |
| 1.8 Synthesis of polythiophene..... | 13 |
| 1.8.1 Electrochemical polymerization | 14 |
| 1.8.2 Oxidative coupling polymerization with iron(III)chloride | 14 |
| 1.8.3 Grignard coupling and other chemical polymerization | 15 |
| 1.9 Plasma..... | 16 |
| 1.10 Plasma polymerization..... | 20 |
| 1.11 Statement of the problem | 25 |
| 1.12 The objective of the research | 26 |
| 1.13 Research Plan and the scope of the research | 26 |
| 1.14 Thesis organization | 27 |

| | |
|--|----|
| CHAPTER II MICROWAVE PLASMA REACTOR | 28 |
| 2.1 The design and construction of the microwave plasma reactor..... | 28 |
| 2.1.1 Vacuum chamber..... | 28 |
| 2.1.2 Rectangular waveguide and excitation mode | 29 |
| 2.1.3 Magnetron power supply | 31 |
| 2.1.4 A matching network (3-stub tuner) | 32 |
| 2.1.5 Monomer vessel..... | 32 |
| 2.1.6 Cold trap | 33 |
| 2.2 Testing of the microwave system | 34 |
| 2.2.1 Testing of the assembly under vacuum | 34 |
| 2.2.2 Testing of chemical recovery by cold trapping | 35 |
| 2.2.3 Determination of plasma temperature | 36 |
| CHAPTER III FABRICATION OF POLYTHIOPHENE FILMS | 39 |
| 3.1 Experimental section..... | 39 |
| 3.1.1 Chemicals | 39 |
| 3.1.2 Instruments | 39 |
| 3.1.3 Preparation of glass substrates..... | 40 |
| 3.1.4 Plasma polymerization of polythiophene | 40 |
| 3.1.5 Plasma polymerization of polythiophene and in situ doping with iodine | 41 |
| 3.1.6 Chemical synthesis of polythiophene | 42 |
| 3.1.7 Characterization of plasma polythiophene | 42 |
| 3.1.7.1 Attenuated Total Reflection Fourier Transform Infrared (ATR FT-IR) Spectroscopy | 42 |
| 3.1.7.2 Solid-state UV-Visible Spectroscopy..... | 42 |
| 3.1.7.3 Scanning Electron Microscopy (SEM)..... | 42 |
| 3.1.7.4 Energy-dispersive X-ray spectroscopy (EDS)..... | 43 |
| 3.1.7.5 Electrical conductivity measurements | 43 |

| | Page |
|--|------|
| 3.2 Results and discussions..... | 43 |
| 3.2.1 Microwave plasma polymerization of thiophene..... | 43 |
| 3.2.2 Characterization of plasma polymerized polythiophene | 44 |
| 3.2.2.1 Functional groups and chemical characteristics | 44 |
| 3.2.2.2 Film morphology | 46 |
| 3.2.2.3 Elemental composition of the films..... | 48 |
| 3.2.2.4 Electrical conductivity | 50 |
| 3.2.2.5 Optical characteristics of the films | 51 |
| 3.2.3 <i>In situ</i> doped polythiophene films | 53 |
| 3.2.4 Characterization of I ₂ -doped plasma-polymerized polythiophene | 54 |
| 3.2.4.1 Functional groups and chemical characteristics | 54 |
| 3.2.4.2 Film morphology | 55 |
| 3.2.4.3 Elemental composition of the films..... | 57 |
| 3.2.4.4 Optical characteristics of the films | 57 |
| 3.2.4.5 Electrical conductivity | 58 |
| CHAPTER IV CONCLUSIONS | 63 |
| 4.1 Conclusions..... | 63 |
| 4.2 Recommendations..... | 64 |
| REFERENCES | 66 |
| APPENDICES | 72 |
| APPENDIX A..... | 73 |
| APPENDIX B..... | 74 |
| APPENDIX C..... | 76 |
| VITAE | 81 |

LIST OF TABLES

| Table | | Page |
|-------|--|------|
| 1.1 | Comparison of some physical properties of semiconductor polymers, metals and insulators..... | 4 |
| 1.2 | Common conducting polymers, conductivities, type of doping, stability and processing attributes | 8 |
| 1.3 | Application of conducting polymers | 12 |
| 2.1 | Argon spectroscopic data | 38 |
| 3.1 | ATR FT-IR band assignments of chemically-synthesized polythiophene and plasma-polymerized polythiophene..... | 45 |
| 3.2 | Film thickness at various microwave power and polymerization time | 46 |
| 3.3 | The elemental composition of chemically-synthesized and plasma-polymerized polythiophene | 49 |
| 3.4 | Electrical conductivity of microwave plasma-polymerized polythiophene | 51 |
| 3.5 | Conclusion of UV-Vis maximum absorption (λ_{max}) of plasma-polymerized polythiophene | 51 |
| 3.6 | Elemental composition of plasma-polymerized I ₂ doped polythiophene..... | 57 |
| 3.7 | Summation of UV-Vis maximum absorption (λ_{max}) of <i>in situ</i> I ₂ doped polythiophene | 58 |
| 3.8 | Electrical conductivity of I ₂ doped plasma-polymerized polythiophene films .. | 59 |
| 3.9 | Electrical conductivity of I ₂ -doped polythiophene by conventional synthetic and different plasma polymerization methods | 60 |
| B.1 | The elemental composition of plasma-polymerized polythiophene..... | 74 |
| B.2 | The elemental composition of I ₂ doped plasma-polymerized polythiophene | 75 |
| C.1 | Electrical conductivity of I ₂ doped plasma polymerized polythiophene films... | 76 |
| C.2 | Electrical conductivity of I ₂ doped microwave plasma-polymerized polythiophene (<i>in situ</i> doping)..... | 77 |
| C.3 | Electrical conductivity of I ₂ doped microwave plasma-polymerized polythiophene (<i>in situ</i> doping) at 250 W, 1 min..... | 77 |
| C.4 | Electrical conductivity of I ₂ doped microwave plasma-polymerized polythiophene (<i>in situ</i> doping) at 300 W, 1 min..... | 78 |

| | | |
|-----|--|----|
| C.5 | Electrical conductivity of I ₂ doped microwave plasma-polymerized polythiophene (<i>in situ</i> doping) at 250 W, 2 min..... | 78 |
| C.6 | Electrical conductivity of I ₂ doped microwave plasma-polymerized polythiophene (<i>in situ</i> doping) at 300 W, 2 min..... | 79 |
| C.7 | Electrical conductivity of microwave plasma-polymerized polythiophene at 150 W, 2 min and I ₂ <i>ex situ</i> doping for 24 hours..... | 79 |
| C.8 | Electrical conductivity of microwave plasma-polymerized polythiophene at 200 W, 1 min and I ₂ <i>ex situ</i> doping for 24 hours..... | 80 |
| C.9 | Electrical conductivity of microwave plasma-polymerized polythiophene at 200 W, 2 min and I ₂ <i>ex situ</i> doping for 24 hours..... | 80 |



ศูนย์วิทยทรัพยากร
จุฬาลงกรณ์มหาวิทยาลัย

LIST OF FIGURES

| Figure | Page |
|--|------|
| 1.1 Structures of some conjugated polymers..... | 2 |
| 1.2 Classification of conducting polymers | 3 |
| 1.3 Schematic representation of the band structure of metal, semiconductor, and insulator. (E_g is the energy gap between the valence band (VB) and the conduction band (CB)). | 4 |
| 1.4 Typical contact geometries used for thin film conductivity measurement..... | 6 |
| 1.5 Schematic representation of polythiophene in the undoped, singly, and doubly oxidized (left), and singly and doubly reduced (right) states | 10 |
| 1.6 Polaron and bipolaron in polythiophene..... | 11 |
| 1.7 Evolution of the polythiophene band structure upon doping: (a) undoped (b) 0.1% doping level, with polaron formation; (c) ~1-20% doping level, with the bipolaron formation; (d) 30% doping level, where the bipolaron states overlap and form two bands; (e) Hypothetical 100% doping level, with quasi-metallic behavior | 11 |
| 1.8 Regioregular of poly(3-alkylthiophene)..... | 13 |
| 1.9 The electropolymerization method for the synthesis of poly(3-alkylthiophene) (R= H, Me, Ph) | 14 |
| 1.10 Oxidative coupling reaction of 3-alkylthiophene by $FeCl_3$ | 14 |
| 1.11 The regiospecific synthesis of poly(3-alkylthiophene)s with almost 100% HT coupling | 15 |
| 1.12 The four states of matter; plasma is sometimes referred to as the fourth state .. | 16 |
| 1.13 General mechanism of gas discharge polymerization..... | 19 |
| 1.14 Polymer prepared from chemical polymerization compared to that from plasma polymerization method..... | 21 |
| 2.1 The drawing of microwave plasma system by AutoCAD and SolidWorks program..... | 28 |
| 2.2 (a) The designed model of vacuum chamber and photographs of the actual vacuum chamber from the: (b) top, (c) front and (d) side views..... | 29 |
| 2.3 Electric and magnetic field lines for TE_{10} mode in rectangular waveguide | 30 |

| Figure | Page |
|--|------|
| 2.4 The photograph of microwave components | 30 |
| 2.5 Circuit diagram of the voltage supplied to the magnetron head..... | 31 |
| 2.6 The magnetron head utilized in this study..... | 31 |
| 2.7 (a) The prototype of 3-stub tuner and 3-stub tuner photographed from the (b) top, (c) front and (d) side views..... | 32 |
| 2.8 (a) The design of monomer vessel in millimeter unit and (b) the photograph of the monomer vessel | 33 |
| 2.9 Illustration of the cold trap written by AutoCAD program. (millimeter unit) (a) and the cold trap used in this study (b)..... | 33 |
| 2.10 The photograph of microwave plasma system | 34 |
| 2.11 The graph of the decrease pressure (a) and increase pressure (b) versus time...35 | 35 |
| 2.12 The dry ice and acetone in region III for the cold trap..... | 35 |
| 2.13 Position of OES probe during plasma temperature measurement..... | 36 |
| 2.14 OES spectra of argon plasma at 0.75 torr..... | 37 |
| 2.15 The peak intensity ratio versus electron temperature | 37 |
| 3.1 The substrate preparation for measurement of electrical conductivity | 40 |
| 3.2 Example polythiophene films by microwave plasma polymerization | 44 |
| 3.3 ATR FT-IR spectra of chemically-synthesized, plasma-polymerized polythiophene at different MW power and polymerization time (a) 1 min, (b) 2 min.... | 44 |
| 3.4 The surface morphology of plasma-polymerized polythiophene films on the glass substrate at 1 min and various microwave power (a) 150, (b) 200, (c) 250 and (d) 300 W | 47 |
| 3.5 The surface morphology of plasma-polymerized polythiophene films on the glass substrate at 2 min and various microwave power (a) 150, (b) 200, (c) 250 and (d) 300 W | 48 |
| 3.6 The microwave power versus C/S ratio..... | 50 |
| 3.7 The plot of current versus voltage at room temperature..... | 50 |
| 3.8 The UV-Vis absorbance spectra of plasma-polymerized polythiophene at different microwave power and polymerization time 1 min | 52 |
| 3.9 The UV-Vis absorbance spectra of plasma-polymerized polythiophene at different microwave power and polymerization time 2 min | 52 |

| | | |
|------|--|----|
| 3.10 | OES spectra of I ₂ doped plasma-polymerized polythiophene | 53 |
| 3.11 | ATR FT-IR spectra of plasma-polymerized I ₂ doped polythiophene | 55 |
| 3.12 | The SEM surface and cross-section of I ₂ -doped plasma-polymerized polythiophene (a) 250 W, 1 min, (b) 300 W, 1 min, (c) 250 W, 2 min, and (d) 300 W, 2 min | 56 |
| 3.13 | UV-Vis spectra of <i>in situ</i> I ₂ doped plasma-polymerized polythiophene | 58 |
| 3.14 | The conductivity of microwave plasma-polymerized polythiophene films and iodine <i>ex situ</i> doping as a function of exposure time | 61 |
| 3.15 | The conductivity of iodine doped microwave plasma-polymerized polythiophene (<i>in situ</i> doping) as a function of exposure time | 61 |
| A.1 | Dimension of standard NW 16 flange | 73 |
| A.2 | Dimension of standard WR 340 flange cover | 73 |
| B.1 | EDS spectra of plasma-polymerized polythiophene at 250 W and 1 min | 74 |
| B.2 | EDS spectra of I ₂ doped plasma-polymerized polythiophene at 250 W and 1 min | 75 |

ศูนย์วิทยทรัพยากร
จุฬาลงกรณ์มหาวิทยาลัย

LIST OF ABBREVIATIONS

| | |
|---------------|---|
| sccm | : Standard Cubic Centimeters per Minute |
| DC | : Direct Current |
| W | : watt |
| S | : siemen |
| μm | : micrometer |
| min | : minute |
| mmol | : millimole |
| ml | : milliliter |
| cm | : centimeter |
| nm | : nanometer |
| m | : meter |
| V | : voltage |
| A | : ammeter |
| I | : current |
| mm^3 | : cubic millimeter |
| MHz | : Mega Hertz |
| GHz | : Giga Hertz |
| ATR | : Attenuated Total Reflection |
| FT-IR | : Fourier Transform Infrared |
| UV | : Ultraviolet |
| SEM | : Scanning Electron Microscope |
| EDS | : Energy-dispersive X-ray spectroscopy |
| OES | : Optical Emission Spectroscopy |
| E_g | : band gap |
| VB | : valence band |
| CB | : conduction band |
| R | : resistance |
| HT | : head-to-tail |
| HH | : head-to-head |
| TT | : tail-to-tail |
| eV | : electron volt |

LIST OF SYMBOLS

| | |
|--------------------|--------------------------|
| σ | : conductivity |
| ρ | : resistivity |
| Ω | : ohms |
| λ | : wavelength |
| I | : intensity |
| A | : transition probability |
| g | : statistical weight |
| E | : Energy level |
| l | : length |
| n | : negative |
| p | : positive |
| $^{\circ}\text{C}$ | : degree celsius |

ศูนย์วิทยทรัพยากร
จุฬาลงกรณ์มหาวิทยาลัย

CHAPTER I

INTRODUCTION

1.1. Evolution of conjugated polymer

Polymers have long been considered as insulating materials. Until 1973, Walatka, Labels, and Perlstein discovered that inorganic poly(sulfur nitride), $(SN)_x$ could be highly conducting, but interest soon turned to organic polymers, in the hope of exploiting conventional plastics processing technology for the processing of the material [1]. In 1997, the simplest conjugated polymer, polyacetylene was synthesized by Macdiarmid, Heeger, Shirakawa, and coworkers [2]. Pristine polyacetylene is an insulator, however, when films of pristine polyacetylene were exposed to vapors of chlorine, bromine, or iodine at room temperature, a dramatic increase in conductivity to about 10^3 S/cm was noticed. Inducing high conductivity in polyacetylene by such oxidation and reduction came to be known as “doping”. This kind of doping changes the electronic profile of the polymers by taking electrons from the valence band (*p*-doping) or by adding electrons to the conduction band (*n*-doping).

Since then, more polymers with conjugated π -electrons were found to undergo transition from insulator to electric conductor after doping with weak oxidants or reducing agents, and the structural formulae of some commonly encountered conjugated polymers are shown in Figure 1.1. Combining moderate electric conductivity and the light weight as well as the flexibility of polymer, it leads to wide range of applications as novel materials in rechargeable batteries, electrochromic display devices, sensors, and the possible extension to even molecular computing and space-craft design in the future.

1.2. Classification of conjugated polymers

Because of the instability of polyacetylene in the environment, the potential of using other types of conjugated molecules were studied to be used as a substitute. A number of conjugated polymer chains consisting of only unsaturated carbon atoms in the backbone or carbon atoms with electron-rich heteroatoms or even totally non-

carbon atom backbones have since been synthesized. A simple classification of conducting polymers on the basis of chain composition is shown in **Figure 1.2**.

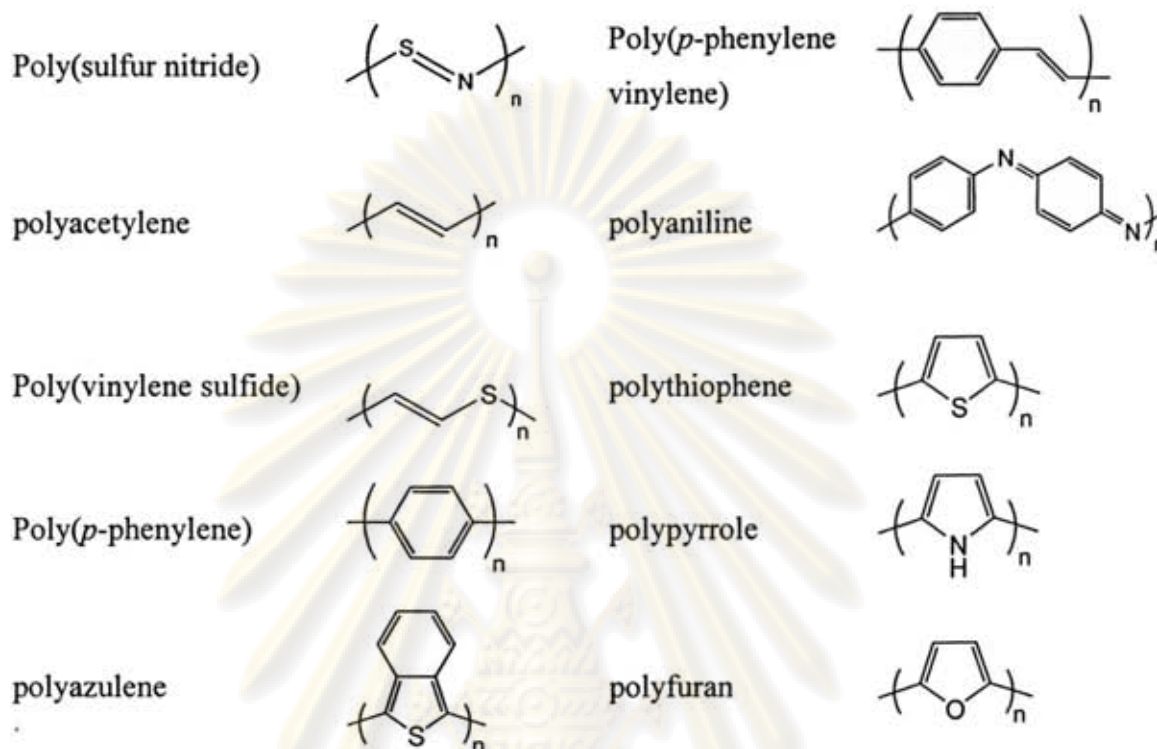


Figure 1.1 Structures of some conjugated polymers.

Polyvinylenes, polyarylenes, and polyheterocycles are the major classes of conducting polymers. Polyvinylenes are well known polymers, which have good thermal stabilities and high electrical conductivities [3]. Poly(*p*-phenylene), polyazulene, and poly(*p*-phenylene vinylene) belong to the family of polyarylenes or polyaromatics. Poly(*p*-phenylene) was the first non-acetylenic hydrocarbon polymer that showed high conductivity on doping which was demonstrated in 1980 [4]. This triggered further research for finding other conducting polymers. Many polyheterocyclics also could be added to the list of organic conducting polymers such as polypyrrole, polythiophene, and polyfuran, all having a five membered ring structure with one heteroatom like oxygen or nitrogen or sulfur [5].

Polyacetylene remains the most crystalline conductive polymer but is not the first conductive polymer to be commercialized. This is due to the fact that it is easily oxidized by oxygen in the air and is also sensitive to humidity. Other polymers studied extensively since the early 1980s include polypyrrole, polythiophene (and

various polythiophene derivatives), poly(*p*-phenylene vinylene), and polyaniline. Polypyrrole and polythiophene differ from polyacetylene most notably in that they may be synthesized directly in the doped form and are very stable in air. Their conductivities are low, however, only around 10^2 S/cm, but this is enough for many practical purposes [6].

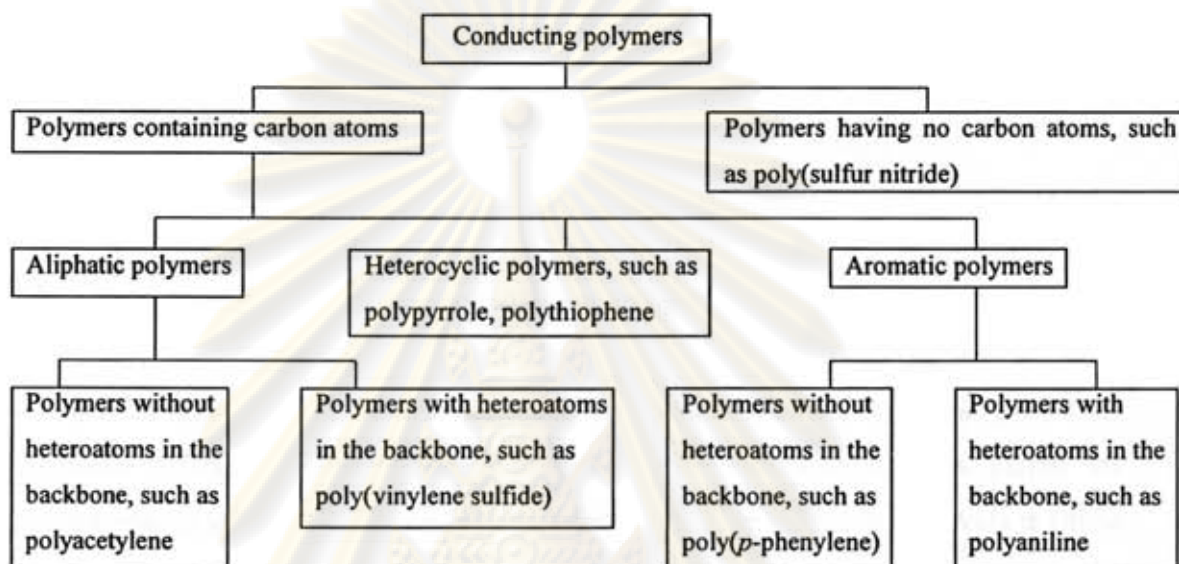


Figure 1.2 Classification of conducting polymers.

1.3. Structure of Conducting Polymers

All existing materials can be divided into three main groups: insulators, semi-conductors and metals. These are differentiated by their ability to conduct electron flow (current). Conducting polymers are generally classified as semi-conductors, although some highly conducting polymers, such as polyacetylene, fall into the metal range. **Table 1.1** compares some of the physical properties of insulators, semi-conductors and metals [7].

As illustrated earlier, polymers that display electron conduction all have a system of conjugated π -bonds, sometimes interspersed with atoms such as nitrogen, sulfur, and oxygen. It was originally believed that the mechanism of conduction in polymeric materials was electron transport through the system of conjugated multiple bonds. With the bonds in a single plane and the π -orbitals parallel, the orbitals of the π electrons overlap to form a single delocalized cloud of π electrons over the entire molecule.

Table 1.1 Comparison of some physical properties of semiconductor polymers, metals and insulators

| Property | Semiconductor Polymers | Metals | Insulators |
|--------------------------------|--|---------------------------------------|-----------------------|
| Electrical conductivity (S/cm) | $10^2 - 10^{11}$ | $10^6 - 10^4$ | $10^{-12} - 10^{-20}$ |
| Carriers | Electrons of conjugated double bonds | Valence electrons of half filled band | - |
| Effect of impurities | Impurities of 0.1-1% change conductivity by 2 to 3 orders of magnitude | Effect comparatively slight | Strong effect |

Analogous to semiconductors, the highest occupied band (originating from the highest occupied molecular orbital (HOMO) of a single thiophene unit) is called the valence band, while the lowest unoccupied band (originating from the lowest unoccupied molecular orbital (LUMO) of a single thiophene unit) is called the conduction band. The difference in energy between these energy band levels is called the band gap energy or simply, band gap (E_g) as indicated in **Figure 1.3**. Generally speaking, because conducting polymers possess delocalized electrons in π -conjugated system along the whole polymeric chain, their conductivity is much higher than that of other polymers with no conjugated system. These latter non-conjugated polymers are usually known to be insulators.

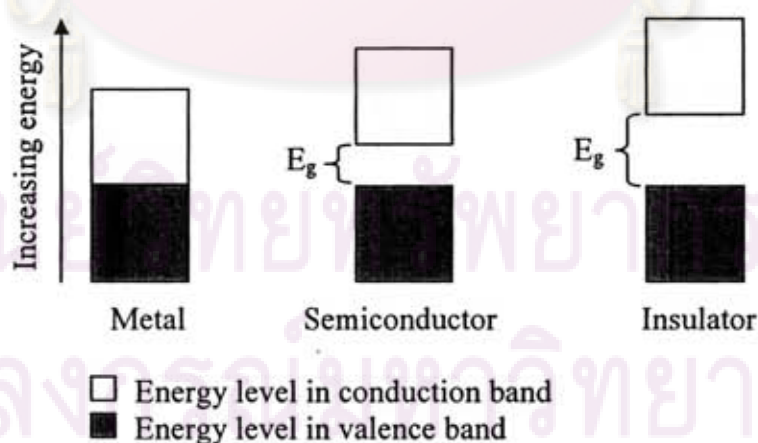


Figure 1.3 Schematic representation of the band structure of metal, semiconductor, and insulator. (E_g is the energy gap between the valence band (VB) and the conduction band (CB)).

The difference between π -conjugated polymers and metals is that in metal, the orbitals of the atoms overlap with the equivalent orbitals of their neighboring atom in all directions to form molecular orbitals similar to those of isolated molecules. With N interacting atomic orbitals we will have N molecular orbitals. In the metal, however, or any continuous solid-state structure, N will be a very large number (typically 10^{22} for a 1 cm^3 metal piece). With so many molecular orbitals spaced together in a given range of energies, they form an apparently continuous band of energies

In insulators, the electrons in the valence band are separated by large gap from the conduction band. However, in conductors like metals, the valence band overlaps with the conduction band. And in semiconductors, there is a small enough gap between the valence and conduction bands that thermal or other excitations can bridge the gap. With such a small gap, the presence of a small percentage of a doping material can increase conductivity dramatically [6].

1.4. Conductivity and doping

As mentioned previously, conducting polymers are unique in that they are organic chains of alternating double- and single-bonded sp^2 hybridized atoms, which endow the polymer with metallike semiconductive properties. The series of alternating single and double bonds, which is generated by electron cloud overlap of p -orbitals to form π molecular orbitals, is referred to as a conjugated system.

Prior to doping, these systems are insulative ($\sim 10^{-10}$ S/cm); however, the electrical conductivity of polyheterocyclic films, for instance, can be increased up to 12 orders of magnitude ($\sim 10^2$ S/cm) depending on the polymer system and the type and extent of doping.

Conductivity is a measure of electrical conduction and thus a measure of the ability of a material to pass a current. Generally, materials with conductivities less than 10^{-8} S/cm are considered insulators, materials with conductivities between 10^{-8} and 10^3 S/cm are considered semiconductors, and materials with conductivities greater than 10^3 S/cm are considered conductors. Conductivity (σ) is the inverse of resistivity (ρ) and therefore has the units of inverse ohms (Ω^{-1}), also known as Siemens (S), per unit of distance, generally centimeters (*i.e.*, S/cm) [8].

In this study, resistivity is determined from a material's resistance (R), which is measured using a 2-point probe technique. The 2-point-probe technique involves

applying voltage (V) across electrodes at the surface of a material and then measuring the change in current (I), according to Ohm's law.

$$R = \frac{V}{I}$$

Where: R = Resistance (ohms, Ω)

V = Voltage (volts, V)

I = Current (amperes, A)

This electrical resistance is proportional to the sample's length and the resistivity and inversely proportional to the sample's cross sectional area.

$$R = \frac{\rho \ell}{A}$$

Where: ρ = Resistivity

A = cross-sectional area

ℓ = length between electrodes

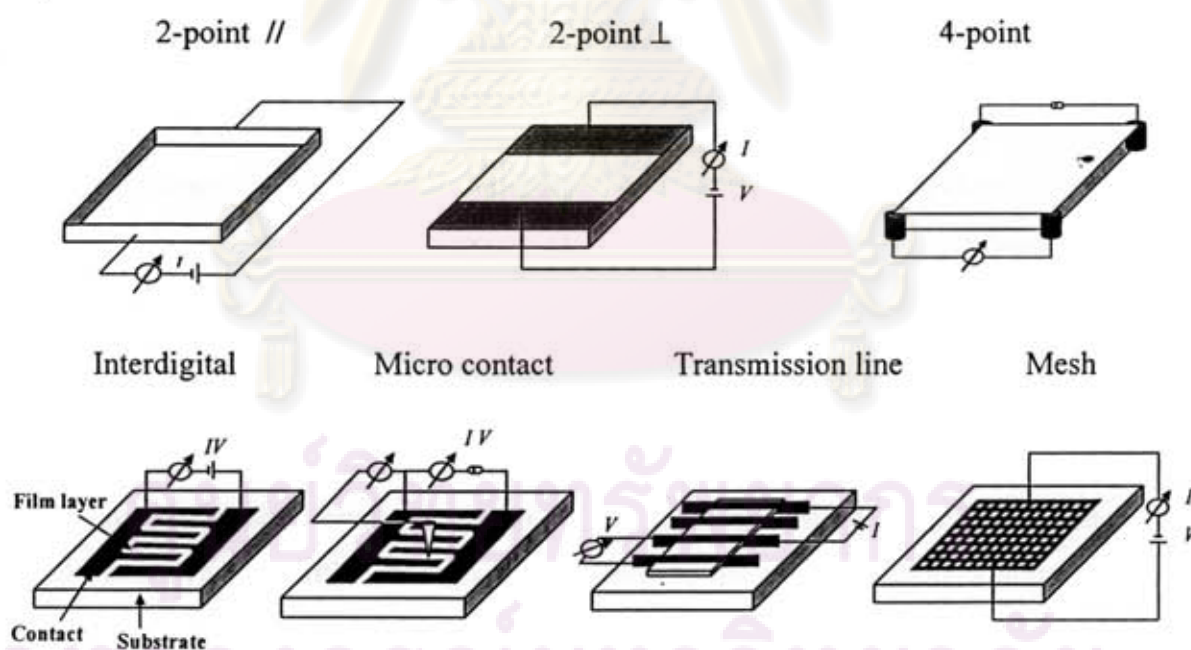


Figure 1.4 Typical contact geometries used for thin film conductivity measurement.

In **Figure 1.4** several different principal types of electrical contacts to thin films are shown [9]. They can be divided into two categories concerning the direction of the measured charge transport with respect to the substrate surface. Most often

devices which measure transport in the direction along the substrate surface are used, because the contacts can be prepared onto the (insulating) substrates before the organic films is prepared and they are often commercially available. Much more complicated is the preparation of top contacts to measure transport perpendicular to the (conducting) substrate surface. If typical evaporation is used for the preparation, a large amount of heat is transferred to the organic film during deposition. Due to the lack of strong intermolecular bonding, the hot metals can easily diffuse into the film.

The doping is an addition of a doping agent into the polymer and expects to improve the conductivity of the polymer. The electrical conductivity results from the existence of charge carriers (through doping) and from the ability of those charge carriers to move along the π -bonded "highway". Consequently, doped conjugated polymers are good conductors for two reasons [10]:

1. Doping introduces carriers into the electronic structure. Since every repeat unit is a potential redox site, conjugated polymers can be doped *n*-type (reduced) or *p*-type (oxidized) to a relatively high density of charge carriers.

2. The attraction of an electron in one repeating unit to the nuclei in the neighboring units leads to carrier delocalization along the polymer chain and to charge carrier mobility, which is extended into three dimensions through interchain electron transfer.

Charge injection onto conjugated, semiconducting macromolecular chains, "doping", leads to the wide variety of interesting and important phenomena that define the field. The doping can be accomplished in a number of ways:

Dopants can be atomic or molecular species, and act as electron donors (Li, Na, K) or electron acceptors (I_2 , Br_2 , AsF_5 , $FeCl_3$, $LiClO_4$). These dopants work by acting as charge transfer agents. They are positioned interstitially between the polymer chains and donate charges to, or accept charges from the polymer backbone. The negative or positive charges being added to the polymer upon doping do not simply begin to fill the conduction or valence bands. A broad range of different conducting polymers and their conductivities is listed in **Table 1.2**.

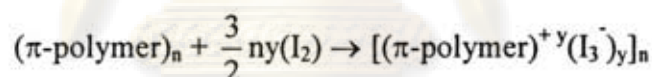
Table 1.2 Common conducting polymers, conductivities, type of doping, stability and processing attributes [8], [11].

| Conducting polymer | Maximum conductivity (after doping) (S/cm) | Type of doping | Stability (doped state) | Processing possibilities |
|-----------------------------------|--|----------------|-------------------------|--------------------------|
| Polyacetylene | 200-1000 | n, p | poor | limited |
| Poly(<i>p</i> -phenylene) | 500 | n,p | poor | limited |
| Poly(<i>p</i> -phenylenesulfide) | 3-300 | p | poor | excellent |
| Poly(<i>p</i> -vinylene) | 1-1000 | p | poor | limited |
| Polypyrrole | 40-200 | p | good | good |
| Polythiophene | 10-100 | p | good | excellent |
| Polyaniline | 5 | n, p | good | good |

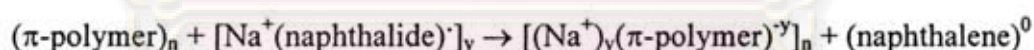
1.4.1 Chemical Doping by Charge Transfer

The initial discovery of the ability to dope conjugated polymers involved charge-transfer redox chemistry, oxidation (*p*-type doping), or reduction (*n*-type doping) as illustrated with the following examples [10]:

1. *p*-type



2. *n*-type



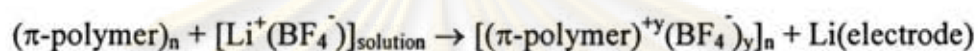
When the doping level is sufficiently high, the electronic structure evolves to that of a metal.

1.4.2 Electrochemical Doping

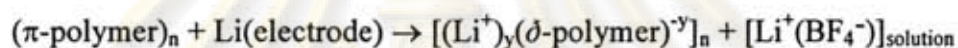
Although chemical (charge transfer) doping is an efficient and straightforward process, it is typically difficult to control. Complete doping to the highest concentrations yields reasonably high quality materials. However, attempts to obtain intermediate doping levels often result in inhomogeneous doping. Electrochemical doping was invented to solve this problem [12]. In electrochemical doping, the electrode supplies the redox charge to the conducting polymer, while ions diffuse into (or out of) the polymer structure from the nearby electrolyte to compensate the

electronic charge. The doping level is determined by the voltage between the conducting polymer and the counter electrode; at electrochemical equilibrium the doping level is precisely defined by that voltage. Thus, doping at any level can be achieved by setting the electrochemical cell at a fixed applied voltage and simply waiting as long as necessary for the system to come to electrochemical equilibrium (as indicated by the current through the cell going to zero). Electrochemical doping is illustrated by the following examples:

1. *p*-type



2. *n*-type



1.5. Mechanism of Conduction by doping [10,11]

One early explanation of conducting polymers used band theory as a method of conduction. This informs that a half-filled valence band would be formed from a continuous delocalized π -system. This would be an ideal condition for conduction of electricity. However, it turns out that the polymer can lower its energy more efficiently by bond alteration (alternating short and long bonds). The polymer is transformed into a conductor by doping with either an electron donor or an electron acceptor. In the doping of silicon-based semiconductors, it is doped with either arsenic or boron. However, while the doping of silicon produces a donor energy level close to the conduction band or an acceptor level close to the valence band, this is not the case with conducting polymers.

In conducting polymers with a non-degenerated ground state, the charge introduced upon doping can be stored in a form of polarons and bipolarons. Polythiophene, polaron, and bipolaron can be visualized as follows (Figure 1.5).

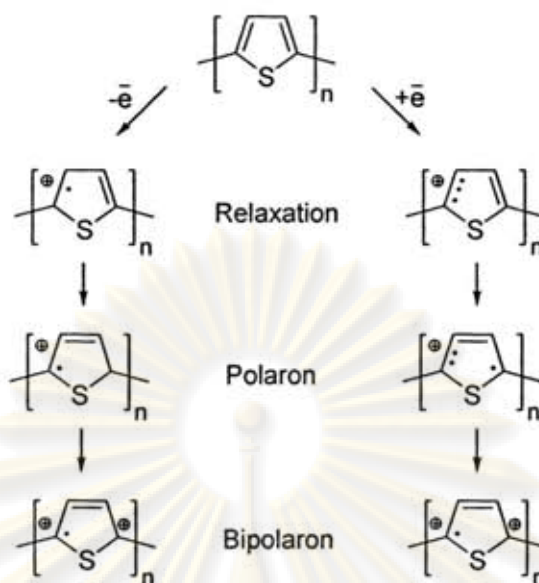


Figure 1.5 Schematic representation of polythiophene in the undoped, singly, and doubly oxidized (left), and singly and doubly reduced (right) states.

Polythiophene and derivatives were often doped by an oxidative doping because they are electron rich and favor to lose electron. The oxidative doping of polythiophene proceeds in the following way shown in **Figure 1.6**. An electron is removed from the π -system of the backbone producing free radical and a spinless positive charge. The radical and cation are coupled to each other via local resonance of the charge and the radical. In this case, a sequence of quinoid-like rings is used. The distortion produced by this is of higher energy than the remaining portion of the chain. The creation and separation of these defects costs a considerable amount of energy. This limits the number of quinoid-like rings that can link these two bound species together. In the case of polythiophene it is believed that the lattice distortion extends over four thiophene rings. This combination of a charge site and a radical is called a polaron. This could be either a radical cation or radical anion. This creates new localized electronic states in the gap, with the lower energy states being occupied by a single unpaired electron.

Upon further oxidation the free radical of the polaron is removed, creating a new spinless defect called a bipolaron. This is of lower energy than the creation of two distinct polarons. At higher doping levels it becomes possible that two polarons combine to form a bipolaron. Thus at higher doping levels the polarons are replaced with bipolarons. This eventually, with continued doping, forms a continuous bipolaron bands. Their band gap also increases as newly formed bipolarons are made

at the expense of the band edges. For a very heavily doped polymer it is conceivable that the upper and the lower bipolaron bands will merge with the conduction and the valence bands respectively to produce partially filled bands and metallic like conductivity. This is shown in **Figure 1.7**.

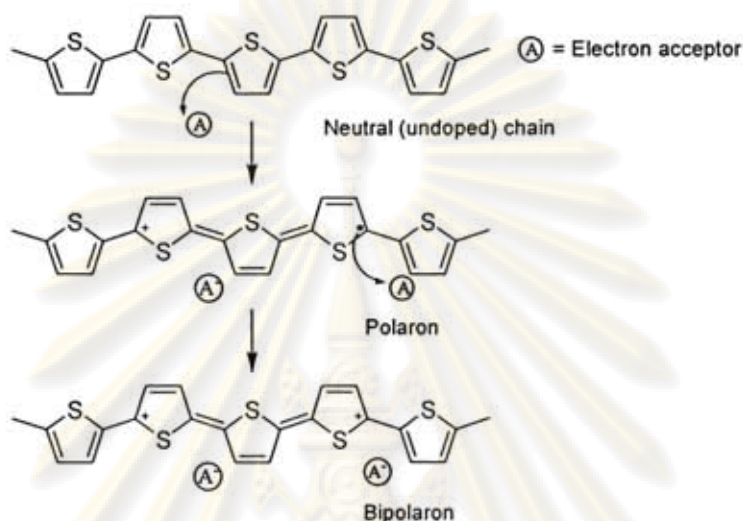


Figure 1.6 Polaron and bipolaron in polythiophene.

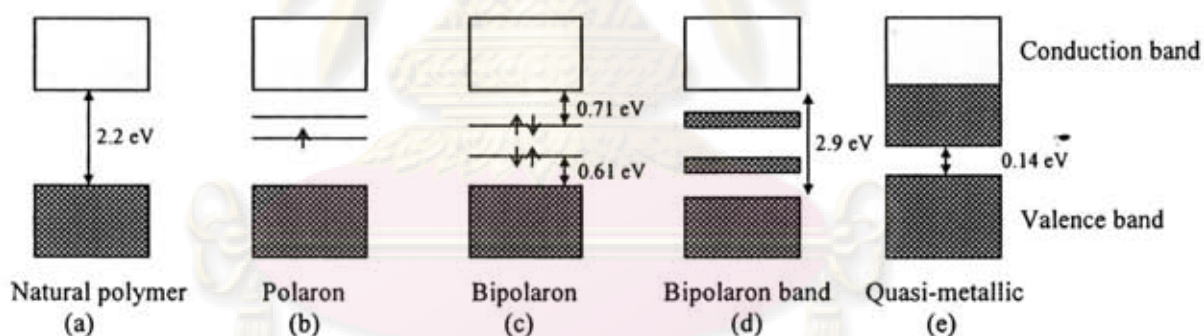


Figure 1.7 Evolution of the polythiophene band structure upon doping: (a) undoped (b) 0.1% doping level, with polaron formation; (c) ~1-20% doping level, with the bipolaron formation; (d) 30% doping level, where the bipolaron states overlap and form two bands; (e) Hypothetical 100% doping level, with quasi-metallic behavior [8].

1.6. Applications of conducting polymers [11]

The extended π -systems of conjugated polymer are highly exposed to chemical or electrochemical oxidation or reduction. These alter the electrical and optical properties of the polymer, and by controlling this oxidation and reduction, it is possible to precisely control these properties. Since these reactions are often reversible, it is possible to methodically control the electrical and optical properties

with a great deal of precision. It is even possible to switch from a conducting state to an insulating state.

There are two main groups of applications for these polymers. The first group utilizes their conductivity as its main property. The second group utilizes this electro activity are shown in **Table 1.3**.

Table 1.3 Application of conducting polymers.

| Group 1 | Group 2 |
|---|---|
| electrostatic materials | molecular electronics |
| conducting adhesives | electrical displays |
| electromagnetic shielding | chemical biochemical and thermal sensors |
| printed circuit boards | rechargeable batteries and solid electrolytes |
| artificial nerves | drug release systems |
| antistatic clothing | optical computers |
| piezoceramics | ion exchange membranes |
| active electronics (diodes transistors) | electromechanical actuators |
| aircraft structures | smart structures |

1.7. Polythiophene [13, 14]

Polythiophene is a polymer composed of five membered heterocyclic monomeric units. Polythiophene with an ideal extended π -conjugation is possible only in polymers with perfectly 2,5-linked repeating units. However, 2,4- and 2,3-couplings as well as hydrogenated thiophene units can also be found in the polymer. It is environmentally stable and highly resistant to heat. Polythiophene attracted much attention as a conducting polymer due to ease of synthesis, high stability, and structural versatility.

A significant discovery demonstrated that polythiophene belongs to one of a few cases in which substitution of hydrogen at the 3-position by an alkyl chain does not affect the conductivity of the polymer, which impart solubility and consequently enhance processibility. The 3- substituent can be incorporated into the polymer chain with two different regioregularities: head-to-tail (HT) and head-to-head (HH) orientations which can result in four triad regioisomers in the polymer chain, *i.e.* HT-HT, HT-HH, TT-HT and TT-HH (**Figure 1.8**).

Both the conducting and semiconducting forms are very stable and readily characterized. Applications of these materials in light-emitting devices, field effect transistors, as well as other molecular electronic devices have been fuelled by the improved solubility and ease of processing of mono-, di-, and ring-substituted polythiophenes, while simultaneously allowing the electronic band gap to be tuned.

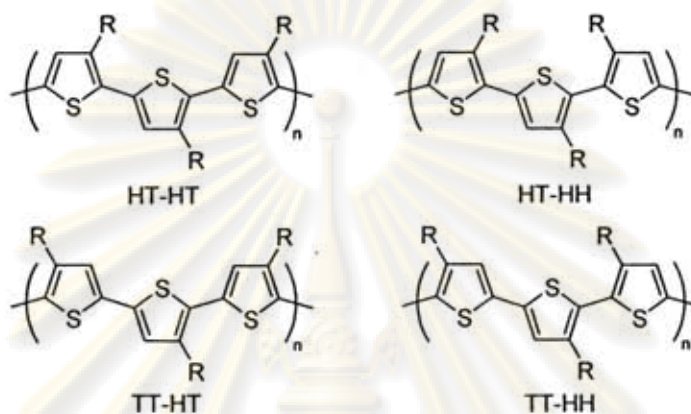


Figure 1.8 Regioregular of poly(3-alkylthiophene).

1.8. Synthesis of polythiophene [15]

Polythiophene has been prepared for the first time by electrochemical polymerization. Since a film is produced on the anode during polymerization, this method is suitable for the preparation of polymers such as polythiophene and poly(3-methylthiophene), which is not processible after polymers are formed. However, in electrochemical polymerization, the yield of polymers is low and the polymers often do not have a well-defined structure. On the other hand, since facile oxidative polymerization with iron(III) chloride produces polythiophene in a high yield, this method is suitable for processing polythiophenes such as poly(3-methylthiophene). The molecular weight of polymer obtained by this method is sufficiently high for a film to be cast. Grignard coupling is also an important route to polythiophene. Polymers produced by this method often show lower conductivity than those obtained by other methods. This technique is still important for the preparation of polymers with a well-defined structure, since no migration of substituents takes place during the coupling reaction. Regioregular poly(3-alkylthiophene) has longer π -electron conjugation along the polymer backbone and shows higher conductivity. In addition, it has a higher stability in the doped state and self-organizing properties. McMullough

et al. [16] prepared the regioregular polymer by Grignard coupling and Rieke *et al.* [17] by the coupling of 2-bromo-5-bromozincio-3-alkylthiophene.

1.8.1 Electrochemical polymerization

A polymeric film can be obtained by electrochemical polymerization, this is a very useful method for preparing polymers such as polythiophene, poly(3-methylthiophene) and poly(3-phenylthiophene) (Figure 1.9), which are insoluble and infusible. When these polymers are obtained in the form of powder we cannot process them into the film or other useful forms.

Polythiophene is not stable at potentials used for electrochemical polymerization of thiophene. Thus, polythiophene deposited on the anode at the earlier stages of the polymerization is overoxidized and has deteriorated, while electrochemical polymerization produces new polymer.

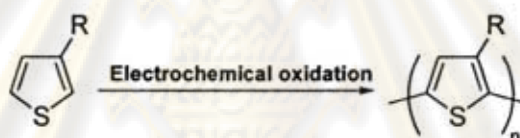


Figure 1.9 The electropolymerization method for the synthesis of poly(3-alkylthiophene) (R= H, Me, Ph).

1.8.2 Oxidative coupling polymerization with iron(III)chloride

This method is easily accessible to almost all scientists who wish to obtain poly(3-alkylthiophene) and will provide sufficient amounts of the polymer for laboratory use. The resulting polymers are soluble in common organic solvents and their film can be formed by simply casting its solution on a substrate. In addition, 3-alkylthiophenes are commercially available (Figure 1.10).

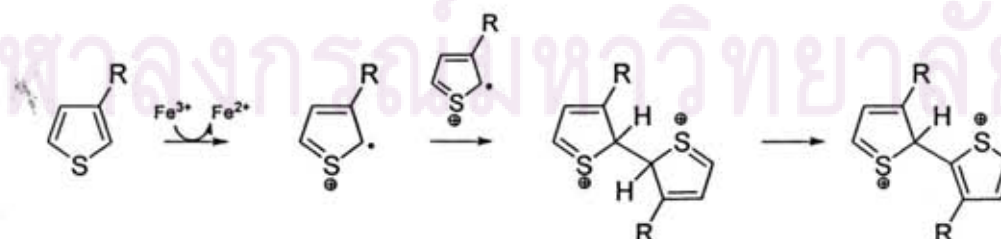


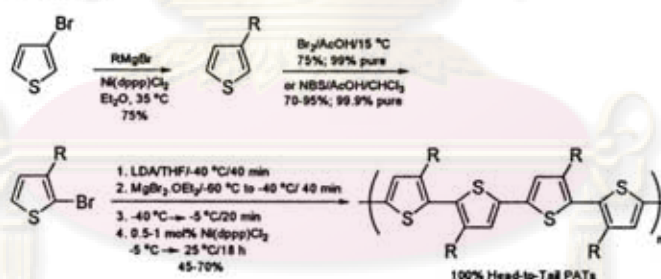
Figure 1.10 Oxidative coupling reaction of 3-alkylthiophene by FeCl_3 .

1.8.3 Grignard coupling and other chemical polymerization

Later developments produced higher molecular weight polythiophenes than those initial efforts, and can be grouped into two categories based on their structure. Regioregular polythiophenes can be synthesized by catalytic cross-coupling reactions of bromothiophenes, while polymers with varying degrees of regioregularity can be simply synthesized by oxidative polymerization.

The first synthesis of perfectly regioregular polyalkylthiophene (PATs) was described by McCullough *et al.* in 1992 [16]. As shown in **Figure 1.11 (a)**, selective bromination produces 2-bromo-3-alkylthiophene, which is followed by metallation and then Kumada cross-coupling in the presence of a nickel catalyst. This method produces approximately 98-100% HT-HT couplings, according to NMR spectroscopy analysis. In the method subsequently described by Rieke *et al.* in 1993 [17], 2,5-dibromo-3-alkylthiophene is treated with highly reactive “Rieke zinc” [18] to form a mixture of organometallic isomers shown in **Figure 1.11 (b)**. Addition of a catalytic amount of $\text{Pd}(\text{PPh}_3)_4$ produces a regiorandom polymer, but treatment with $\text{Ni}(\text{dppf})\text{Cl}_2$ yields regioregular PAT in quantitative yield [19].

(a) McCullough method



(b) Rieke method

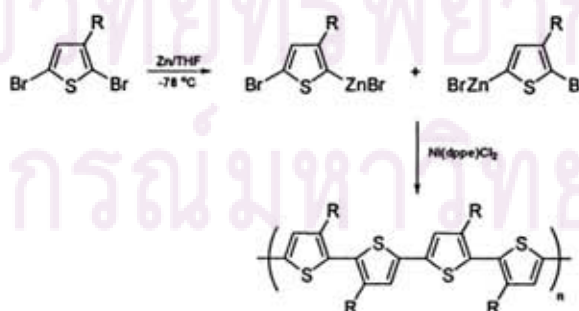


Figure 1.11 The regiospecific synthesis of poly(3-alkylthiophene)s with almost 100% HT coupling.

An alternative method, plasma polymerization, makes use of molecules occurring in various plasma environments. This technique results in very thin but uniform polymeric layers that strongly adhere to a desired substrate. It has been found that the plasma polymerized films are usually highly cross-linked and are resistant to higher temperatures and chemicals. The disadvantage is the poor predictability of the chemical structure of the resulting plasma polymerized layer. Several monomers have been plasma polymerized with the objective to obtain conductive surfaces. Success in synthesizing processible conducting polymer has promised their potential application in electronic devices [20].

1.9. Plasma

As the temperature increases the substance passes from solid to liquid, through gas, to plasma (**Figure 1.12**). The solid, the liquid and the gas are composed of a very large number of molecules (or atoms). In these phases of matter the heat is an expression of the molecular motion. In these three phases the molecules or atoms are moving as one unit. Plasma is composed of a very large number of free electrons and ions and in this phase of matter the heat is the expression of the separate electron and ion motion. Gas is normally an electrical insulator, that is, electric currents cannot easily pass through it. However, by heating gas to appropriate temperature, physicists found that insulator gas becomes a good electrical conductor. Gas is transformed into plasma which consists of free electrons: the carriers of the electric currents [21].

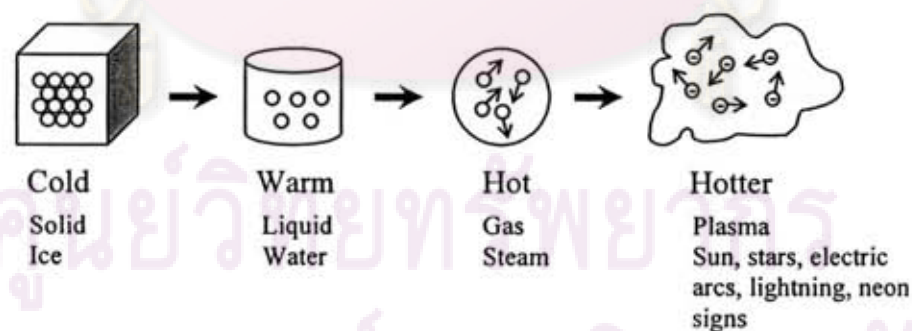


Figure 1.12 The four states of matter; plasma is sometimes referred to as the fourth state.

Plasma is a partially ionized gas containing free electrons, ions, radicals and photons with equal numbers of positive and negative charge carriers. In this situation, plasmas are termed quasi-neutral. Quasi-neutral refers to there being about equal

numbers of positive ions and negative electrons in the gas, and thus most of plasmas are electrically neutral. Quasi-neutrality demands that

$$n_i \cong n_e \cong n_s$$

where n_s is the number density (*i.e.*, the number of particles per cubic meter) of species [22].

Plasma states can be divided in two main categories: Hot Plasmas (near-equilibrium plasmas) and Cold Plasmas (non-equilibrium plasmas). Hot plasmas are characterized by very high temperatures of electrons and heavy particles, both charged and neutral, and they are close to maximal degrees of ionization (100%). Cold plasmas are composed of low temperature particles (charged and neutral molecular and atomic species) and relatively high temperature electrons and they are associated with low degrees of ionization (10^{-4} – 10%). Hot plasmas include electrical arcs, plasma jets of rocket engines, thermonuclear reaction generated plasmas, *etc.* while cold plasmas include low-pressure direct current (DC), radio frequency (RF), and microwave (MW) power, discharges from fluorescent (neon) illuminating tubes. Corona discharges are also identified as cold plasmas.

In this case, utilizing microwave source for generating plasma, these plasmas are sustained by microwave energy dissipated into the reaction media by waveguides in the case of higher powers. The physical dimensions of waveguides are selected according to the microwave frequency. Microwave discharges are more difficult to sustain under low-pressure conditions (<1 torr). In a collisionless condition the energy gained by an electron during one cycle is too small to produce ionization. In collisional plasmas at constant power density and electric field, the average microwave power transferred from the driving field has a maximum value when the collision frequency equals the driving frequency. The absorption of microwave power depends on the collision frequency of the electrons which is controlled by the atomic and molecular species. At comparable plasma parameters, RF discharges most often fill the entire reactor whose dimensions are usually smaller than the wavelength of the RF field (13.56 MHz corresponds roughly to 22 m). Microwave plasmas exhibit a strong peaking in field intensity at the coupling to the microwave cavity that diminishes gradually with increased distance from the coupling owing to the energy

originating at the microwave coupling, rather than being deposited throughout the discharge ($\lambda = 12.24$ cm at 2.54 GHz) [23].

The energy of the electrons in the plasma produced by a glow discharge is 1-30 eV and their density (10^9 - 10^{12} cm⁻³) is dependent on plasma source. For deposition of plasma polymers several types of plasmas can be used, for example; RF, DC, and MW. Possible areas of application of plasma treatment and plasma polymerization are listed below.

1. Electronics (integrated circuits, resists with a high degree of integration, amorphous semiconductors, etching of fine amorphous ceramics).
2. Electrical engineering (insulators, thin film dielectrics, separators for galvanic elements).
3. Chemical technology (reverse-osmotic, semi-permeable, gas-separation membranes, lubricants, insolubilization).
4. Surface modification (improved adhesion, protective, abrasion-resistant and strengthening coats).
5. Optics (antireflecting and antimisting coatings, improved transparency, optical fibers, laser and optical windows, contact lenses).
6. Textile industry (anti-igniters and antistatic treatment, improved dyeing qualities, hydrophilization, water-repellant properties, anti-creasing).
7. Biomedicine (immobilization of enzymes, organelles and cells, regulation of the release of drugs and pesticides, sterilization and pasteurization, artificial soil, blood vessels, teeth, anticoagulants).

Plasma chemistry includes four types of main reactions: 1) surface reactions of polymers (plasma treatment); 2) plasma polymerization; 3) plasma-initiated polymerization; and 4) plasma reduction [24].

The individual steps or reactions that are involved in the process of polymer formation in a glow discharge are extremely complex and are dependent on the system. Several important types of phenomena can be identified for the purpose of constructing a general picture of the glow discharge polymerization. This process is represented by the Competitive Ablation and Polymerization (CAP) mechanism schematically shown in **Figure 1.13**. The direct route shown in the Figure is referred

to as plasma-induced polymerization which is referred to as plasma-initiated polymerization while the indirect route is referred to as plasma polymerization [25].

The plasma initiated polymerization comprises exposing a monomer vapor equilibrated with a liquid or solid monomer to a plasma for a short time thereby producing a polymerically active seed and then allowing the polymerically active seed produced in the plasma to come into contact with the surface of the liquid or solid monomer thereby starting polymerization growing in the liquid or solid monomer. Unlike the ordinary plasma polymerization such as the plasma vapor-phase polymerization wherein all the component steps including start of polymerization, growth, migration, recombination, and restart take place in the presence of plasma, the plasma-initiated polymerization occurs in the vapor phase and the subsequent reaction for growth and stop of polymerization occur in the condensate phase. In various fields, such polymers by the plasma polymerization have come to attract growing attention in recent years. The plasma polymerization has been principally used in vapor phase polymerization or applied for surface treatment [26].

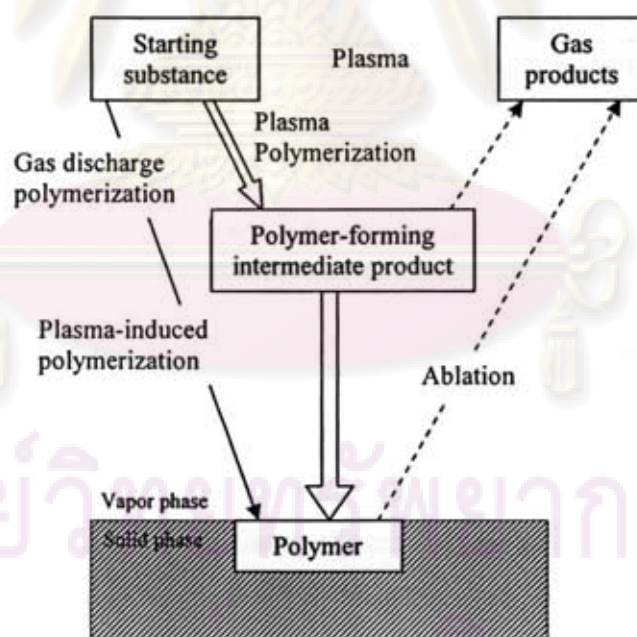


Figure 1.13 General mechanism of gas discharge polymerization.

1.10. Plasma polymerization

Plasma treatment, which is an electric gas discharge, is typically performed in a vacuum equipment in a pressure range of 0.0075 – 0.075 torr. An electric field, which is applied to the gas under vacuum conditions, causes the acceleration of free electrons. The kinetic energy of the electrons is then high enough for basic reactions like ionization, fragmentation, and excitation of the gas species in the case of the ignition of the plasma, which can be observed by its characteristic visible glow. Atoms and molecules are ionized, excited and fragmented and thus form a highly reactive gaseous mixture, which is able to react chemically with exposed surfaces. The resulting surface properties are mainly dependant on the process gas used and its chemical properties [27].

Plasma polymerization is the most important technique for fabricating thin polymer films (sub-micrometer (μm) range) from almost any organic vapor. Unlike conventional polymers, plasma polymers do not consist of chains with a regular repeat unit (see **Figure 1.14**). The chemical structure and physical properties may be quite different from conventional polymer which is derived from the same starting materials. Plasma-polymerized films are generally chemically inert, insoluble, mechanically tough, thermally stable, and have been used in a wide variety of applications such as permselective membranes, protective coatings, electrical, optical and biomedical films. The process offers several advantages over conventional polymer synthesis, as follows

1. the starting feed gases used may not contain the type of functional groups normally associated with conventional polymerization
2. such films are often highly coherent and adherent to a variety of substrates, including conventional polymers, glasses, and metals
3. polymerization may be achieved without the use of solvents
4. plasma polymer films can be easily produced with thicknesses of 500 \AA to 1 μm
5. ultrathin, "pin-hole" free films may be prepared
6. through careful control of the polymerization parameters, it is possible to tailor the films with respect to specific chemical functionality, thickness and other chemical and physical properties [28].

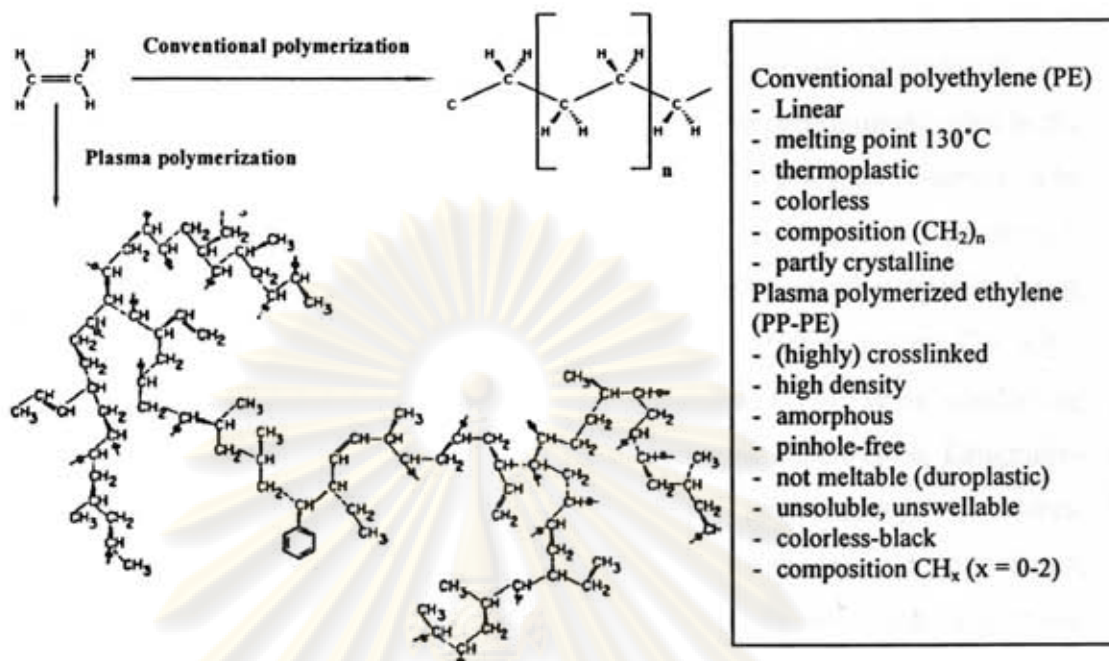
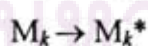


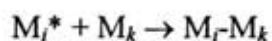
Figure 1.14 Polymer prepared from chemical polymerization compared to that from plasma polymerization method [27, 29].

The mechanism of plasma polymerization of organic compounds is very complex. The overall polymer formation is the consequence of many complex reactions, and the polymer deposition rate as well as the properties of polymers are dependent on many experimental factors such as types of electric discharge, conditions of the discharge, geometrical factors of the reaction vessel, and the properties of substrate upon which a polymer deposits. Consequently, the plasma polymerization cannot be specifically described for the general case. However, a series of recent studies has projected reasonable overall mechanisms of the plasma polymerization of organic compounds, which seem to be able to apply in many cases. The overall mechanisms can be represented by

Initiation:



Propagation:



Where i and k are numbers of repeating units (*i.e.*, $i = k = 1$ for the monomer) and the M^* are reactive species which can be ions of either charge, an excited molecule, or a free radical. Although the kind of reactive species that play predominant roles in the plasma polymerization has been a subject of debate for past years, there seems to be no conclusive evidence which enables us to exclude any specific species. Therefore, it seems most reasonable to assume that any energetic and/or reactive species being created in plasma can contribute to the overall polymer formation in plasma [25, 30]

Common techniques developed for the synthesis of thin layer conducting polymers include electrochemical growth on modified electrode surfaces, Langmuir-Blodgett deposition, spin-coating and self-assembly of polyelectrolyte structures. These deposition approaches usually require complex experimental procedures, solubility of the starting materials, and often result in less oriented macromolecular structures. Conducting polymers prepared using conventional polymerization procedures result, in most cases, in the formation of insoluble powdery materials which are difficult to convert into uniform, thin layer, ordered networks. Attempts initiated for the generation of processible conducting polymer structures using chemical derivatives of aniline, pyrrole and thiophene, or by employing chemical modification techniques for altering the structures of conventionally synthesized conducting polymers, have not always generated the expected results. These approaches usually require complex synthetic routes, and the purification of the resulting polymer-containing final products are rather difficult. Solubility can also be a disadvantage in some applications. Deposition of water-soluble polyaniline-derivatives (e.g. sulfonated-polyaniline) on various substrates, for instance, hardly can be considered for biosensor applications. It is still an unsolved problem to learn how to deposit uniform and insoluble thin conducting polymer layers with good adhesion characteristics on various substrate surfaces, starting from soluble polymeric precursors.

Plasma chemistry was recently considered an alternative for overcoming these drawbacks. Pyrrole, thiophene and aniline were mainly investigated for plasma deposition of conductive (conjugated) polymeric layers since these polymers synthesized by conventional polymerization techniques showed promising electrical behavior [23].

In 1993, Sadhir and Schoch [31] prepared conducting films of polythiophene by RF (13.56 MHz) plasma polymerization at RF (4 W) and 5 hr duration of polymerization. In this technique, ionized argon is the initiating species for the polymerization of thiophene in a region away from the high RF flux-density. These films displayed a conductivity of 1.8×10^{-4} S/cm after doping with iodine by exposing the films to iodine vapor in a sealed container overnight at room temperature.

In 1993, Kruse and coworkers [32] studied a new method of doping using an iodine-containing monomer, 2-iodothiophene, with a 2.45 GHz microwave plasma at 300 W and 5 min. Poly(2-iodothiophene) were formed and had exhibited good electrical conductivity between 10^{-6} and up to 10^{-1} S/cm. For comparison, conventional electrochemically prepared polythiophene had a conductivity of 10^2 S/cm and other plasma polymers produced in 7.3 kHz audio frequency (AF) or 13.56 MHz RF plasma discharges had an electrical conductivity of 2.2×10^{-3} S/cm and 4.3×10^{-4} S/cm, respectively. It was found that the content and the chemical state of iodine correlated with electrical properties of the films. The sulfur and iodine content in the plasma polymer was much lower than one would expect from the atomic composition of the monomer. The reason may be that in the plasma process iodine can form various volatile species such as ICH_3 , HI and H_2S .

In 1996, Ryan and coworkers [33] synthesized poly(2-iodothiophene) using continuous wave RF plasma polymerization at 2-20 W, and reaction time of 1 min to provide sufficient plasma polymer for XPS analysis and at reaction time of 10 min to generate films thick enough for IR characterization. This method produced a polymeric network which retained many of the structural characteristics by associated with the original precursor molecule. Sulfur and iodine incorporation into the growing plasma polymer layer drops with increasing glow discharge power due to the weaker C-S and C-I bond linkages present in the monomer.

In 1998, Bhat and coworker [34] synthesized polythiophene under an RF-inductively tubular reactor. Thiophene-based films were deposited onto aluminum, glass, and NaCl crystal substrates. The electrical conductivity of the films was found in the range of 10^{-15} – 10^{-10} S/cm which was rather low as compared to other methods of preparation. It was suggested that this could be due to higher crosslinking and that it was in an undoped state. By suitable doping, the conductivity could be increased.

In 1999, Kiesod and Heilmann [35] use thiophene and 2-iodothiophene to synthesize conductive thin polymeric layers without additional doping. These plasma-polymer films were deposited using an AC plasma technique, during which an additional silver-particles-embedding process was performed. It was shown, that low plasma power densities and high monomer flow rates resulted in the best electrical conductivities of the deposited layers (1.3×10^{-6} S/cm).

In 2000, Groenewoud and coworkers [36] synthesized highly transparent (>80%) layers with conductivities (10^{-6} S/cm) in the range of antistatic applications by pulsed plasma polymerization of thiophene and doped immediately after deposition by placing in an iodine vapor for 5 min. The influence of power, pressure, pulse time, duty cycle, and position in the reactor on the conductivity of the resulting plasma polymerized thiophene (PPT) layers was evaluated. In the used ranges, only pressure had a significant influence on the conductivity of the deposited layer. The results could be correlated to the effect of the deposition parameters on the fragmentation of the thiophene monomer. At high pressure and short pulse times there was less fragmentation of thiophene, resulting in a higher conductivity of the layer.

Two years later, Groenewoud and coworkers [37] synthesized polythiophene by pulsed plasma polymerization at high (0.225 torr) and low (0.045 torr) pressure. The iodine doping process of plasma polymerized thiophene films was conducted by placing the films in a sealed container containing iodine crystals. For the iodine doping the initial increase in conductivity was faster for the high pressure plasma polythiophene layers compared with the low pressure and showed a higher stability towards exposure to air after doping than low pressure-plasma polymerized thiophene. This can be explained by the longer conjugation length in the HP-PPT layers. At longer conjugation lengths, both the rate of formation and the mobility of charge carriers are higher.

In 2004, Wang and coworkers [38] prepared polythiophene via chemical and plasma polymerization at different RF power input. The FT-IR, SEM, and conductivity results indicated that the structures of plasma polymerized thiophene were rather different from those of polymers synthesized by conventional chemical methods, due to a higher degree of crosslinking and branching reactions in plasma polymerization. A higher and more stable conductivity could be obtained with

chemically synthesized polythiophene, but the thin films generated from the plasma polymerization process were much smoother and more uniform.

Besides, the application of microwave heating interest continues to grow concerning in chemical processes. Correa *et al.* [39] prepared polystyrene by emulsion polymerization under both microwave radiation and a conventional heating method. It was found that using microwave radiation resulted in a significant saving of energy and time.

Blagojevic *et al.* [40] studied the comparison of some properties of denture base polymers processed by both microwave and water-bath methods. It was demonstrated that in general, water-bath polymerization with a long curing cycle and a 3-h terminal boil produced superior properties. Although these two methods were inter-changeable for the conventionally heat cured material, consistently superior results were produced by following the method recommended by the manufacturer. Microwave polymerization resin improved mechanical properties and reduced residual monomer.

The aforementioned reports showed that plasma polymerization proves to be an excellent alternative to conventional polymerization of conducting films. Therefore, we would like to explore more into details.

1.11. Statement of the problem

Polythiophene is a polymer of high environmental stability and can also be used in electronic devices such as light emitting diode, solar cell, field-effect transistor, and battery. However, in an undoped state, the conductivity is low (10^{-15} - 10^{-10} S/cm). In order to increase the conductivity, conventional doping by exposing the chemically synthesized films to saturated iodine vapor in a sealed container is usually carried out. This disadvantage of this method is the leach of iodine from surface over time resulting in a regeneration of the undoped material.

The general synthesis of polymer can be synthesized by chemical polymerization and electrochemical polymerization. In addition, plasma polymerization can be an alternative to other conventional polymerization method because of high quality, adherent and pinhole-free film with a high degree of crosslinking.

This research is part of an effort to utilize an alternative method for thin film fabrication as opposed to conventional chemical or electrochemical processes. Efforts will also be made to introduce a dopant *in situ*.

1.12. The objective of the research

The aim of this study is to design and assemble a microwave plasma reactor for the synthesis of polythiophene films by microwave plasma polymerization. An *in situ* doping of plasma polymerized thiophene with iodine will also be investigated to increase electrical conductivity of the films.

1.13. Research Plan and the scope of the research

The following research plan will be conducted.

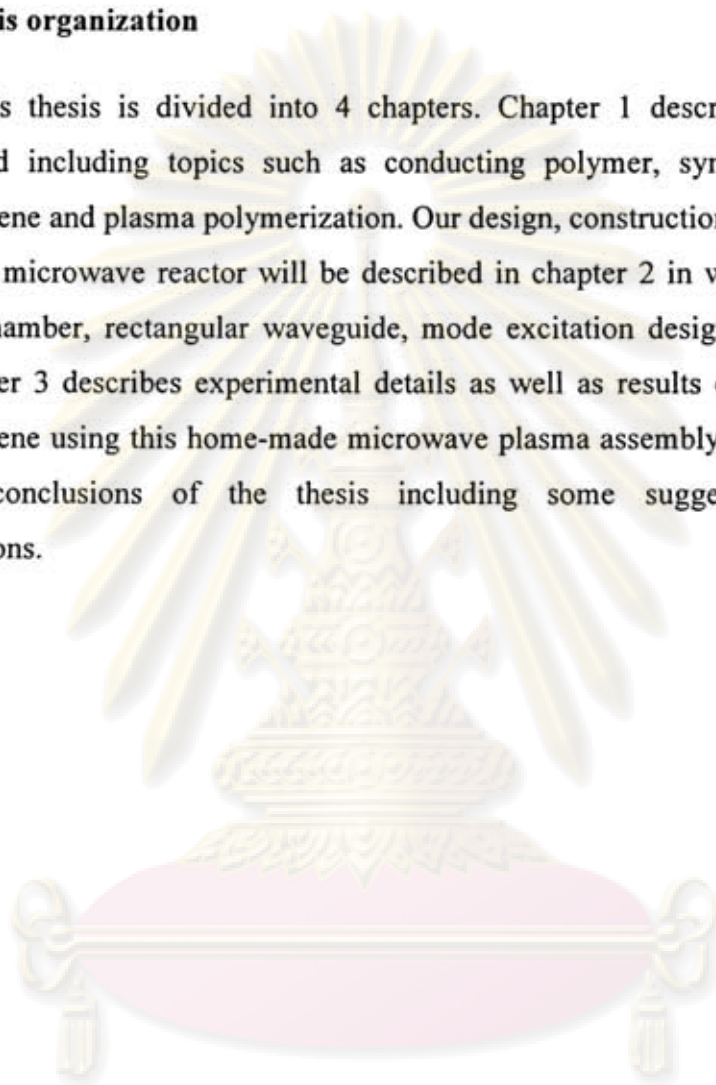
1. Design and construction of microwave plasma system
2. Testing of the microwave plasma reactor and the entire assembly with Optical emission spectroscopy (OES) to determine electron temperature
3. Synthesis of polythiophene by plasma polymerization under various conditions, for instance:
 - 3.1 microwave power: 150, 200, 250, and 300 Watt
 - 3.2 polymerization time: 1 and 2 minutes
4. Synthesis of doped polythiophene by *in situ* doping with iodine
 - 4.1 microwave power: 250 and 300 Watt
 - 4.2 polymerization time: 1 and 2 min
5. Synthesis of polythiophene by chemical polymerization for comparison
6. Characterization of polythiophenes: analyses with the following techniques will be carried out:
 - 6.1 Attenuated Total Reflection Fourier Transform Infrared (ATR FT-IR) Spectroscopy to characterize important functional groups in the material
 - 6.2 Solid-state UV-Visible absorption (UV-Vis) to determine optical properties of the material obtained
 - 6.3 Scanning Electron Microscopy (SEM) to investigate surface morphology of the fabricated material
 - 6.4 Energy-dispersive X-ray spectroscopy (EDS) to determine elemental composition of the material

6.5 Electrical conductometric determination to measure electrical conductivity of the fabricated material

7. Data analysis

1.14. Thesis organization

This thesis is divided into 4 chapters. Chapter 1 describes the necessary background including topics such as conducting polymer, synthetic methods of polythiophene and plasma polymerization. Our design, construction, and testing of the assembled microwave reactor will be described in chapter 2 in which the details of vacuum chamber, rectangular waveguide, mode excitation design, *etc.* will be laid out. Chapter 3 describes experimental details as well as results on the synthesis of polythiophene using this home-made microwave plasma assembly. Finally, chapter 4 presents conclusions of the thesis including some suggestions for future investigations.



ศูนย์วิจัยทรัพยากร
จุฬาลงกรณ์มหาวิทยาลัย

CHAPTER II

MICROWAVE PLASMA SYSTEM

2.1 The design and construction of the microwave plasma system

The microwave plasma reactor was designed to be assembled as an economical home-made prototype, the layout of which is as shown in **Figure 2.1**. The system consists of a power supply, a vacuum chamber, a microwave generator, a waveguide, a 3-stub tuner, a monomer vessel, and a cold trap.

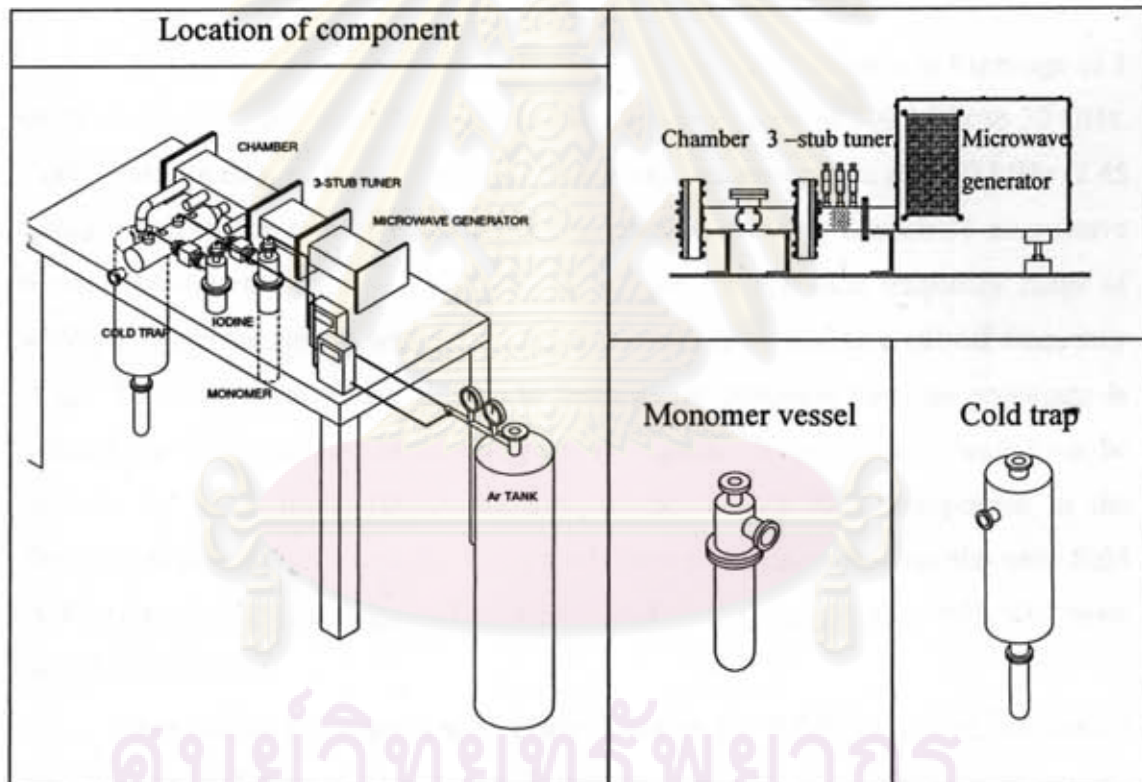


Figure 2.1 The drawing of microwave plasma system by AutoCAD and SolidWorks program.

2.1.1 Vacuum chamber

The vacuum chamber with a $86 \times 290 \times 43 \text{ mm}^3$ rectangular cavity and a circular flange (180 mm outside diameter) was made from stainless steel (**Figure 2.2**). Circular glass plates must be utilized here in order to allow microwave transmission into the vacuum system. The vacuum chamber is equipped with four ports leading to a

cold trap, a leak valve, an Edwards Pirani gauge, and a feed line for gaseous reagents. The dimension of the four ports is NW 16 the detail of which is explained in **Appendix A.1.**

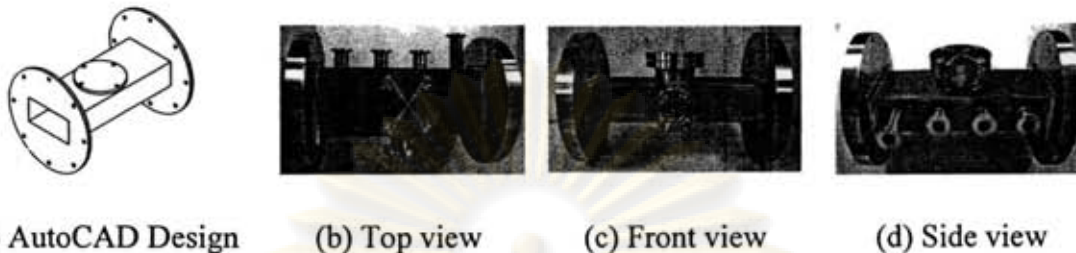


Figure 2.2 (a) The designed model of vacuum chamber and photographs of the actual vacuum chamber from the: (b) top, (c) front and (d) side views.

2.1.2 Rectangular waveguide and excitation mode [41]

Microwave is an electromagnetic radiation with wavelengths in the range of 1 cm to 1 m which corresponds to the frequency in the range of 300 MHz to 30 GHz. Traditional microwave plasma research mostly utilizes microwave at 2450 MHz (2.45 GHz) which is the same frequency as that used in ordinary household microwave ovens. The dimensions of a waveguide depend on the specified frequency range of which its electromagnetic wave can propagate and are related to a cut-off frequency ($f_{c,mn}$). The lowest frequency of an electromagnetic radiation that can propagate is called a cut-off frequency. In a rectangular waveguide, the propagation waves can be in both the TE_{mn} mode (transverse electric, no electric field component in the direction of propagation) and the TM_{mn} mode (transverse magnetic, no magnetic field in the direction of propagation) where m and n are the integers followed from Helmholtz equation.

An air-filled rectangular waveguide based on the WR340 standard (86.4×43.2 mm²) has been designed. Due to this dimension, only the TE_{10} mode can propagate the electric and magnetic field lines as shown in **Figure 2.3**. The dimension is related to the cut-off frequency shown in equation (1).

$$f_{c,mn} = \frac{c}{2\pi} \left[\left(\frac{n\pi}{a} \right)^2 + \left(\frac{m\pi}{b} \right)^2 \right]^{1/2} \quad (1)$$

when a = width of the waveguide
 b = height of the waveguide
 c = velocity of light

For the WR340, the cut-off frequency is 1.72 GHz (inside width (a) = 86.4 mm, and inside height (b) = 43.2 mm) which is less than 2.45 GHz, therefore, the electromagnetic wave can propagate.

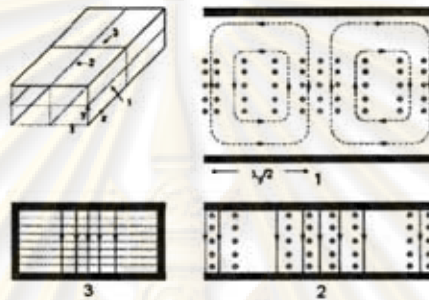
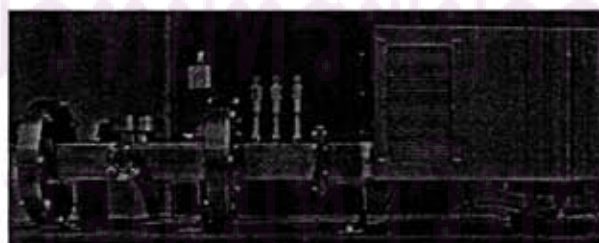


Figure 2.3 Electric and magnetic field lines for TE_{10} mode in a rectangular waveguide [42].

Furthermore, the wavelength within the waveguide (λ_g) also relates to the free space wavelength ($\lambda_0 = 121.6$ mm), by the relation [43];

$$\lambda_g = \frac{\lambda_0}{\sqrt{1 - (f_c/f)^2}}$$

For f_c of 1.72 GHz and f of 2.45 GHz, the value of λ_g becomes 170 mm. Rectangular waveguide is designed with the length of 685 mm, as shown in **Figure 2.4**.



Chamber 3-stub tuner Microwave generator

Figure 2.4 The photograph of microwave components.

2.1.3 Magnetron power supply

The circuit diagram consists of two main parts which are low and high voltage circuits (Figure 2.5). For the low voltage circuit, an applied voltage of around 3-4 V and a 10 A current would produce electrons around the cathode. The high voltage provides potential difference between the anode and the cathode of about 3000 V. This causes the electrons to blast off from the cathode and accelerate straight towards the anode. The potential difference between the anode and the cathode is adequate to generate a radiation of electromagnetic waves which are the output of the magnetron head. The power supply of this magnetron can be adjusted to the power in the range of 0-500 Watt.

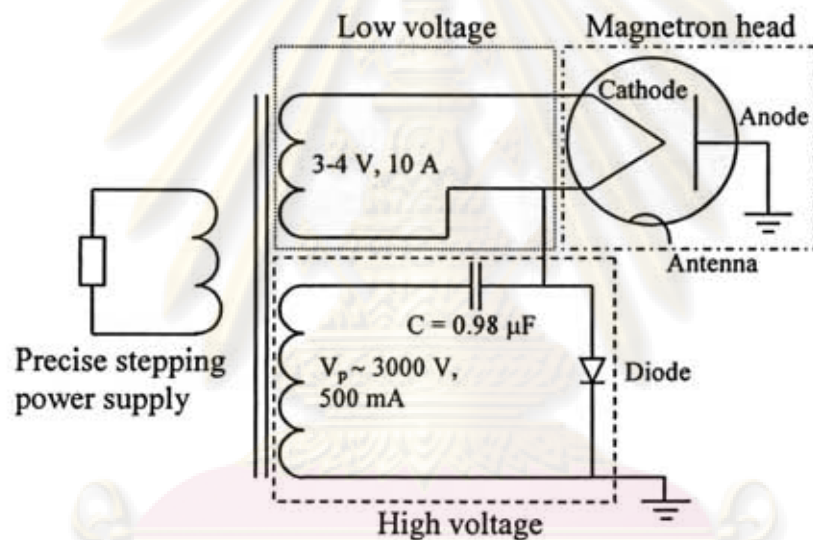


Figure 2.5 Circuit diagram of the voltage supplied to the magnetron head.

In this study, the microwave energy source (magnetron head) was taken from a Daewoo microwave oven. The magnetron head is shown in Figure 2.6.

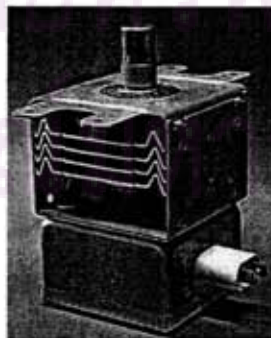


Figure 2.6 The magnetron head utilized in this study.

2.1.4 A matching network (3-stub tuner)

The role of a 3-stub tuner is to act as a matching network to minimize microwave reflection which causes damage to the magnetron head. Thus, 3-stub is necessary for an efficiency enhancement of a microwave transfer from the magnetron to the vacuum chamber. The micrometers apply to the part of 3-stub tuner which consist of three stubs were inserted to the waveguide. The distance of each stub is approximately 3 cm. The 3-stub was made from stainless steel and dimension is of the same as WR340 size which was joined with rectangular flanges cover as shown in **Figure 2.7**. The description of the flange cover is covered in **Appendix A.2**.

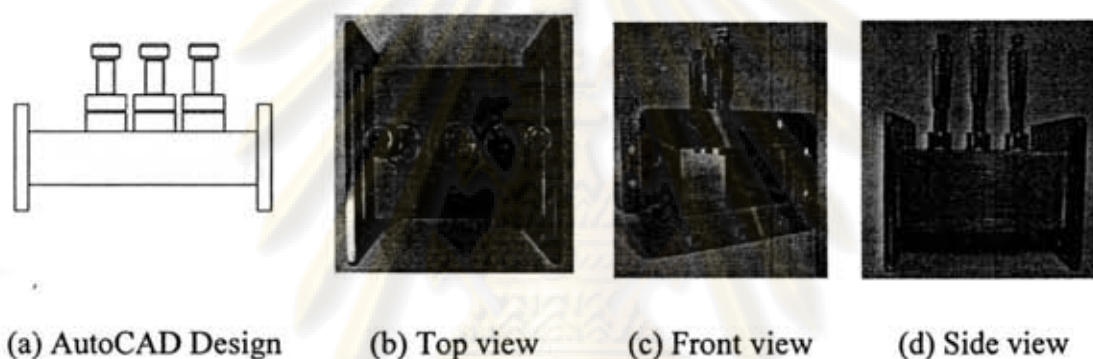


Figure 2.7 (a) The prototype of the 3-stub tuner and 3-stub tuner photographed from the (b) top, (c) front and (d) side views.

2.1.5 Monomer vessel

The compartments in which chemicals will be handled are composed of a monomer vessel and a cold trap (**Figures 2.8 and 2.9**).

The monomer vessel is consisting of the stainless steel (upper part) and borosilicate monomer container (lower part). The upper part consists of two ports. The top port designed to uptake a carrier gas feed, is connected with an argon cylinder. The bottom part is designed to contain a monomer. Argon as a carrier gas would be fed into the monomer container though the inner tube in order to purge the containing monomer vaporizing and flowing into the chamber.

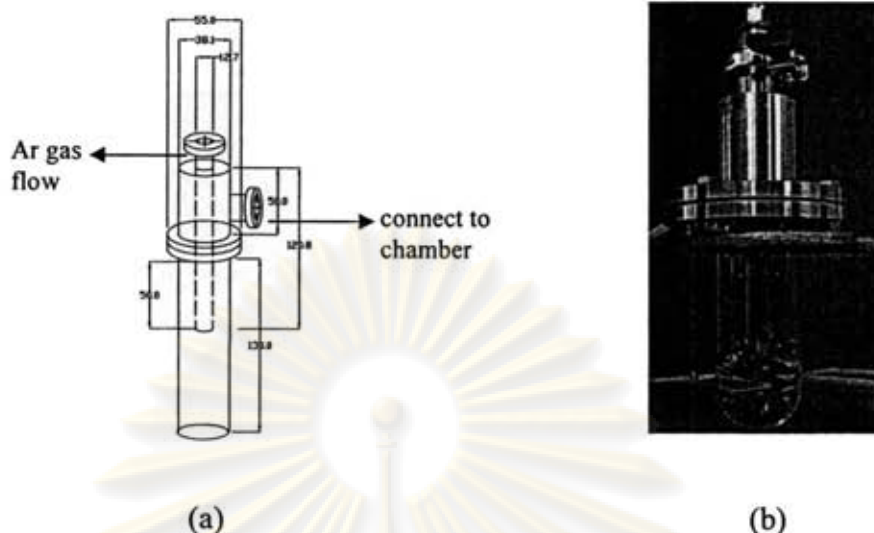


Figure 2.8 (a) The design of monomer vessel in millimeter unit and (b) the photograph of the monomer vessel.

2.1.6 Cold trap

The cold trap is a cylindrical stainless steel tube with a 114.3 mm diameter and a 290 mm length. The cold trap is also designed to accommodate a middle tube with a 76.2 mm diameter and a 235 mm length. In addition, an inner stainless steel tube of 21.6 mm diameter by 235 mm length has also been designed to connect with the reactor chamber using a NW 16 flange (Appendix A.1). This compartment is designed to collect any gas residue which would pass into the inner tube and condensed into a borosilicate receiver which uses dry ice and acetone as a coolant was covered the borosilicate receiver. The cold trap is used in conjunction with the rotary vane pump.

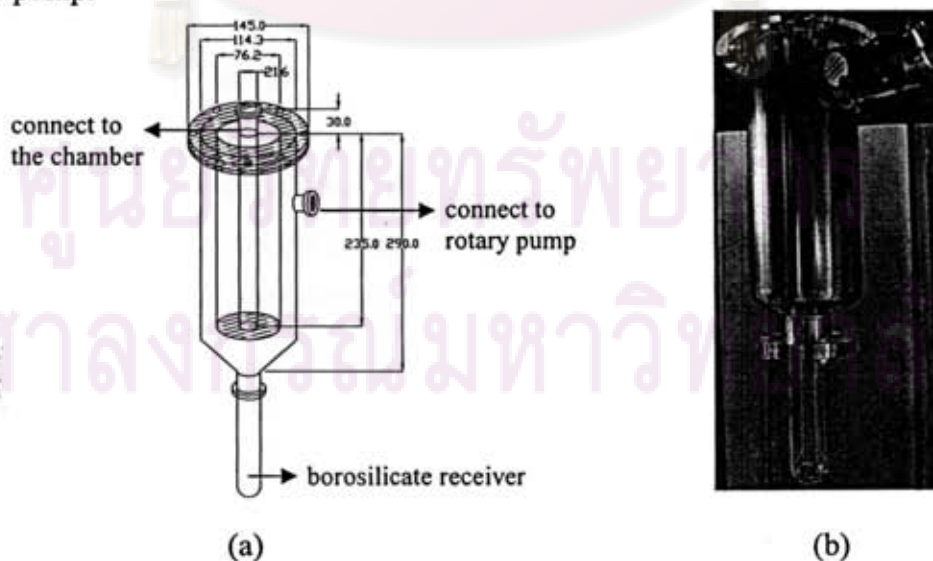


Figure 2.9 Illustration of the cold trap written with AutoCAD program. (millimeter unit) (a) and the cold trap used in this study (b).

The complete microwave plasma assembly was displayed in **Figure 2.10**.

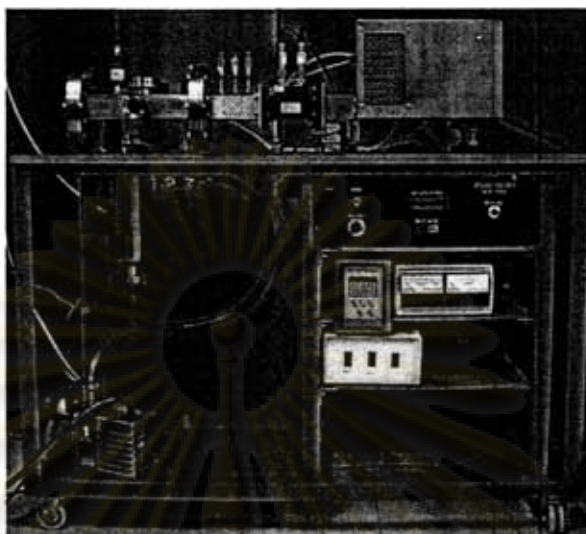


Figure 2.10 The photograph of microwave plasma system.

2.2 Testing of the microwave system

Test runs had been performed to verify if the system was ready to be utilized. Major concern included the following:

2.2.1 Testing of the assembly under vacuum

The entire microwave plasma reactor was assembled and tested for vacuum maintaining efficiency. The chamber was evacuated using a rotary pump until the chamber pressure approached a relatively constant value. The base pressure was determined to be approximately 2×10^{-2} torr. In general this base pressure can be reached within 60 minutes. A relationship between the pressure (torr) as a function of evacuation time (min) was plotted as illustrated in **Figure 2.11 (a)**. After the base pressure had been achieved, the valve to the pump was closed and the assembly was tested for the ability to hold a vacuum. Again, a relationship between the pressure (torr) as a function of evacuation time (min) was plotted the slope of which (shown in **Figure 2.11 (b)**) is an increase ratio of pressure with respect to time (approximately 0.0022 torr/min). It is indicated that air leakage into the chamber within 1 min is less than 0.3% when compared with pressure of 1 torr. This proved that the system pressure was appropriate for the plasma technology which, in general, is in the pressure range of about 25 torr to 1×10^{-3} torr [44]. Attempts have been made to ensure that this can be reproduced when the reactor is in operation.

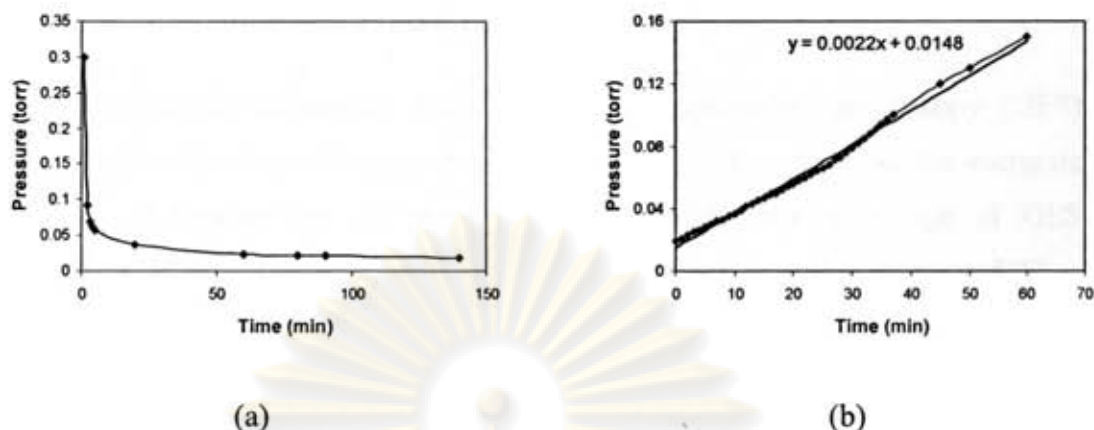


Figure 2.11 The graph of the decrease pressure (a) and increase pressure (b) versus time.

2.2.2 Testing of chemical recovery by cold trapping

The cold trap is a stainless steel cylinder which has a smaller internal stainless steel tube connected to the chamber. All excess vapor content from the reactor chamber was passed through the trap by means of a rotary pump. The trap was designed to let the residues pass through the inside tube (region I) and condense with cooling (region II, shaded) and collected in a borosilicate receiver (**Figure 2.12**). In order to check for trapping efficiency, thiophene monomer was evaporated into the chamber without a microwave transport and cooling system was applied.

It was found that efficient trapping of all vapor content from the chamber outlet was achieved when adequate cooling with dry ice/acetone was applied in region III. Without a microwave discharge, a quantitative amount of the monomer which was purged through the chamber with Ar carrier gas was recovered.

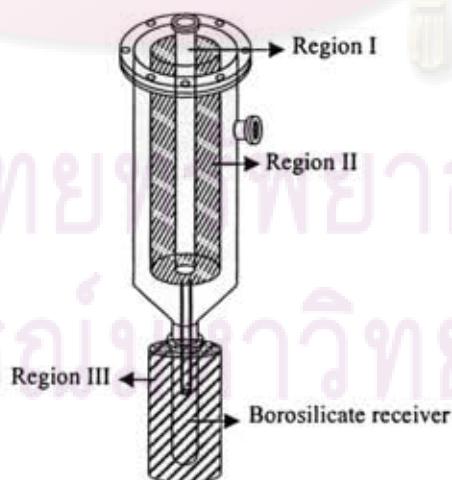


Figure 2.12 The dry ice and acetone in region III for the cold trap.

2.2.3 Determination of plasma temperature

The plasma diagnostics techniques, optical emission spectroscopy (OES) allows an identification of reactive species and gives information on the energetic properties of plasma and on plasma processes. The main advantage of OES comparing to other plasma diagnostics techniques is its non-intrusive character [45].

In the measurement step, at the beginning, the chamber was evacuated with a rotary pump to the base pressure of around 0.03 torr. Then an argon flow was introduced into the chamber to provide the desired pressure. Subsequently, the input power was supplied to the magnetron in order to generate a microwave which was then transmitted through the waveguide to produce plasma glow discharge in the chamber. During the time of plasma glow the plasma illuminated in a violetish pale blue color. Characterization of plasma phase was analyzed by OES. An HR4000 spectrophotometer including an OOIBase 32 software program was employed in the OES. Spectra were recorded from 300 to 1100 nm at 0.75 torr with an input microwave power of 250 watt and an argon flow rate of 10 sccm (mL/min). The measuring probe was placed at the outside of the chamber. The plasma discharge could be observed through a glass window on the side of the chamber (**Figure 2.13**).



Figure 2.13 Position of OES probe during plasma temperature measurement.

In the OES spectrum depicted in **Figure 2.14**, most of the Ar I peaks were observed in the range of 720-950 nm. The emission spectra data of argon were obtained from NIST Atomic Spectra Database [46]. **Table 2.1** lists the spectroscopic data needed for the thirteen argon transition used in this work. From the OES result, a graph between ratio of Ar II peak intensity to that of Ar I vs. electron temperature in accordance with Boltzmann equation (2) [47] was plotted. From the intensity ratio of

Ar II (at 387.45 nm) and Ar I (at 750.13 nm) it can be seen that both regions of the spectrum have a high transition probability. The electron temperature (T_e) can then be determined from the graph to be approximately 1.62 eV as shown in **Figure 2.15**.

$$R = \frac{I_2}{I_1} = \left(\frac{A_2}{A_1}\right)\left(\frac{g_2}{g_1}\right)\left(\frac{\lambda_1}{\lambda_2}\right) \cdot \exp(-(E_2 - E_1)/kT_e) \quad (2)$$

When A_i = Transition probability line i

g_i = Statistical weight line i

λ_i = wavelength line i

E_i = Energy level line i

T_e = Electron temperature

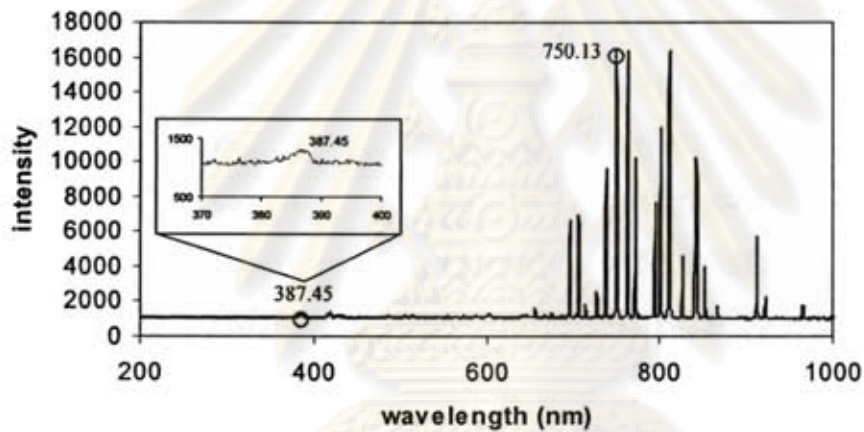


Figure 2.14 OES spectra of argon plasma at 0.75 torr.

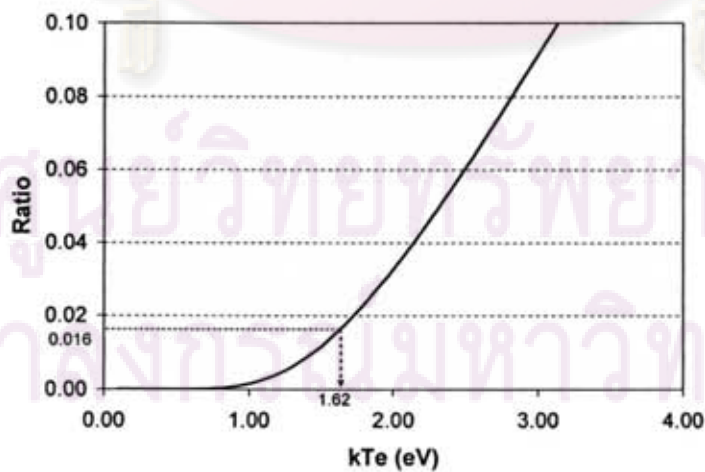


Figure 2.15 The peak intensity ratio versus electron temperature.

Table 2.1 Argon spectroscopic data.

| Spectrum | Wavelength (nm) | A_i (s^{-1}) | E_i (cm^{-1}) | g_i |
|----------|-----------------|--------------------|---------------------|-------|
| Ar II | 387.45 | 8.2×10^6 | 158428.1087 | 2 |
| Ar I | 696.52 | 6.39×10^6 | 107496.4166 | 3 |
| Ar I | 738.28 | 8.47×10^6 | 107289.7001 | 5 |
| Ar I | 750.13 | 4.45×10^7 | 108722.6144 | 1 |
| Ar I | 763.47 | 2.45×10^7 | 106237.5518 | 5 |
| Ar I | 772.27 | 5.18×10^6 | 106087.2598 | 3 |
| Ar I | 794.59 | 1.86×10^7 | 107131.7086 | 3 |
| Ar I | 811.84 | 3.31×10^7 | 105462.7596 | 7 |
| Ar I | 826.20 | 1.53×10^7 | 107496.4166 | 3 |
| Ar I | 842.25 | 2.15×10^7 | 105617.27 | 5 |
| Ar I | 851.94 | 1.39×10^7 | 107131.7086 | 3 |
| Ar I | 867.08 | 2.43×10^7 | 106087.2598 | 3 |
| Ar I | 912.04 | 1.89×10^7 | 104102.0990 | 3 |
| Ar I | 922.37 | 5.03×10^6 | 106237.5518 | 5 |
| Ar I | 965.76 | 5.43×10^6 | 104102.0990 | 3 |

ศูนย์วิทยทรัพยากร
จุฬาลงกรณ์มหาวิทยาลัย

CHAPTER III

FABRICATION OF POLYTHIOPHENE FILMS

3.1 Experimental section

3.1.1 Chemicals

Chemical used in this research were purchased from the following vendors. Reagent grade chemicals were used without purification prior to use. Commercial grade solvents were distilled before use.

1. Thiophene (purity $\geq 98\%$) : SIGMA-ALDRICH
2. Iodine (pro analysis) : MERCK
3. Acetone (commercial grade) : ZEN POINT
4. Methanol (commercial grade) : CTL
5. Argon gas (Ultra high purity grade) : TIG

3.1.2 Instruments

Fabricated polythiophene films were analyzed with the following equipment. Characterization details are described in section 3.1.7.

3.1.2.1 Attenuated Total Reflection Fourier Transform Spectroscopy (ATR FT-IR): NICOLET 6700 FT-IR spectrometer

Thermo Corporation connected with Continuum infrared microscope

3.1.2.2 UV-Visible absorption: SHIMADZU, UV-2250

3.1.2.3 Scanning Electron Microscope (SEM): JEOL, JSM-6480LV

3.1.2.4 Energy-dispersive X-ray spectroscopy (EDS): OXFORD, INCAX-sight 7573

3.1.2.5 Electric conductivity: HP 4140B pA meter / DC voltage source

3.1.3 Preparation of glass substrates

Prior to a plasma polymerization process, preparation of glass substrates need to be carried out. Glass substrates ($1.2 \times 2.5 \text{ cm}^2$) were first cleaned by acetone, methanol and deionized water in an ultrasonic bath for 5 minutes. And then the clean substrates are dried in an oven (100°C) for 2 minutes then transferred to be stored in a desiccator ready for use. Substrates for preliminary experiments carried out to determine optimum condition of the process were used as such.

Glass substrates which will be used in a fabrication process where electrical conductivity of the film would be measured are required to be treated by the following method prior to film fabrication. In order for the electrical conductivity of the film to be determined by the 2-point probe measurement, two copper electrodes had to be fabricated on each end of the glass substrates. This was conducted using a DC sputtering method operated at 0.004 torr, 45 W, and 15 min to afford coated copper electrodes with the size of $0.6 \times 1.2 \text{ cm}^2$. After polythiophene film deposition (*vide infra*), a sample would appear as shown in **Figure 3.1**.

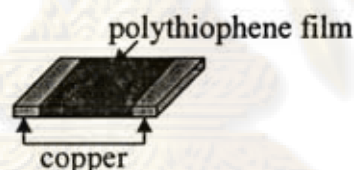


Figure 3.1 The substrate preparation for measurement of electrical conductivity.

3.1.4 Plasma polymerization of polythiophene

At the beginning, the clean glass substrates were placed in the chamber. Then the system was evacuated to the base pressure of around 0.03-0.05 torr and argon gas was introduced into the chamber for plasma pre-treatment process which was ongoing for 1 minute. In this pre-treatment step, the flow rate of argon gas was fixed at 5 sccm, the pressure at 0.75 torr and the microwave power at 200 W. After the pre-treatment, the chamber was evacuated again. Argon was bubbled through a monomer vessel at room temperature. Argon was used as a carrier gas to transport the thiophene vapor into the chamber. The argon gas flow rate and pressure of the system were kept at the same conditions in all experiments. Plasma-polymerized films were fabricated under various microwave power (150-300 W) and the polymerization times were 1-2 min while a constant pressure of 2.5 torr was used. The syntheses of plasma polymerized

polythiophene were carried out in two series. In the first series, the reaction time of 1 minute was used. In the other series, the reaction time of 2 minutes was used. In each series, microwave power of 150, 200, 250, and 300 W were utilized. For each reaction condition, for example at 150 W and 1 minute, experiments were carried out in duplicate. Therefore, 8 samples were obtained in each series and a total of 16 samples were subsequently analyzed. After the experiments were complete, glass substrates fabricated with polythiophene were analyzed with various methods described in section 3.1.7.

3.1.5 Plasma polymerization of polythiophene and *in situ* doping with iodine

In doping method, iodine crystals were placed on a glass slide and then placed into the chamber. The vacuum was applied to the system. As a consequence, iodine started to sublime more rapidly to generate a purple vapor all over the chamber. Subsequently thiophene monomer purged with argon gas was fed into the chamber. Then microwave discharge was applied to generate plasma. At the same time, OES technique was carried out to analyze the plasma phase to verify that iodine species were present. The measuring probe was placed at the outside glass window of the chamber at which the plasma discharge can be seen. The plasma polymerized films were produced at the microwave power of 250 and 300 W, the polymerization times were 1 and 2 min the chamber pressure during film growing was maintained at approximately 3.5 torr. The *in situ* doping plasma polymerized polythiophene were carried out in two series. In the first series, the reaction time of 1 minute was used. In the other series, the reaction time of 2 minutes was used. In each series, microwave power of 250 and 300 W were utilized. For each reaction condition, for example at 250 W and 1 minute, experiments were carried out in duplicate. Therefore, 4 samples were obtained in each series and a total of 8 samples were subsequently analyzed. Glass substrates fabricated with I₂ doped polythiophene were analyzed with various methods described in section 3.1.7.

3.1.6 Chemical synthesis of polythiophene

Thiophene monomer (3 mmol) was dissolved in 5 mL of dichloromethane. The solution was slowly added into a stirred suspension of 4 mmol of anhydrous ferric chloride in 5 mL of dichloromethane. When the addition was complete, the mixture was stirred for an additional 6 hours at 0 °C. After the reaction mixture was allowed to warm to room temperature and stirred overnight for 18 hours. The precipitate was filtered and rinsed with methanol until the washed solution was colorless. The remaining ferric chloride in the precipitate was extracted out by Soxhlet extraction with methanol for 24 hours.

3.1.7 Characterization of plasma-polymerized polythiophene

The obtained films were subjected to thorough analyses by the following methods:

3.1.7.1 Attenuated Total Reflection Fourier Transform Infrared (ATR FT-IR) Spectroscopy

ATR FT-IR investigates functional groups as well as structural relationships in films and the chemical states. The ATR spectra of polythiophene films deposited on glass substrate were recorded using Continuum infrared microscope attached to the Nicolet 6700 FT-IR spectrometer. The spectra were detected in the range of 750 - 4000 cm^{-1} . The plasma-polymerized polythiophene was scraped from substrate and then ground with a mortar before characterization.

3.1.7.2 Solid-state UV-Visible Spectroscopy

The UV-Visible absorption spectra were obtained using a Shimadzu, UV-2250 spectrophotometer. Barium sulfate (BaSO_4) was used as a reference. The spectra were scanned in the range of 200 - 800 nm.

3.1.6.3 Scanning Electron Microscopy (SEM)

Surface morphology and film thickness were investigated using a JEOL, JSM-6480LV scanning electron microscope. A cross sectional mode was used

in the thickness measurement and each value reported herein was an average of five readings.

3.1.6.4 Energy-dispersive X-ray spectroscopy (EDS)

EDS is an analytical technique used for elemental analysis of samples. The technique utilizes x-rays that are emitted from the sample during bombardment by an electron beam to characterize the elemental composition of the analyzed volume. This study was performed on an OXFORD, INCAX-sight 7573. For quantitative analysis, samples were scanned at the 3000 \times magnification in an area-averaged mode. All measured data are reported in **Appendix B**.

3.1.6.5 Electrical conductivity measurements

The electric conductivity was measured through using a two-probe. The current (I) was measured as a function of the applied voltage (V) from 0 to 100 V using HP 4140B pA meter / DC voltage source, including Lab View program. The conductivity of each sample was measured in triplicate and the average value was reported herein. All conductivity data are reported in **Appendix C**.

3.2 Results and discussions

3.2.1 Microwave plasma polymerization of thiophene

In general, fabricated undoped polythiophene films by microwave plasma polymerization were obtained as light-brown to black films on the glass slide substrates (**Figure 3.2**). It was found that the color of the films became more intense in color when an increasing power and polymerization time were employed. During optimization to determine appropriate range of microwave power, it was found that power between 150-300 W was suitable. Therefore, samples were produced at 150, 200, 250 and 300 W in all cases.

Preliminary investigation showed that a great deal of heat was generated when prolonged reaction time was used. It was cautioned that this may lead to decomposition of film already deposited. Furthermore, it was envisaged that a lifetime of the reactor could be shortened. Therefore, polymerization time of 1 and 2

minutes were used. These time period were proven to be optimal since an adequate amount of good quality material was afforded for characterization.

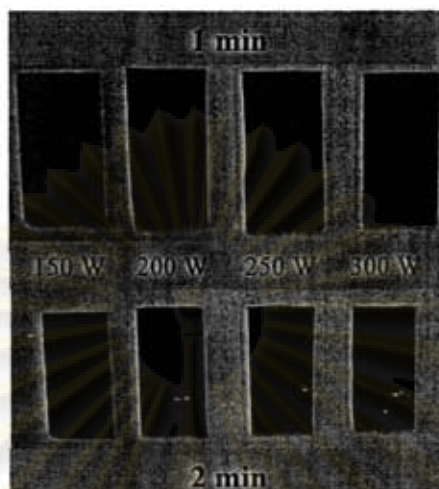


Figure 3.2 Example of polythiophene films by microwave plasma polymerization.

3.2.2 Characterization of plasma-polymerized polythiophene

3.2.2.1 Functional groups and chemical characteristics

ATR FT-IR spectroscopic analysis was performed on the microwave plasma polythiophene films in order to determine important functional groups present in the material. Representative spectra obtained from films grown at 150, 200, 250, and 300 W are presented in **Figure 3.3**.

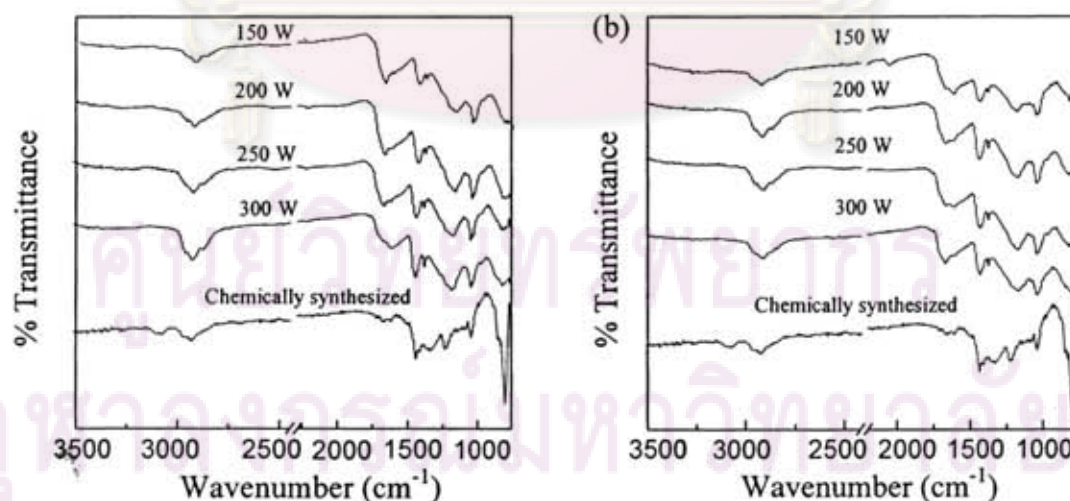


Figure 3.3 ATR FT-IR spectra of chemically-synthesized, plasma-polymerized polythiophene at different MW power and polymerization time (a) 1 min, (b) 2 min.

A spectrum from chemically-synthesized polythiophene obtained by conventional solution polymerization was also included for comparison. The transmittance spectra exhibit the following characteristic peaks: aromatic or olefinic =C-H stretching at around 3084 cm^{-1} ; -C-H stretching around 2924 cm^{-1} ; symmetric C=C stretching mode around 1450 cm^{-1} ; C-C stretching of the thiophene rings around 1370 cm^{-1} ; =C-H bending around 1046 cm^{-1} and C-S stretching around 795 cm^{-1} . The data are summarized again in **Table 3.1**

Table 3.1 ATR FT-IR band assignments of chemically-synthesized polythiophene and plasma-polymerized polythiophene.

| Assignments | Wavenumber (cm^{-1}) | |
|-----------------------------|--------------------------------------|----------------------------------|
| | Chemically-synthesized polythiophene | Plasma-polymerized polythiophene |
| aromatic or =C-H stretching | 3084 | weakened & broadened |
| aliphatic C-H stretching | 2924 | 2914 |
| C=C alkene stretching | - | 1660 |
| C=C ring stretching | 1440, 1330 | 1427, 1370 |
| C-C stretching | 1230 | 1170 |
| C-H aromatic bending | 1046 | 1046 |
| C-S stretching | 795 | 817 |

In general, observed peaks of the films are broader than that of chemically-synthesized polythiophene. This is consistent with amorphous structure of the plasma polymerized material. Since numerous different fragments, radicals, ions, *etc.* are generated in the plasma process due to its high energy, a high degree of crosslinking would take place. It is not surprising to observe that in the spectra of plasma polythiophene a =C-H stretching of the thiophene ring around 3080 cm^{-1} are weakened or in some case almost disappeared. In general, signals for sp^2 -C-H bond are already rather weak in nature. Amorphous structure of the plasma-polymerized polythiophene resulting from myriad structural differences would no doubt result in really weak signals. The previously non-existing wavenumber at 1660 cm^{-1} representing C=C stretching of alkene in the spectrum of the plasma-polymerized polythiophene is somewhat suggestive of fragmentation of thiophene ring. The most distinct feature in plasma polythiophene spectra is the weakened band at 817 cm^{-1}

assigned to the C-S stretching. This result also suggests a certain degree of thiophene ring fragmentation which is in good agreement with literature report [48]. Despite of some evidence for ring fragmentation, aromatic C=C stretching around 1427 and 1370 cm^{-1} confirm existence of cyclic structure. In addition, spectra in the fingerprint region still show relatively well maintained characteristics of the thiophene rings.

3.2.2.2 Film morphology

The morphology of the plasma-polymerized polythiophene films was observed by SEM analysis to be a globular structure under most conditions used. As the microwave power increased, the extended spherical agglomerate afforded smoother surface as shown in **Figure 3.4**. SEM analysis also revealed a relatively uniformly distributed deposition of the so-formed polymer films.

The thickness of plasma-polymerized polythiophene films is significantly affected by microwave power and polymerization time. The thickness ranges from 1.04-1.34 μm for plasma polymerization time 1 min. The thickness at 2 min ranges from 1.39-1.90 μm (**Table 3.2**). In addition, SEM cross-section realizes that plasma-polymerized polythiophene films are dense and pinhole-free as shown in **Figure 3.4** and **Figure 3.5**.

Table 3.2 Film thickness at various microwave power and polymerization time.

| MW Power (W) | Thickness (μm) | |
|-----------------|-----------------------------|-------|
| | 1 min | 2 min |
| 150 | 1.04 | 1.39 |
| 200 | 1.29 | 1.68 |
| 250 | 1.34 | 1.90 |
| 300 | 1.22 | 1.61 |

ศูนย์วิจัยเทคโนโลยี
จุฬาลงกรณ์มหาวิทยาลัย

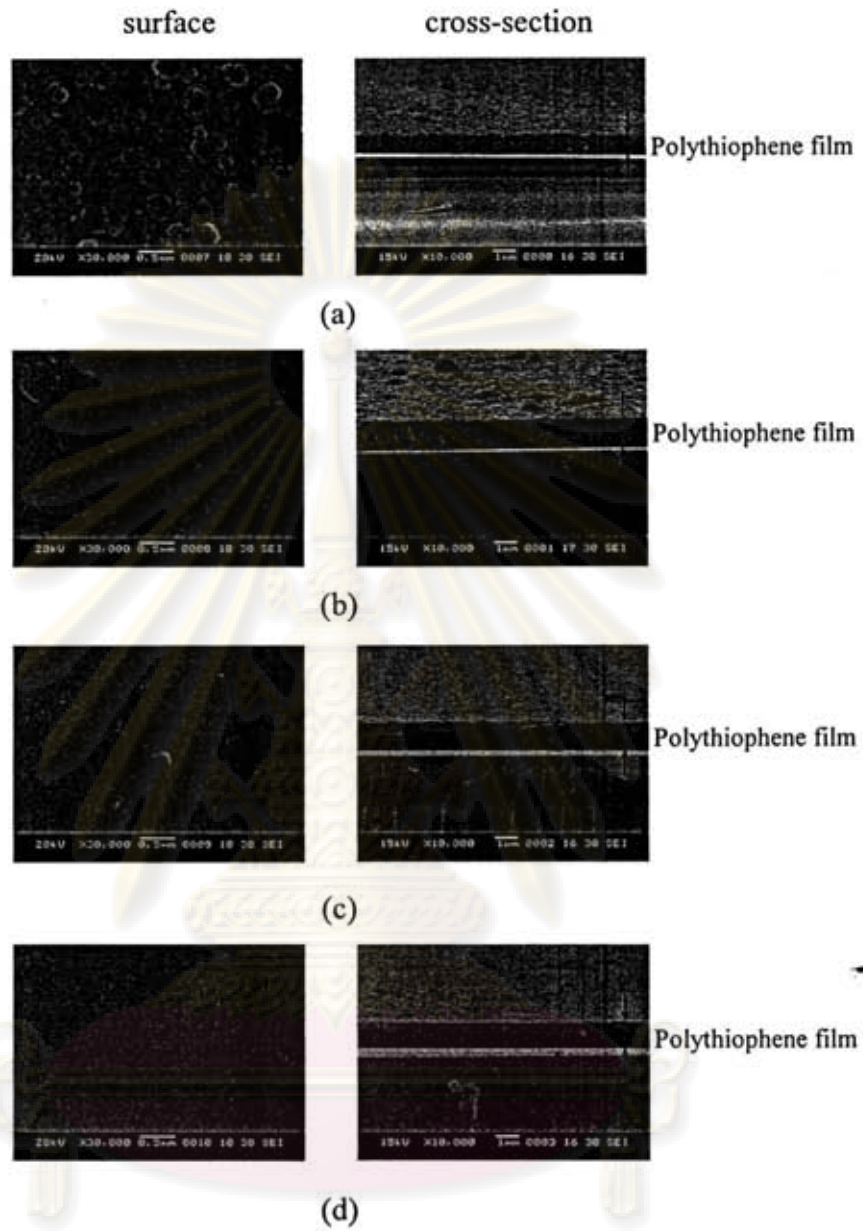


Figure 3.4 The surface morphology of plasma-polymerized polythiophene films on the glass substrate at 1 min and various microwave power (a) 150, (b) 200, (c) 250 and (d) 300 W.

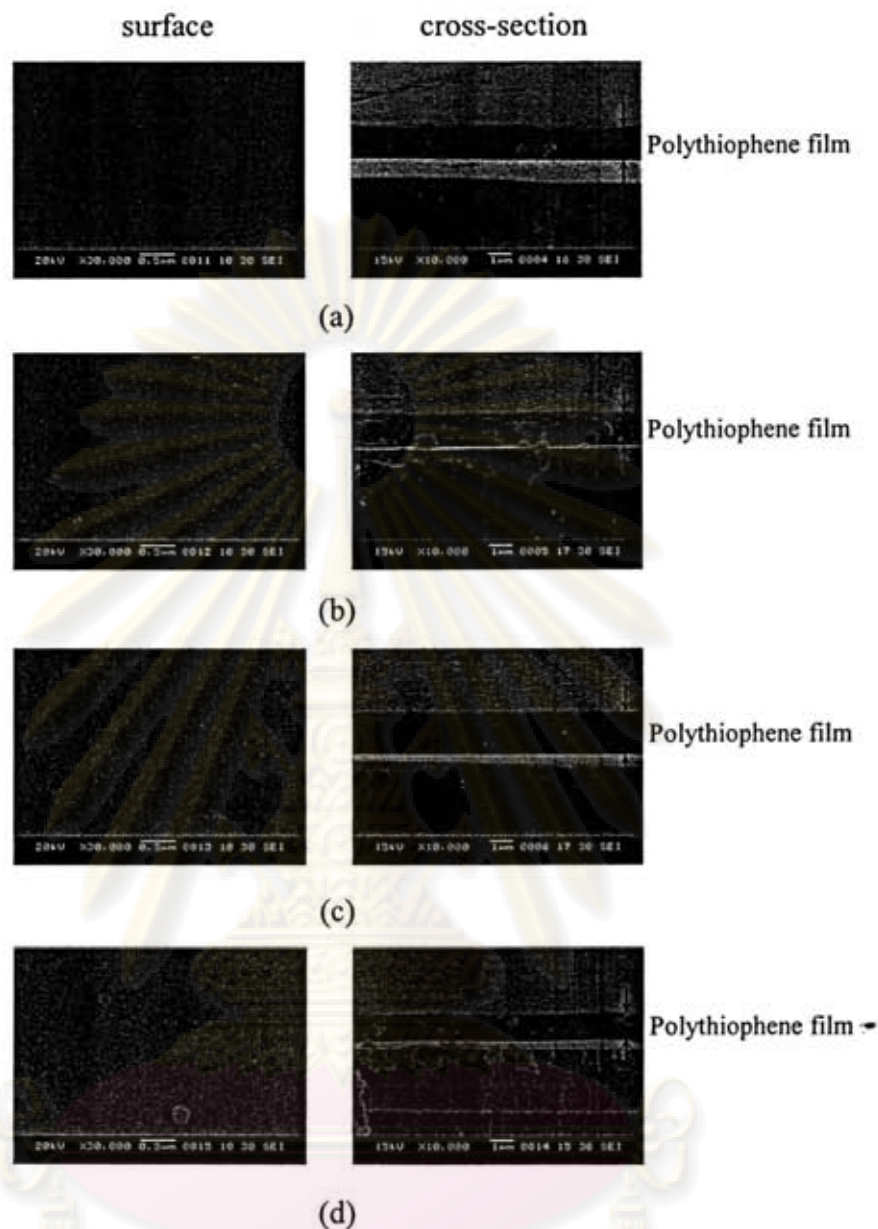


Figure 3.5 The surface morphology of plasma-polymerized polythiophene films on the glass substrate at 2 min and various microwave power (a) 150, (b) 200, (c) 250 and (d) 300 W.

3.2.2.3 Elemental composition of the films

Elemental analysis for sulfur content by conventional method was proven to be too costly at this stage. Alternatively, quantitative determination of elemental composition of materials by means of EDS analysis can serve as an acceptable preliminary substitute for such a purpose. Results from the elemental analysis of plasma-polymerized polythiophene as by EDS are shown in **Table 3.3** and raw data are tabulated in **Appendix B.1**.

In the chemically-synthesized polythiophene, the carbon to sulfur ratio of 4.6:1 was observed. This is not exactly consistent with theoretical value of 4:1. The elemental compositions of plasma-polymerized polythiophene were compared with the value from the chemically-synthesized polythiophene. In this case, a C/S ratio close to the chemically-synthesized would indicate that the plasma-polymerized polythiophene was not much damaged.

Table 3.3 The elemental composition of chemically-synthesized and plasma polymerized polythiophene.

| MW power (W) | Carbon content (%) | | Sulfur content (%) | | C/S | |
|------------------------|--------------------|-------|--------------------|-------|-------|-------|
| | 1 min | 2 min | 1 min | 2 min | 1 min | 2 min |
| 150 | 89.6 | 87.2 | 10.4 | 12.8 | 8.7 | 7.0 |
| 200 | 88.2 | 89.7 | 11.8 | 10.3 | 7.8 | 8.7 |
| 250 | 89.3 | 90.2 | 10.7 | 9.8 | 8.6 | 9.3 |
| 300 | 88.2 | 90.7 | 11.8 | 9.3 | 7.5 | 10.4 |
| Chemically-synthesized | 82.2 | | 17.8 | | 4.6 | |

However, from the data presented in **Table 3.3**, it can be clearly seen that most plasma-polymerized thiophene films have a C/S ratio higher than 4.6 ranging from approximately 7-10. This is suggestive of a decrease in sulfur content from the main structure of chemically-synthesized. It is noteworthy that as the microwave power increased, the C/S ratio is higher. This is highly possible since a more energetic plasma environment may be experienced by the existing film. Moreover, C-C and C=C bonds are stronger (290 and 720 kJ mol⁻¹, respectively) than the C-S bond (272 kJ mol⁻¹). The effect of the microwave power employed on the C/S ratio may be explained by the increase in electron density with increasing power input. At higher power input more electrons with adequate energy to break the C-S bond attack the already deposited polythiophene layer which resulted in a higher C/S ratio. Furthermore, the increase in electron density may result in an increase in the number of collisions between electrons and other plasma species [36]. The hydrogen content was not taken into account because EDS is unable to detect hydrogen. A relationship between microwave power utilized in the experiments and the C/S ratios are illustrated in **Figure 3.6**.

From the plot between microwave power and C/S ratio in **Figure 3.6** at polymerization time 2 min, a small trend can be observed that as the microwave power increased, the C/S ratio increased. At polymerization time 1 min, however, when the microwave power increased, the C/S ratio fluctuated.

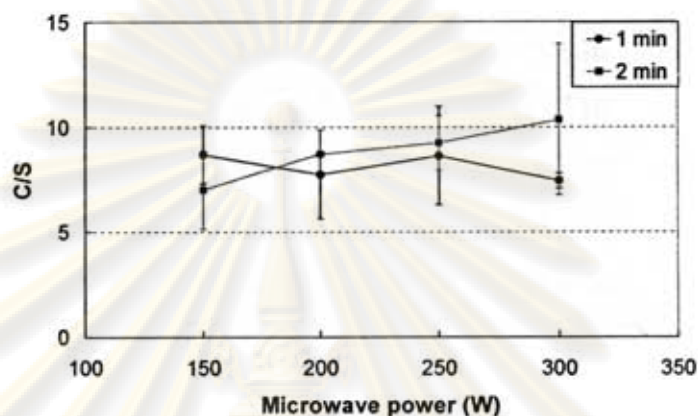


Figure 3.6 The microwave power versus C/S ratio.

3.2.2.4 Electrical conductivity

The conductivity of the plasma-polymerized polythiophene films deposited on glass slide were measured using a two-probe method. The I - V characteristics were measured between 0 to 100 V. The typical plot for current versus voltage is depicted in **Figure 3.7**. In this study I - V characteristic show linearity which obeys Ohmic's law.

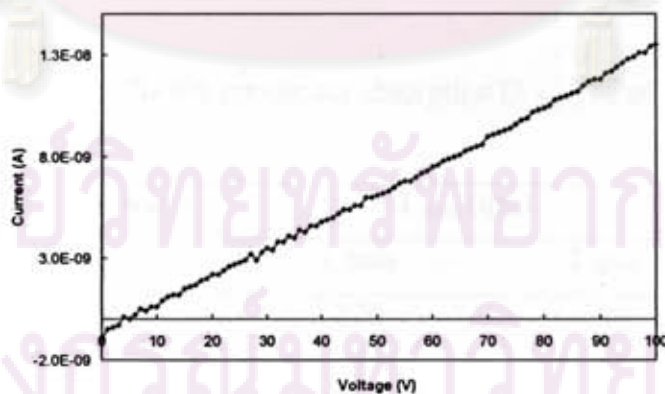


Figure 3.7 The plot of current versus voltage at room temperature.

Table 3.4 summarized conductivity of the fabricated films at various microwave powers at 1 and 2 minute reaction time. The conductivity of microwave plasma-polymerized polythiophene films is in the range of 5.4×10^{-7} to 1.9×10^{-6} S/cm.

Table 3.4 Electrical conductivity of microwave plasma-polymerized polythiophene.

| MW power (W) | Conductivity (S/cm) | |
|-----------------|----------------------|----------------------|
| | 1 min | 2 min |
| 150 | 1.4×10^{-6} | 9.3×10^{-7} |
| 200 | 1.9×10^{-6} | 6.9×10^{-7} |
| 250 | 5.8×10^{-7} | 6.3×10^{-7} |
| 300 | 1.5×10^{-6} | 5.4×10^{-7} |

3.2.2.5 Optical characteristics of the films

The UV-Vis maximum absorption of the plasma-polymerized films at different microwave power and polymerization time is summarized in **Table 3.5**. The UV-Vis spectra illustrated that the absorption maxima of polythiophene fabricated by plasma polymerization at 1 min (**Figure 3.8**) and 2 min reaction time (**Figure 3.9**) which were assigned to the $\pi-\pi^*$ transition were noticed at around 375-415 nm and 389-418 nm, respectively. A shift to a longer wavelength with an increasing microwave power was also observed. Furthermore, the broadening of absorption band was observed in a higher degree with an increase in the microwave power used.

Table 3.5 Conclusion of UV-Vis maximum absorption (λ_{max}) of plasma-polymerized polythiophene.

| MW power (W) | λ_{max} (nm) | |
|-----------------|----------------------|-------|
| | 1 min | 2 min |
| 150 | 376 | 389 |
| 200 | 374 | 397 |
| 250 | 398 | 406 |
| 300 | 415 | 418 |

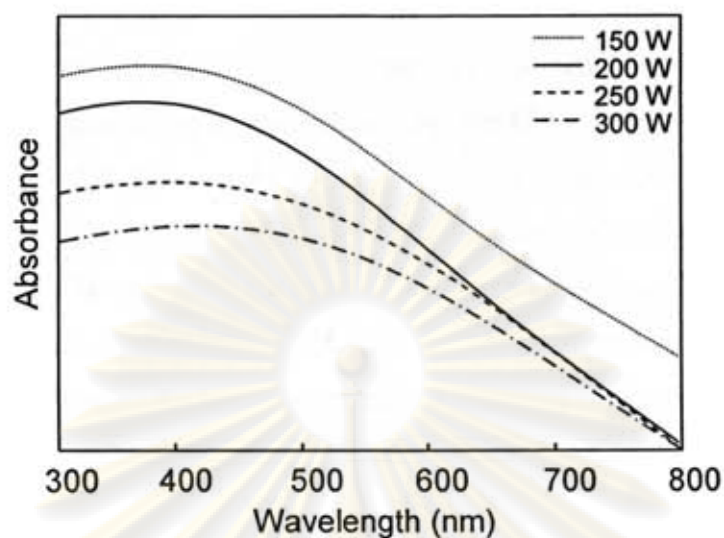


Figure 3.8 The UV-Vis absorbance spectra of plasma-polymerized polythiophene at different microwave power and polymerization time 1 min.

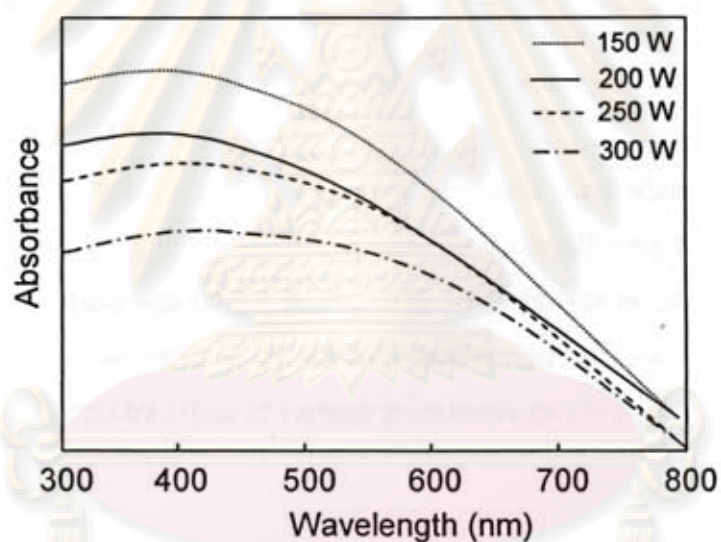


Figure 3.9 The UV-Vis absorbance spectra of plasma-polymerized polythiophene at different microwave power and polymerization time 2 min.

It has been shown here that as the microwave power increased, an absorption was observed at relatively longer wavelength. This is suggestive of a longer π -electron conjugation length in the plasma-polymerized polythiophene films and high degree of crosslinking which resulted in a red shift with microwave power increasing.

3.2.3 *In situ* doped polythiophene films

The purpose of this study is a part of an effort to increase electrical conductivity by incorporating dopant species into the films during fabrication process. It was envisaged that this means of doping would result in a higher and more sustainable electrical conductivity of the films. In this study, iodine was used as a dopant. Iodine has been one of the most studied doping agents in plasma polymers, due to its high electronegativity and high vapor pressure, which facilitates the introduction of its vapor into vacuum plasma reactors [49].

At the beginning, the doping method was carried out by feeding the monomer vapor and the iodine vapor into the vacuum chamber simultaneously through 2 separate gas inlets. Analysis of the films deposited on the glass substrates using this method showed only a trace amount of incorporated iodine. Attempts have been made to modify iodine pressure intake, as well as other parameters in order to improve the amount of iodine passing into the chamber. None was satisfactory. Therefore, an alternative method had been utilized.

This was performed by placing iodine crystals on a glass slide then placed inside the chamber. Sublimation of iodine was visible all over the chamber. When plasma-polymerization was taking place, OES analysis was performed to ensure the presence of iodine as well as to identify active iodine species involved in the experiments. OES spectra taken at various microwave powers are as shown in **Figure 3.10** and the position of iodine peaks (804.34, 885.64, 890.09, 902.18, 905.88, 911.30, 933.67 and 973.33) [46].

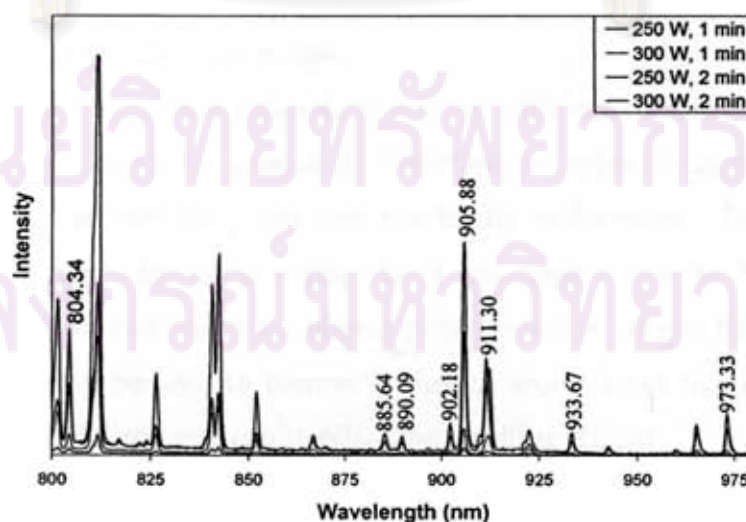


Figure 3.10 OES spectra of I₂ doped plasma-polymerized polythiophene.

The appearance of the film by this method ranged from a light brown to a dark brown color depending on the microwave power and the polymerization time used. In the doping studies, only the microwave power at 250 W and 300 W as well as polymerization time of 1 and 2 min were used. Attempts to utilize microwave power at 150 W and 200 W failed to generate plasma discharge. This was accounted for by the fact that while iodine was introduced in the chamber, the pressure of the system increased. As a result, higher microwave power must be applied in order to generate plasma.

3.2.4 Characterization of I₂-doped plasma-polymerized polythiophene

3.2.4.1 Functional groups and chemical characteristics

The ATR FT-IR spectra of I₂ doped polythiophene by microwave plasma polymerization are shown in Figure 3.11. As mentioned earlier that in the plasma process numerous different fragments, for instance radicals, ions, *etc.* could be generated, therefore complex chemical structures of plasma-polymerized polythiophene are not totally unforeseen. Moreover, many reactions with iodine may occur during the *in situ* doping process. This may also result in an even more amorphous structure of the films. Consequently, the ATR FT-IR spectra are broad. However, attempts are made here to identify some transmittance which might be suggestive of certain structural features related to incorporation of iodine in the films. For instance, an ATR FT-IR peak around 960 cm⁻¹, might be assigned to the C-I vibration. Furthermore, the new transmittance band around 1540-1590 cm⁻¹ may be described as -CH₂I or -CI=CH₂ groups.

In the plasma process, numerous different fragments, for instance radicals, ions, *etc.* could be generated. Therefore, complex chemical structures of plasma polymerized polythiophene are not totally unforeseen. Moreover, many reactions with iodine may occur during the *in situ* doping process. Iodine probably reacted with residual radicals in the plasma polymerized thiophene films. In addition, iodine radicals may be able to remove hydrogen atoms from thiophene structures because the aromatic structure can stabilize the resulting radical.

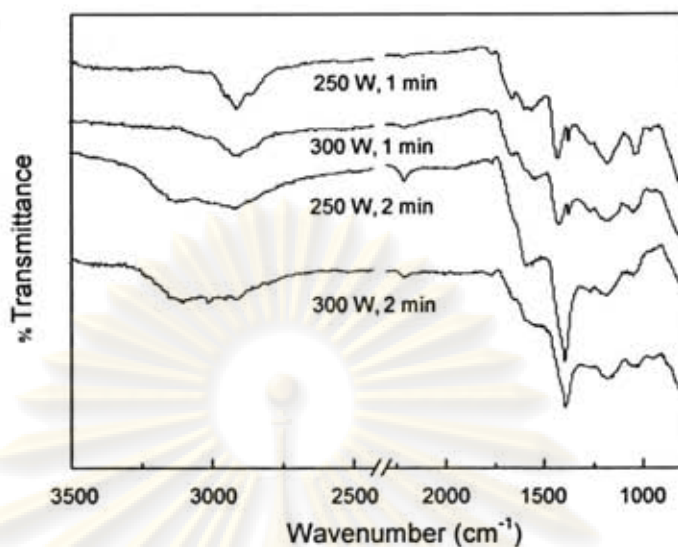
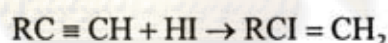
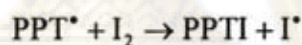


Figure 3.11 ATR FT-IR spectra of plasma-polymerized I₂ doped polythiophene.

Subsequently, the so-formed HI can react with C≡C as evident from a report by Groenewoud as shown in equations below. The radical on the thiophene structure can in its turn react with other iodine radicals to form mono-substituted thiophene, *etc.* [50].



3.2.4.2 Film morphology

The *in situ* I₂ doped polythiophene by microwave plasma polymerization were obtained as thinner films compared to those of the undoped polythiophene films. I₂ doped polythiophene films were found to be in the range of 100 nm to 1.50 μm thickness as determined by SEM analysis. The effects of microwave power and polymerization time on the morphology are shown in **Figure 3.12**. At higher the microwave power and longer polymerization time, a more globular particle and smoother surface were observed. At a 1 minute polymerization time a platelet structure was exhibit while at 2 minute polymerization time, the films appear to be increasingly a globular structure.

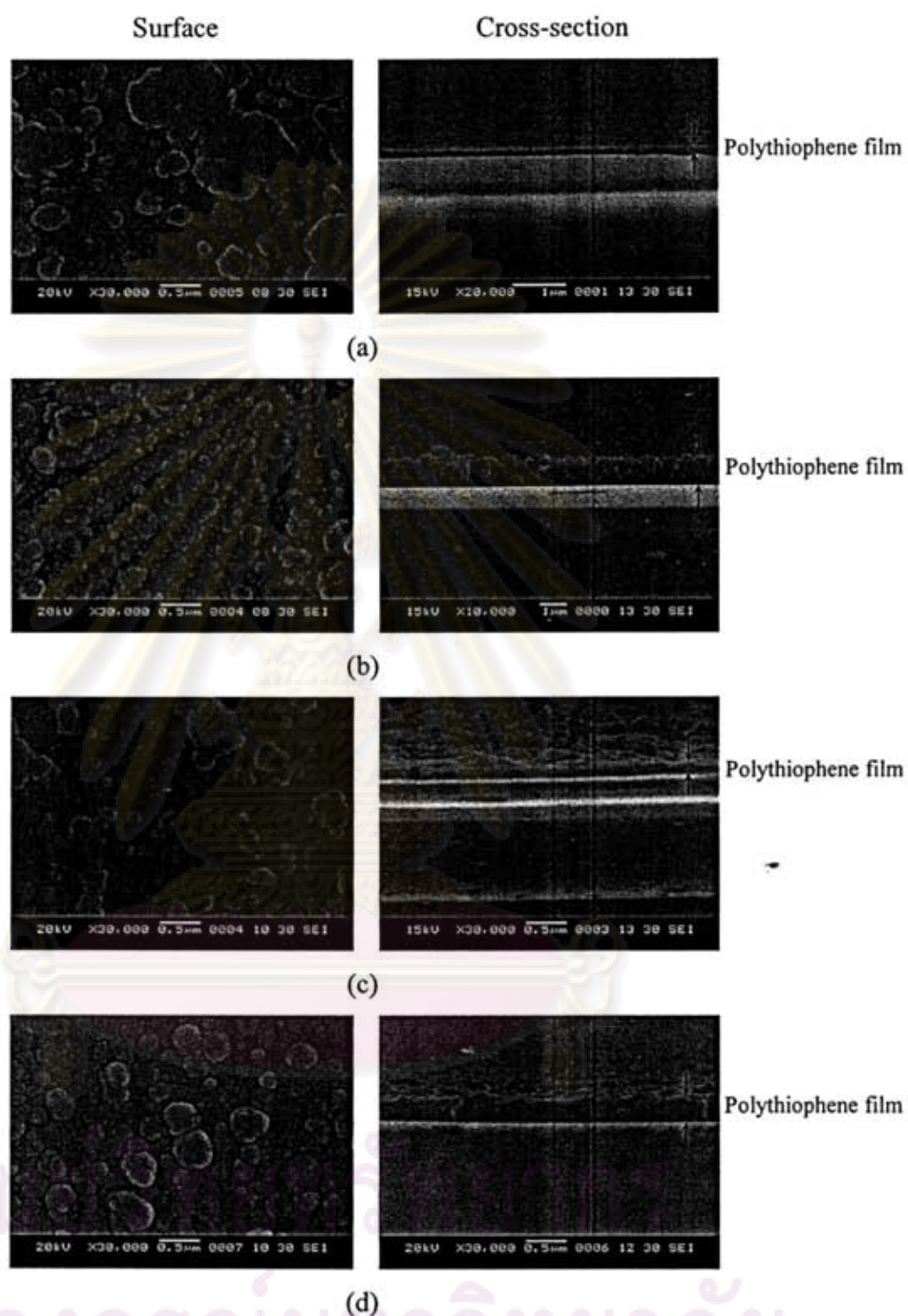


Figure 3.12 The SEM surface and cross-section of I₂-doped plasma-polymerized polythiophene (a) 250 W, 1 min, (b) 300 W, 1 min, (c) 250 W, 2 min, and (d) 300 W, 2 min.

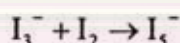
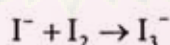
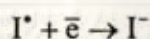
3.2.4.3 Elemental composition of the films

EDS characterization verified the presence of iodine in the *in situ*-doped films. The atomic percentage of iodine in these polythiophene ranged from 4.6 to 9.8 (Table 3.6). Raw data are presented in Appendix B.2.

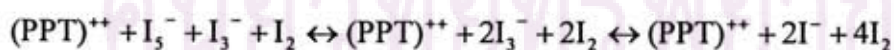
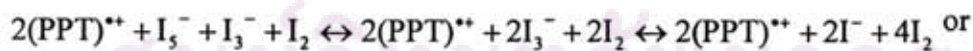
Table 3.6 Elemental composition of plasma polymerized I₂ doped polythiophene

| MW power (W) | Carbon content (%) | | Sulfur content (%) | | C/S | | Iodine content (%) | |
|-----------------|-----------------------|-------|-----------------------|-------|-------|-------|-----------------------|-------|
| | 1 min | 2 min | 1 min | 2 min | 1 min | 2 min | 1 min | 2 min |
| | 250 | 85.5 | 83.9 | 5.7 | 6.4 | 15.1 | 13.2 | 8.9 |
| 300 | 84.2 | 84.9 | 11.3 | 9.1 | 7.5 | 9.3 | 4.6 | 5.9 |

It was proposed by Groenewoud that when the iodine vapor suffers the plasma, iodine molecule is broken into iodine radicals. An iodine radical can then capture an electron from plasma environment resulting in the formation of monoiodine ion (I⁻). Even with the detection of the I⁻ ion, it was found that I₃⁻ and I₅⁻ are the most important forms [50].



The following equilibrium has been proposed for I₂-doped plasma-polymerized polythiophene [50]:



3.2.4.4 Optical characteristics of the films

The *in situ* I₂ doped polythiophene films by microwave plasma polymerization gave products that showed a maximum absorption around 439 to 535 nm as shown in Figure 3.13 and summarized in Table 3.7.

Table 3.7 Summation of UV-Vis maximum absorption (λ_{\max}) of *in situ* I₂ doped polythiophene.

| MW power (W) | λ_{\max} (nm) | |
|-----------------|-----------------------|-------|
| | 1 min | 2 min |
| 250 | 478 | 535 |
| 300 | 439 | 511 |

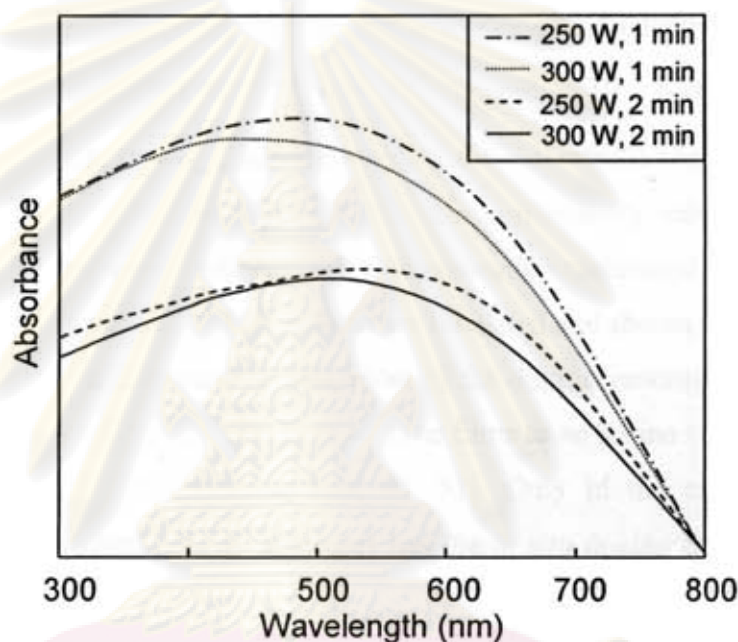


Figure 3.13 UV-Vis spectra of *in situ* I₂ doped plasma-polymerized polythiophene.

A red shift to a longer wavelength than those of undoped polythiophene (374 to 417 nm) were evident. This confirms the incorporation of iodine in the films. The shift of UV absorption is strongly suggestive of the formation of the (PPT)⁺I⁻ charge-transfer complex. Consequently, an enhanced electrical conductivity was also observed (*vide infra*).

3.2.4.5 Electrical conductivity

The conductivity of an *in situ* doped I₂ plasma polythiophene is summarized in **Table 3.8**.

Table 3.8 Electrical conductivity of I₂ doped plasma-polymerized polythiophene films.

| MW power (W) | Conductivity (S/cm) | |
|-----------------|----------------------|----------------------|
| | 1 min | 2 min |
| 250 | 1.0×10^{-4} | 4.6×10^{-5} |
| 300 | 1.8×10^{-5} | 1.4×10^{-5} |

It is evident that the measured values (1.4×10^{-5} to 1.0×10^{-4} S/cm) are upto three orders of magnitude higher than the usual range of conductivity of undoped plasma-polymerized polythiophene (5.4×10^{-7} to 1.9×10^{-6} S/cm). This result indicated that the *in situ* doping can indeed enhance the electrical conductivity of the films. For comparison purposes, reported electrical conductivity values of I₂-doped conventional chemically-synthesized, electrochemically-synthesized polythiophene and other plasma-polymerized polythiophene are tabulated and shown in **Table 3.9**.

From the literature reports, most of the doping processes were carried out after the synthesis of the films by exposing the films to an iodine vapor in a sealed container at various lengths of time [36, 48, 51]. Only in the case of plasma-polymerization of 2-iodothiophene monomer has the *in situ* doping been carried out. By this means of doping, the dopant element iodine was introduced directly with the monomer into the plasma process [32]. In general it can be seen that in the case of conventional electrochemical as well as chemically-polymerized film, after being doped initial electrical conductivity were exhibited. However, over a period of time, conductivities were reported to decrease to more or less a value of an undoped material.

In order to study and compare the difference in the lifetime of doped state of polythiophene obtained from different methods, the following experiments were carried out. Polythiophene films prepared by microwave plasma polymerization were doped by placing them in a sealed container containing iodine crystals for 24 hours (*ex situ*). Subsequently, the conductivity of these materials were determined by a two point probe method.

Table 3.9 Electrical conductivity of I₂-doped polythiophene by conventional synthetic and different plasma polymerization methods.

| Entry | Polymerization method | Doping method (Doping period) | Conductivity (S/cm) | Ref. |
|-------|-----------------------|--|--|----------|
| 1 | Electrochemical | I ₂ chamber, ^a (unspecified) | 1.5×10^1 | [30, 48] |
| 2 | Chemical | I ₂ chamber, ^a (unspecified) | 1.4×10^1 | [31] |
| 3 | AF-plasma | I ₂ chamber, ^a 5 h | 2.2×10^{-3} | [48] |
| 4 | RF-plasma | I ₂ chamber, ^a 5 h | 4.3×10^{-4} | [48] |
| 5 | MW-plasma | <i>in situ</i> doping ^b | 10^{-6} to 2.6×10^{-1} | [32] |
| 6 | Pulsed plasma | I ₂ chamber, ^a 5 min | 5.6×10^{-5} | [51] |
| 7 | Pulsed plasma | I ₂ chamber, ^a 5 min | 3×10^{-8} to 5×10^{-6} | [36] |

Remark: AF = Audio frequency, RF = Radio frequency, MW = Microwave

^a Preformed films were exposed to a saturated vapor of I₂ in a sealed container.

^b *in situ* doping by using an iodine containing monomer (2-iodothiophene) was performed.

The measurements revealed that these films exhibited conductivity in the range of 1.5×10^{-4} to 1.9×10^{-3} S/cm which are higher than *in situ* I₂ doped in this study (1.4×10^{-5} to 1.0×10^{-4} S/cm). After the doping process, the films were taken out of the chamber and were let stand in ambient atmosphere. Conductivity of the films was measured at intervals of time to determine the decreasing rate of conductivity. A relationship between standing time and conductivity was plotted as depicted in **Figure 3.14**. It was found that during the post-doping period, conductivity of the doped materials rapidly decreased to more or less that of undoped material in approximately 48 hours (2880 min).

The fast decay is not surprising since iodine could only be adsorbed mostly on the surface of the polythiophene films. This physical interaction is rather weak. As a result diffusion of the adsorbed iodine can occur over time.

จุฬาลงกรณ์มหาวิทยาลัย

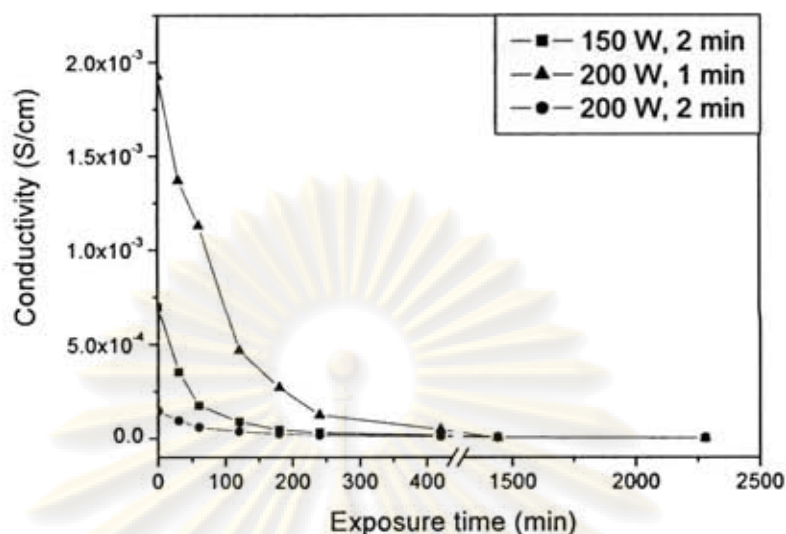


Figure 3.14 The conductivity of microwave plasma-polymerized polythiophene films and iodine *ex situ* doping as a function of exposure time.

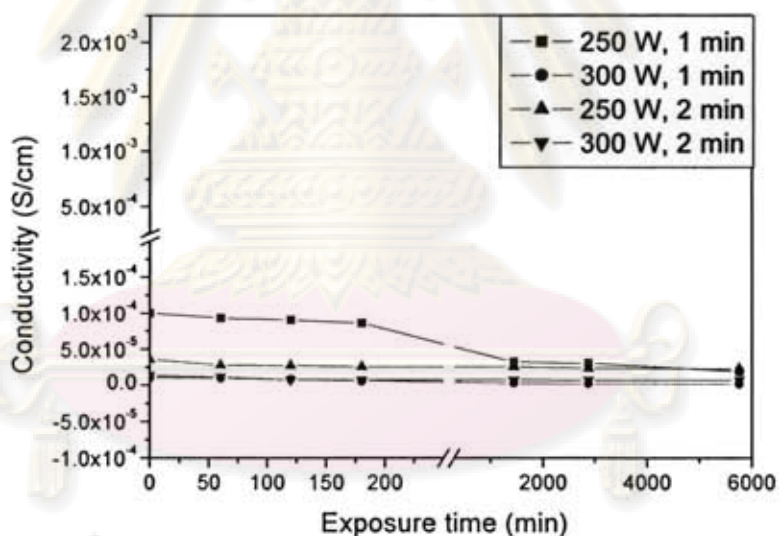


Figure 3.15 The conductivity of iodine doped microwave plasma-polymerized polythiophene (*in situ* doping) as a function of exposure time.

Determination of a decrease in film conductivity of the *in situ* doped plasma polymerized polythiophene was also carried out in a parallel fashion. Freshly fabricated *in situ*-doped films were also subjected to conductivity measurements at intervals of time. Film conductivity has been plotted as a function of time (**Figure 3.15**). Apparently, the films lost their conductivity in a longer period of time compared to the results obtained from traditional doping method. Therefore, the *in*

situ doping had presumably evenly distributed iodine dopant all over the entire bulk of the films [52]. It can be proven that *in situ* doping provides the increased conductivity and high stability for a long time.

Results presented thus far in this thesis have shown that microwave plasma polymerization process can be an efficient method for fabricating conducting polymer films. Future work may include optimization of reaction conditions, testing of other possible substances as dopants, modification of dopant introduction into the films, as well as finding good conditions to maintain conjugating system in the materials.



ศูนย์วิจัยทรัพยากร
จุฬาลงกรณ์มหาวิทยาลัย

CHAPTER IV

CONCLUSIONS

4.1 Conclusions

The home-made economical prototype microwave plasma system was designed and constructed for polythiophene synthesis. This system can be divided into two main parts; plasma part and chemical part. In the plasma part consisted of a vacuum chamber and a microwave generator. In addition, the system also consisted of a waveguide and a 3-stub tuner. The vacuum chamber was made from stainless steel with $86 \times 290 \times 43 \text{ mm}^3$ rectangular cavity. The waveguide and 3-stub tuner purpose that to transfer microwave and minimize microwave reflection or maximize the transfer of power, respectively. Another main part comprised of monomer vessel and cold trap. Liquid monomer was contained into monomer vessel which purges argon gas in order to carry monomer vapor into the chamber. The cold trap was used in conjunction with Edwards rotary vane pump to collect condensation produced from residue monomer. The optical emission spectroscopy (OES) technique determines electron temperature (T_e) in plasma reactor. It found that T_e of argon plasma is 1.62 eV at 0.75 torr, 250 W and argon flow rate 10 sccm.

The syntheses of polythiophene were varied the condition of pressure (150, 200, 250, and 300 W) and plasma polymerization time (1 and 2 min). The effect of microwave power was explained by the increase in electron density with increasing microwave power input which results in an increase in the number of collisions between electrons and other plasma species. And the using longer plasma polymerization time as though monomer vapor suffer plasma generated for a long time. It causes fragmentation. The effect of microwave power and plasma polymerization time on chemical structure, morphology, elemental composition, and electrical conductivity are summarized. The transmittance ATR FT-IR spectra at 3048 cm^{-1} are absent which represent $=\text{C-H}$ stretching and weaken the band at 817 cm^{-1} assigned to the $=\text{C-H}$ out-of-plane deformation. This result clearly indicates that the thiophene ring is destructed by plasma polymerization. The elemental compositions of

plasma polymerized thiophene have C/S ratio in the range 7.02 to 10.36 which higher than chemical synthesis (4.62). This result can also verify the thiophene structure was damaged. The result of elemental composition affect to the conductivity. The C/S ratio increase which the conductivity decrease. The electrical conductivity is range of 5.39×10^{-7} to 1.96×10^{-6} S/cm. It solid-state UV-Vis spectra showed an absorption maximum around 374 to 417.5 nm. In addition, the surface morphology of polythiophene is a globular structure. Besides, polythiophene films have a dense, pinhole-free film, and the thickness about 1.04 to 1.90 μm .

The *in situ* doping with iodine is to increase the electrical conductivity. This method feed monomer vapor and iodine vapor, which iodine crystal was placed inside the chamber, into the vacuum chamber. After, generate microwave plasma to deposit I₂ doped polythiophene on a glass slide substrate. From ATR FT-IR and EDS results indicated that iodine exists in the polythiophene films. Because the appearance of C-I at 805 cm^{-1} and $-\text{CH}_2\text{I}$ or $-\text{CI}=\text{CH}_2$ around $1540\text{-}1590 \text{ cm}^{-1}$. Moreover, the atomic percentage of iodine in I₂ doped polythiophene films is range of 4.58 to 9.75%. The I₂ doped polythiophene by microwave plasma polymerization gave products that showed λ_{max} around 439 to 511 nm. This *in situ* doping is successful at increasing the conductivity. These I₂ doped polythiophene are 4.64×10^{-5} to 1.02×10^{-4} S/cm, which were lower than plasma-polymerized films which were doped with conventional method (1.47×10^{-4} to 1.93×10^{-3} S/cm) even though thickness range of 100 nm to 1.50 μm . Furthermore, this *in situ* doping method is more stable than conventional doping (post doping with iodine for 24 hours).

4.2 Recommendations

Besides, the process parameters such as pressure, discharge power, flow rate of feed gases *et al.* can affect the elemental composition of material and fragmentation during deposition. For instance, the thiophene monomer structure with electron-donating substituents such as methyl groups was used as a monomer to minimize fragmentation during plasma polymerization, plasma-polymerized polythiophene from methylated thiophenes contained a high amount of conjugated structure. Consequently, after iodine doping a higher conductivity compared with non-substituted thiophene [51]. Thus, the chemical structure of monomer with substituents maybe used to minimize fragmentation. In the doping step, should modification of

dopant introduction into the films in order to increase electrical conductivity. In an earlier study, the use of plasma treatment technique after the doping process (*ex situ*) investigated for improving both the conductivity and stability of iodine doped [53]. This results maybe it is an alternative method for future work.



ศูนย์วิจัยทรัพยากร
จุฬาลงกรณ์มหาวิทยาลัย

REFERENCES

- [1] Saxena, V., and Malhotra, B.D. Prospects of conducting polymers in molecular electronics. **Curr. Appl. Phys.** 3 (2003): 293–305.
- [2] (a) Shirakawa, H., Louis, E.J., MacDiarmid, A.G., Chiang C.K., and Heeger A.J. Synthesis of electrically conducting organic polymers: halogen derivatives of polyacetylene, $(\text{CH})_x$. **J. Chem. Soc., Chem. Commun.** (1977): 578-580.
- (b) Park, Y.W., Druy, M. A., Chiang, C.K., MacDiarmid, A.G., and Heeger A.J. Anisotropic electrical conductivity of partially oriented polyacetylene. **J. Polym. Sci. Polym. Lett. Ed.** 17 (1979): 195-201.
- [3] MacDonald, R.N., and Campbell, J. The wittig reaction as a polymerization method. **J. Am. Chem. Soc.** 82 (1960): 4669-4671.
- [4] Shacklette, L.W., Elsenbaumer, R.L., Chance, R.R., Sowa, J.M., Ivory, D.M., Miller, G.G., and Baughman, R.H. Electrochemical doping of poly-(*p*-phenylene) with application to organic batteries. **J. Chem. Soc., Chem. Commun.** (1982): 361 – 362.
- [5] Pfluger, P., and Street, G.B. Chemical electronic and structural properties of conducting heterocyclic polymers: a view by XPS. **J. Chem. Phys.** 80 (1984): 544.
- [6] Shirakawa, H., MacDiarmid, A.G., and Heeger, A.J. **The Nobel Prize in chemistry, 2000: conductive polymers.** Available from: http://nobelprize.org/nobel_prizes/chemistry/laureates/2000/chemadv.pdf [2006, June 29]
- [7] Paushkin, Y.M., Vishnyakova, T.P., Lunin, A.F., and Nizova, S.A. **Organic polymeric semiconductors.** Halsted Press: Nazareth, 1974.
- [8] Guimard, N.K.; Gomez, N.; Schmidt, C.E. Conducting polymers in biomedical engineering. **Prog. Polym. Sci.** (32) 2007: 876-921.

- [9] Ziegler, C. **Thin Film Properties of Oligothiophenes**. John Wiley & Sons Ltd: Chichester, 1997.
- [10] Heeger, A.J. Semiconducting and Metallic Polymers: The Fourth Generation of Polymeric Materials. **J. Phys. Chem. B.** 105(36) 2001: 8475-8491.
- [11] Colin, P. **Conducting Polymers**. 1996. Available from: <http://homepage.ntlworld.com/colin.pratt/cpoly.pdf> [2006, June 29]
- [12] Nigrey, P.J., MacDiarmid, A.G., and Heeger, A.J. Electrochemistry of polyacetylene, $(CH)_x$: electrochemical doping of $(CH)_x$ films to the metallic state. **J. Chem. Soc., Chem. Commun.** 96 (1979): 594-595.
- [13] Nalwa, H.S. **Handbook of Organic Conductive Molecules and Polymers: Vol.3. Spectroscopy and Physical Properties**. John Wiley & Sons Ltd: Chichester, 1997.
- [14] Pomerantz, M., Tseng, J.J., Zhu, H., Sproull, S.J., Reynolds, J.R., Uitz, R., Arnott, H.J., and Haider, M.I. Processable polymers and copolymers of 3-alkylthiophenes and their blends. **Synth. Met.** 41 (1991): 825-830.
- [15] Nalwa, H.S. **Handbook of organic conductive molecules and polymers: vol.2. conductive polymers: synthesis and electrical properties**. John Wiley & Sons Ltd: Chichester, 1997.
- [16] McCullough, R. D., and Lowe, R. D. Enhanced electrical conductivity in regioselectively synthesized poly(3-alkylthiophenes). **J. Chem. Soc., Chem. Commun.** (1992): 70-72.
- [17] Chen, T. A., O'Brien, R. A., and Rieke, R. D. Use of highly reactive zinc leads to a new facile synthesis for polyarylenes. **Macromolecules** 26 (1993): 3462-3463.
- [18] Zhu, L., Wehmeyer, R. M., and Rieke, R. D. The direct formation of functionalized alkyl(aryl)zinc halides by oxidative addition of highly reactive zinc with organic halides and their reactions with acid chlorides,

alpha, beta-unsaturated ketones and allylic, aryl, and vinyl halides. **J. Org. Chem.** 56 (1991): 1445–1453.

- [19] Chen, T. A., and Rieke, R. D. The first regioregular head-to-tail poly(3-hexylthiophene-2,5-diyl) and a regiorandom isopolymer: nickel versus palladium catalysis of 2(5)-bromo-5(2)-(bromozincio)-3-hexylthiophene polymerization. **J. Am. Chem. Soc.** 114 (1992): 10087–10088.
- [20] Saxena, V., and Malhotra, B.D. Prospects of conducting polymers in molecular electronics. **Curr. Appl. Phys.** 3 (2003): 293–305.
- [21] Eliezer, S., and Eliezer, Y. **The fourth state of matter: an introduction to plasma science.** CRC Press: Cambridge, 2001.
- [22] Fitzpatrick, R. **Introduction to plasma physics: a graduate level course.** pp.10.
- [23] Denes, F.S., and Manolache, S. Macromolecular plasma-chemistry: an emerging field of polymer science. **Prog. Polym. Sci.** 29 (2004): 815–885.
- [24] Osada, Y. Plasma polymerization and plasma treatment of polymers. **Polymer Science U.S.S.R.** 30 (1988): 1922-1941.
- [25] Yasuda, H.K. Competitive ablation and polymerization (CAP) mechanisms of glow discharge polymerization. **American Chemical Society Symposium**, pp. 37-52. Washington, D.C., 1979.
- [26] Takeshi, S., and Tohru, T. **Method for plasma-initiated polymerization.** United States: Patent 4705612.
- [27] **Plasma polymerization pretreatment and finishing of polymer surfaces in the field of medical plastics.** EUROPLASMA, Oudenaarde (Belgium)
Available from: www.europlasma.be [2007, April 21]
- [28] Shi, F. F. Recent advances in polymer thin films prepared by plasma polymerization: synthesis, structural characterization, properties and applications. **Surf. Coating. Tech.** 82 (1996): 1-15.

- [29] Shen, M., and Bell, A.T. A review of recent advances in plasma polymerization. **American Chemical Society Symposium**, pp. 1-33. Washington, D.C., 1979.
- [30] Yasuda, H., and Hsu, T. Some aspects of plasma polymerization investigated by pulsed R.F. discharge. **J. Polymer Sci. Polymer Chem. Ed.** 15 (1977): 81-97.
- [31] Sadhir, R.K., and Schoch, K.F. Preparation and properties of plasma-polymerized thiophene (PPT) conducting films. **Thin Solid Films** 223 (1993): 154-160.
- [32] (a) Kruse, A., Baalman, A., Budden, W., and Schlett, V. Thin conductive coatings formed by plasma polymerization of 2-iodothiophene **Surf. Coat. Tech.** 59 (1993): 359-364.
- (b) Kruse, A., Schlett, V., Baalman, A., and Hennecke, M. Structural investigations of electrical conducting plasma polymerized films from 2-iodothiophene. **Fresenius J. Anal. Chem.** 346 (1993): 284-289.
- [33] Ryan, M. E., Hynes, A. M., Wheale, S. H., and Badyal, J. P. S. Plasma polymerization of 2-iodothiophene. **Chem. Mater.** 8 (1996): 916-921.
- [34] Bhat, N.V., and Wavhal, D.S. Preparation and characterization of plasma-polymerized thiophene films. **J. Appl. Polym. Sci.** 70 (1998): 203-209.
- [35] Kiesow, A., and Heilmann, A. Deposition and properties of plasma polymer films made from thiophenes. **Thin Solid Films** 343-344 (1999): 338-341.
- [36] Groenewoud, L. M. H., Engbers, G. H. M., Terlingen, J. G. A., Wormeester, H., and Feijen, J. Pulsed plasma polymerization of thiophene. **Langmuir** 16 (2000): 6278-6286.
- [37] Groenewoud, L.M.H., Weinbeck, A.E., Engbers, G.H.M., and Feijen, J. Effect of dopants on the transparency and stability of the conductivity of plasma polymerised thiophene layers. **Synth. Met.** 126 (2002): 143-149.

- [38] Wang, J., Neoh, K.G., and Kang, E.T. Comparative study of chemically synthesized and plasma polymerized pyrrole and thiophene thin films. **Thin Solid Films** 446 (2004): 205–217.
- [39] Correa, R., Gonzalez, G., and Dougar, V. Emulsion polymerization in a microwave reactor. **Polymer** 39 (1998): 1471-1474.
- [40] Blagojevic, V., and Murphy, V.M. Microwave polymerization of denture Base materials: a comparative study. **J. Oral Rehab.** 26 (1999): 804-808.
- [41] Collin, R. E. **Foundations for microwave engineering**. 2nd ed. Singapore: McGraw-Hill, Inc, 1992.
- [42] Pozar, D. M. **Microwave Engineering**. 2nd ed. USA: John Wiley & Sons, Inc., 1998.
- [43] Spanel, P., Hall, E. F. H., Workman, C.T., and Smith, D. A directly coupled monolithic rectangular resonator forming a robust microwave plasma ion source for SIFT-MS. **Plasma Sourc. Sci. Tech.** 13 (2004): 282-284.
- [44] Phongbandhu, S. **System Characteristic and parameters analysis of a vacuum system**. Department of Physics, Faculty of Science, Chulalongkorn University, 2004.
- [45] Jamroz, P., and Zyrmicki, W. Optical emission characteristics of glow discharge in the $N_2-H_2-Sn(CH_3)_4$ and $N_2-Ar-Sn(CH_3)_4$ mixtures. **Surf. Coating. Tech.** 201 (2006): 1444–1453.
- [46] **National instrument of standard and technology, NIST atomic spectra database** Available from: <http://www.physics.nist.gov/cgi-bin/ASD/line1.pl> [2007, October 10]
- [47] Konuma, M. **Plasma Techniques for Film Deposition**. Alpha Science, International Ltd: Middlesex. 2005.
- [48] Tanaka, K., Yoshizawa, K., Takeuchi, T., and Yamabe, T. Plasma polymerization of thiophene and 3-methylthiophene. **Synth. Met.** 38 (1990): 107-116.

- [49] Vásquez, M., Cruz, G.J., Olayo, M.G., Timoshina, T., Morales, J., and Olayo, R. Chlorine dopants in plasma synthesized heteroaromatic polymers. **Polymer** 47 (2006): 7864-7870.
- [50] Groenewoud, L.M.H., Engbers, G.H.M., White, R., and Feijen, J. On the iodine doping process of plasma polymerized thiophene layers. **Synth. Met.** 125 (2002): 429-440.
- [51] Groenewoud, L. M. H., Engbers, G. H. M., and Feijen, J. Plasma polymerization of thiophene derivatives. **Langmuir** 19 (2003): 1368-1374.
- [52] Dams, R. **Plasma Deposition of Conjugated Polymers at Atmospheric Pressure.** 2007. Available from: www.vito.be/VITO/OpenWoDocument.aspx?wovitoguid=83E8BC70-2CA9-45DC-8F3C884C0E97E8B2. [2008, August 26]
- [53] Tu, D.M., Zhuang, G.P., and Kao, K.C. Electrical conductivity of plasma-treated poly(*p*-phenylene sulfide) doped with iodine. **J. Appl. Polym. Sci.** 43 (1991): 1625-1632.

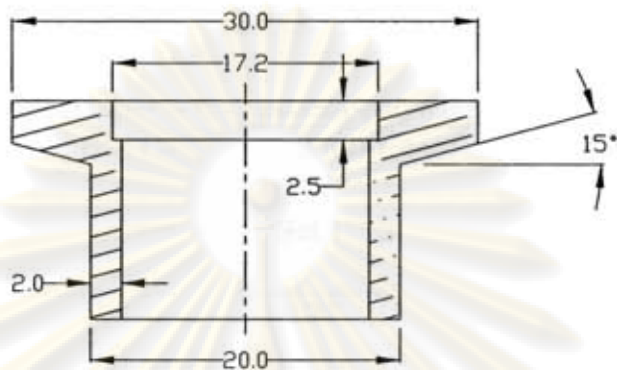
ศูนย์วิทยทรัพยากร
จุฬาลงกรณ์มหาวิทยาลัย



ศูนย์วิทยทรัพยากร
จุฬาลงกรณ์มหาวิทยาลัย

APPENDIX A

Detail of reactor design



NW 16

Figure A.1 Dimension of standard NW 16 flange

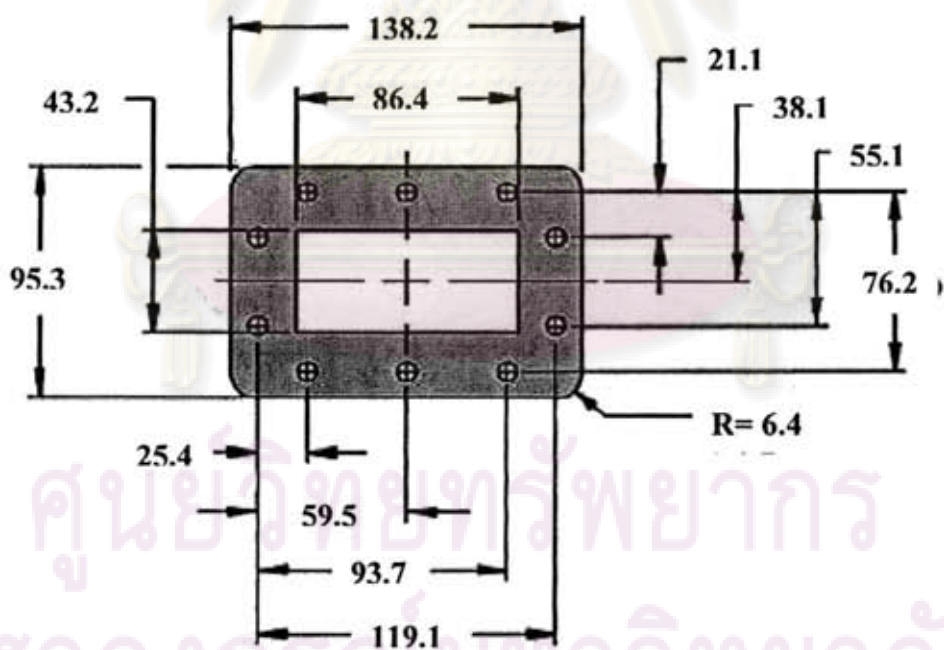


Figure A.2 Dimension of standard WR 340 flange cover

APPENDIX B

Elemental composition of samples determined by Energy-Dispersive X-Ray Spectroscopy (EDS)

Table B.1 The elemental composition of plasma-polymerized polythiophene.

| Condition | | Carbon content (%) | | | Sulfur content (%) | | | C/S | | |
|------------|-----------|--------------------|-------|---------|--------------------|-------|---------|-------|-------|---------|
| Time (min) | Power (W) | Set 1 | Set 2 | Average | Set 1 | Set 2 | Average | Set 1 | Set 2 | Average |
| 1 | 150 | 90.63 | 88.54 | 89.59 | 9.37 | 11.46 | 10.42 | 9.67 | 7.73 | 8.70 |
| | 200 | 90.24 | 86.23 | 88.24 | 9.76 | 13.77 | 11.77 | 9.25 | 6.26 | 7.76 |
| | 250 | 87.47 | 91.15 | 89.31 | 12.53 | 8.85 | 10.69 | 6.98 | 10.30 | 8.64 |
| | 300 | 88.50 | 87.79 | 88.15 | 11.50 | 12.21 | 11.86 | 7.70 | 7.19 | 7.45 |
| 2 | 150 | 85.06 | 89.29 | 87.18 | 14.94 | 10.71 | 12.83 | 5.69 | 8.34 | 7.02 |
| | 200 | 90.51 | 88.79 | 89.65 | 9.49 | 11.21 | 10.35 | 9.54 | 7.92 | 8.73 |
| | 250 | 91.05 | 89.29 | 90.17 | 8.95 | 10.71 | 9.83 | 10.17 | 8.34 | 9.26 |
| | 300 | 92.81 | 88.65 | 90.73 | 7.19 | 11.35 | 9.27 | 12.91 | 7.81 | 10.36 |

Data was obtained using an OXFORD, INCAX-sight 7573 spectrometer.

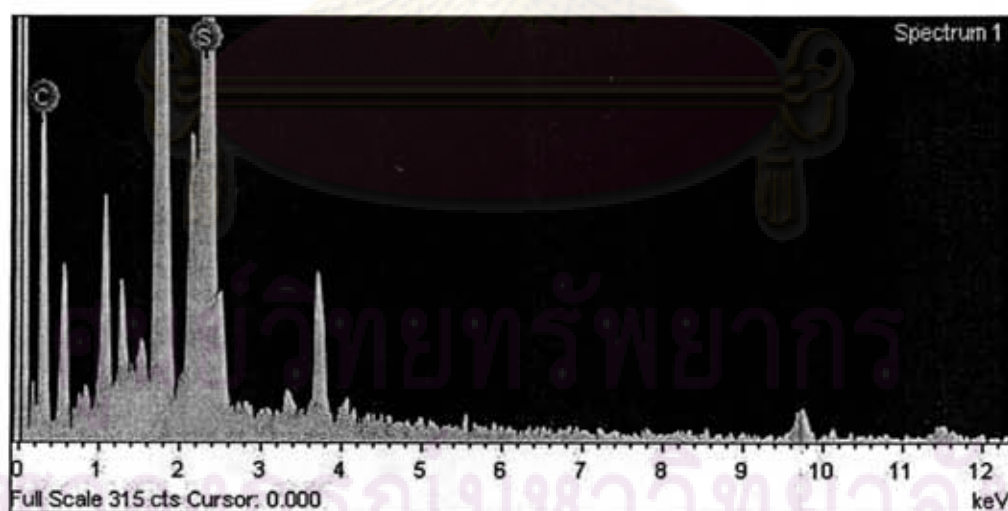


Figure B.1 EDS spectra of plasma-polymerized polythiophene at 250 W and 1 min.

Table B.2 The elemental composition of I₂ doped plasma-polymerized polythiophene.

| Condition | | Carbon content (%) | | | Sulfur content (%) | | | C/S | | | Iodine content (%) | | |
|------------|-----------|--------------------|-------|---------|--------------------|-------|---------|-------|-------|---------|--------------------|-------|---------|
| Time (min) | Power (W) | Set 1 | Set 2 | Average | Set 1 | Set 2 | Average | Set 1 | Set 2 | Average | Set 1 | Set 2 | Average |
| 1 | 250 | 80.01 | 90.97 | 85.49 | 6.14 | 5.17 | 5.66 | 13.03 | 17.60 | 15.12 | 13.85 | 3.86 | 8.86 |
| | 300 | 83.44 | 84.90 | 84.17 | 10.79 | 11.72 | 11.26 | 7.73 | 7.24 | 7.48 | 5.77 | 3.38 | 4.58 |
| 2 | 250 | 81.73 | 86.09 | 83.91 | 7.44 | 5.26 | 6.35 | 10.99 | 16.37 | 13.21 | 10.83 | 8.66 | 9.75 |
| | 300 | 84.38 | 85.46 | 84.92 | 9.91 | 8.31 | 9.11 | 8.51 | 10.28 | 9.32 | 5.71 | 6.23 | 5.97 |

Data was obtained using an OXFORD, INCAX-sight 7573 spectrometer.

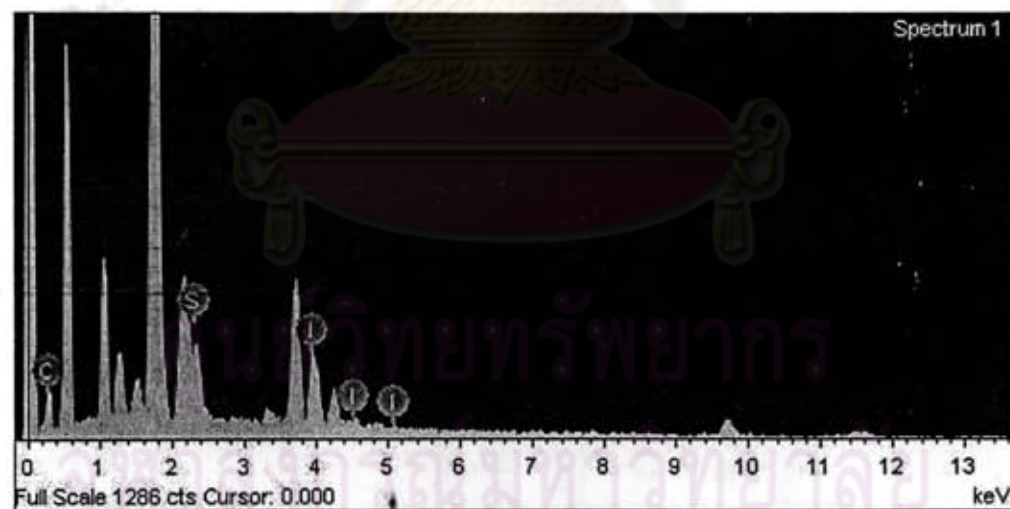


Figure B.2 EDS spectra of I₂ doped plasma-polymerized polythiophene at 250 W and 1 min.

APPENDIX C

Electrical Conductivity of Samples

$$\sigma = \frac{\ell}{Rwt}$$

When: σ = conductivity (S/cm)

ℓ = length between electrodes (cm)

R = Resistance (ohms, Ω)

w = the width of electrodes (cm)

t = thickness of films (cm)

Table C.1 Electrical conductivity of microwave plasma-polymerized polythiophene

| Condition | | R (Ω) | | t (μm) | | Conductivity (S/cm) | | |
|------------|-----------|--------------------|---------------------|-----------------------|-------|-----------------------|-----------------------|-----------------------|
| Time (min) | Power (W) | Set 1 | Set 2 | Set 1 | Set 2 | Set 1 | Set 2 | Average |
| 1 | 150 | 7.21×10^9 | 6.81×10^9 | 0.94 | 1.14 | 1.48×10^{-6} | 1.28×10^{-6} | 1.38×10^{-6} |
| | 200 | 5.53×10^9 | 3.17×10^9 | 1.36 | 1.22 | 1.33×10^{-6} | 2.59×10^{-6} | 1.96×10^{-6} |
| | 250 | 7.91×10^9 | 4.02×10^9 | 1.29 | 1.40 | 0.98×10^{-6} | 0.18×10^{-6} | 0.58×10^{-6} |
| | 300 | 9.06×10^9 | 3.7×10^9 | 1.19 | 1.25 | 0.93×10^{-6} | 2.16×10^{-6} | 1.54×10^{-6} |
| 2 | 150 | 5.24×10^9 | 9.50×10^9 | 1.31 | 1.48 | 1.21×10^{-6} | 0.65×10^{-6} | 0.93×10^{-6} |
| | 200 | 7.11×10^9 | 9.09×10^9 | 1.90 | 1.45 | 0.62×10^{-6} | 0.76×10^{-6} | 0.69×10^{-6} |
| | 250 | 6.50×10^9 | 8.85×10^9 | 1.88 | 1.93 | 0.68×10^{-6} | 0.59×10^{-6} | 0.63×10^{-6} |
| | 300 | 6.94×10^9 | 9.244×10^9 | 2.02 | 1.19 | 0.47×10^{-6} | 0.61×10^{-6} | 0.54×10^{-6} |

ศูนย์วิทยทรัพยากร
จุฬาลงกรณ์มหาวิทยาลัย

Table C.2 Electrical conductivity of I₂ doped microwave plasma-polymerized polythiophene (*in situ* doping).

| Condition | | R (Ω) | | t (nm) | | Conductivity (S/cm) | | |
|------------|-----------|----------------------|----------------------|--------|-------|-----------------------|-----------------------|-----------------------|
| Time (min) | Power (W) | Set 1 | Set 2 | Set 1 | Set 2 | Set 1 | Set 2 | Average |
| 1 | 250 | 4.83×10 ⁸ | 9.81×10 ⁹ | 126 | 252 | 16.4×10 ⁻⁵ | 4.04×10 ⁻⁵ | 10.2×10 ⁻⁵ |
| | 300 | 3.95×10 ⁸ | 3.93×10 ⁸ | 1080 | 1910 | 2.34×10 ⁻⁵ | 1.33×10 ⁻⁵ | 1.84×10 ⁻⁵ |
| 2 | 250 | 2.58×10 ⁸ | 2.00×10 ⁸ | 114.4 | 85.4 | 3.39×10 ⁻⁵ | 5.88×10 ⁻⁵ | 4.64×10 ⁻⁵ |
| | 300 | 2.16×10 ⁸ | 2.16×10 ⁸ | 346 | 307 | 1.34×10 ⁻⁵ | 1.51×10 ⁻⁵ | 1.43×10 ⁻⁵ |

Table C.3 Electrical conductivity of I₂ doped microwave plasma-polymerized polythiophene (*in situ* doping) at 250 W, 1 min.

| Time (min) | R (Ω) | | Conductivity (S/cm) | | |
|------------|----------------------|----------------------|-----------------------|-----------------------|-----------------------|
| | Set 1 | Set 2 | Set 1 | Set 2 | Average |
| 0 | 4.53×10 ⁸ | 1.56×10 ⁹ | 17.5×10 ⁻⁵ | 2.55×10 ⁻⁵ | 10.0×10 ⁻⁵ |
| 60 | 4.82×10 ⁸ | 1.83×10 ⁹ | 16.5×10 ⁻⁵ | 2.17×10 ⁻⁵ | 9.32×10 ⁻⁵ |
| 120 | 4.95×10 ⁸ | 1.93×10 ⁹ | 16.0×10 ⁻⁵ | 2.06×10 ⁻⁵ | 9.02×10 ⁻⁵ |
| 180 | 5.20×10 ⁸ | 1.98×10 ⁹ | 15.3×10 ⁻⁵ | 2.00×10 ⁻⁵ | 8.60×10 ⁻⁵ |
| 1440 | 1.72×10 ⁹ | 2.04×10 ⁹ | 4.61×10 ⁻⁵ | 1.95×10 ⁻⁵ | 3.22×10 ⁻⁵ |
| 2880 | 1.85×10 ⁹ | 2.17×10 ⁹ | 4.29×10 ⁻⁵ | 1.83×10 ⁻⁵ | 3.03×10 ⁻⁵ |
| 5760 | 2.09×10 ⁹ | 2.23×10 ⁹ | 3.80×10 ⁻⁵ | 1.78×10 ⁻⁵ | 1.90×10 ⁻⁵ |

Table C.4 Electrical conductivity of I₂ doped microwave plasma-polymerized polythiophene (*in situ* doping) at 300 W, 1 min.

| Time (min) | R (Ω) | | Conductivity (S/cm) | | |
|---------------|----------------------|----------------------|-----------------------|-----------------------|-----------------------|
| | Set 1 | Set 2 | Set 1 | Set 2 | Average |
| 0 | 0.96×10 ⁹ | 0.80×10 ⁹ | 9.60×10 ⁻⁶ | 11.6×10 ⁻⁶ | 10.6×10 ⁻⁶ |
| 60 | 1.02×10 ⁹ | 0.85×10 ⁹ | 9.04×10 ⁻⁶ | 10.9×10 ⁻⁶ | 9.97×10 ⁻⁶ |
| 120 | 1.17×10 ⁹ | 1.10×10 ⁹ | 7.93×10 ⁻⁶ | 8.42×10 ⁻⁶ | 8.17×10 ⁻⁶ |
| 180 | 1.54×10 ⁹ | 1.50×10 ⁹ | 6.01×10 ⁻⁶ | 6.17×10 ⁻⁶ | 6.09×10 ⁻⁶ |
| 1440 | 2.26×10 ⁹ | 2.15×10 ⁹ | 4.10×10 ⁻⁶ | 4.31×10 ⁻⁶ | 4.20×10 ⁻⁶ |
| 2880 | 2.4×10 ⁹ | 2.32×10 ⁹ | 3.86×10 ⁻⁶ | 3.99×10 ⁻⁶ | 3.92×10 ⁻⁶ |
| 5760 | 2.52×10 ⁹ | 2.42×10 ⁹ | 3.67×10 ⁻⁶ | 3.83×10 ⁻⁶ | 3.75×10 ⁻⁶ |

Table C.5 Electrical conductivity of I₂ doped microwave plasma-polymerized polythiophene (*in situ* doping) at 250 W, 2 min.

| Time (min) | R (Ω) | | Conductivity (S/cm) | | |
|---------------|----------------------|----------------------|-----------------------|-----------------------|-----------------------|
| | Set 1 | Set 2 | Set 1 | Set 2 | Average |
| 0 | 2.90×10 ⁹ | 2.85×10 ⁹ | 3.02×10 ⁻⁵ | 4.11×10 ⁻⁵ | 3.57×10 ⁻⁵ |
| 60 | 3.60×10 ⁹ | 3.71×10 ⁹ | 2.43×10 ⁻⁵ | 3.16×10 ⁻⁵ | 2.79×10 ⁻⁵ |
| 120 | 3.65×10 ⁹ | 3.85×10 ⁹ | 2.39×10 ⁻⁵ | 3.04×10 ⁻⁵ | 2.72×10 ⁻⁵ |
| 180 | 3.83×10 ⁹ | 4.01×10 ⁹ | 2.28×10 ⁻⁵ | 2.92×10 ⁻⁵ | 2.60×10 ⁻⁵ |
| 1440 | 4.00×10 ⁹ | 4.06×10 ⁹ | 2.19×10 ⁻⁵ | 2.88×10 ⁻⁵ | 2.54×10 ⁻⁵ |
| 2880 | 4.18×10 ⁹ | 4.51×10 ⁹ | 2.09×10 ⁻⁵ | 2.60×10 ⁻⁵ | 2.34×10 ⁻⁵ |
| 5760 | 4.39×10 ⁹ | 4.57×10 ⁹ | 1.99×10 ⁻⁵ | 2.56×10 ⁻⁵ | 2.28×10 ⁻⁵ |

ศูนย์วิทยทรัพยากร
จุฬาลงกรณ์มหาวิทยาลัย

Table C.6 Electrical conductivity of I₂ doped microwave plasma-polymerized polythiophene (*in situ* doping) at 300 W, 2 min.

| Time (min) | R (Ω) | | Conductivity (S/cm) | | |
|---------------|--------------------|--------------------|-----------------------|-----------------------|-----------------------|
| | Set 1 | Set 2 | Set 1 | Set 2 | Average |
| 0 | 2.37×10^9 | 2.19×10^9 | 1.22×10^{-5} | 1.49×10^{-5} | 1.35×10^{-5} |
| 60 | 2.83×10^9 | 2.54×10^9 | 1.02×10^{-5} | 1.28×10^{-5} | 1.15×10^{-5} |
| 120 | 4.00×10^9 | 3.86×10^9 | 7.22×10^{-6} | 8.45×10^{-6} | 7.83×10^{-6} |
| 180 | 4.09×10^9 | 4.07×10^9 | 7.07×10^{-6} | 8.01×10^{-6} | 7.54×10^{-6} |
| 1440 | 4.11×10^9 | 4.09×10^9 | 7.03×10^{-6} | 7.97×10^{-6} | 7.50×10^{-6} |
| 2880 | 4.16×10^9 | 4.24×10^9 | 6.95×10^{-6} | 7.69×10^{-6} | 7.32×10^{-6} |
| 5760 | 4.29×10^9 | 4.18×10^9 | 6.74×10^{-6} | 7.80×10^{-6} | 7.27×10^{-6} |

Table C.7 Electrical conductivity of microwave plasma-polymerized polythiophene at 150 W, 2 min and I₂ *ex situ* doping for 24 hours.

| Time (min) | R (Ω) | | Conductivity (S/cm) | | |
|---------------|--------------------|--------------------|-----------------------|-----------------------|-----------------------|
| | Set 1 | Set 2 | Set 1 | Set 2 | Average |
| 0 | 1.39×10^7 | 8.01×10^6 | 5.48×10^{-4} | 8.64×10^{-4} | 6.97×10^{-4} |
| 30 | 2.33×10^7 | 1.77×10^7 | 3.27×10^{-4} | 3.83×10^{-4} | 3.55×10^{-4} |
| 60 | 6.42×10^7 | 2.91×10^7 | 1.19×10^{-4} | 2.33×10^{-4} | 1.76×10^{-4} |
| 120 | 1.45×10^8 | 5.29×10^7 | 5.26×10^{-5} | 1.28×10^{-4} | 9.03×10^{-5} |
| 180 | 2.87×10^8 | 1.00×10^8 | 2.66×10^{-5} | 6.78×10^{-5} | 4.72×10^{-5} |
| 240 | 4.33×10^8 | 1.46×10^8 | 1.76×10^{-4} | 4.64×10^{-5} | 3.20×10^{-5} |
| 420 | 9.25×10^8 | 2.60×10^8 | 8.24×10^{-6} | 2.61×10^{-5} | 1.71×10^{-5} |
| 1440 | 1.70×10^9 | 6.28×10^8 | 4.48×10^{-6} | 1.08×10^{-5} | 7.64×10^{-6} |
| 2880 | 4.85×10^9 | 1.32×10^9 | 1.57×10^{-6} | 5.13×10^{-6} | 3.35×10^{-6} |

ศูนย์วิทยทรัพยากร
จุฬาลงกรณ์มหาวิทยาลัย

Table C.8 Electrical conductivity of microwave plasma-polymerized polythiophene at 200 W, 1 min and I₂ *ex situ* doping for 24 hours.

| Time (min) | R (Ω) | | Conductivity (S/cm) | | |
|---------------|----------------------|----------------------|-----------------------|-----------------------|-----------------------|
| | Set 1 | Set 2 | Set 1 | Set 2 | Average |
| 0 | 3.78×10 ⁶ | 4.27×10 ⁶ | 1.94×10 ⁻³ | 1.92×10 ⁻³ | 1.93×10 ⁻³ |
| 30 | 5.70×10 ⁶ | 5.62×10 ⁶ | 1.29×10 ⁻³ | 1.46×10 ⁻³ | 1.37×10 ⁻³ |
| 60 | 6.90×10 ⁶ | 6.86×10 ⁶ | 1.06×10 ⁻³ | 1.19×10 ⁻³ | 1.13×10 ⁻³ |
| 120 | 1.95×10 ⁷ | 1.46×10 ⁷ | 3.76×10 ⁻⁴ | 5.61×10 ⁻⁴ | 4.69×10 ⁻⁴ |
| 180 | 2.95×10 ⁷ | 2.77×10 ⁷ | 2.49×10 ⁻⁴ | 2.96×10 ⁻⁴ | 2.72×10 ⁻⁴ |
| 240 | 6.39×10 ⁷ | 6.02×10 ⁷ | 1.15×10 ⁻⁴ | 1.36×10 ⁻⁴ | 1.25×10 ⁻⁴ |
| 420 | 1.23×10 ⁸ | 2.17×10 ⁸ | 5.96×10 ⁻⁵ | 3.78×10 ⁻⁵ | 4.87×10 ⁻⁵ |
| 1440 | 2.27×10 ⁹ | 1.24×10 ⁹ | 3.23×10 ⁻⁶ | 6.61×10 ⁻⁶ | 4.92×10 ⁻⁶ |
| 2880 | 5.23×10 ⁹ | 3.34×10 ⁹ | 1.40×10 ⁻⁶ | 2.45×10 ⁻⁶ | 1.93×10 ⁻⁶ |

Table C.9 Electrical conductivity of microwave plasma-polymerized polythiophene at 200 W, 2 min and I₂ *ex situ* doping for 24 hours.

| Time (min) | R (Ω) | | Conductivity (S/cm) | | |
|---------------|----------------------|----------------------|-----------------------|-----------------------|-----------------------|
| | Set 1 | Set 2 | Set 1 | Set 2 | Average |
| 0 | 3.64×10 ⁷ | 4.62×10 ⁷ | 1.45×10 ⁻⁴ | 1.49×10 ⁻⁴ | 1.47×10 ⁻⁴ |
| 30 | 5.33×10 ⁷ | 7.54×10 ⁷ | 9.87×10 ⁻⁵ | 9.13×10 ⁻⁵ | 9.50×10 ⁻⁵ |
| 60 | 8.63×10 ⁷ | 1.15×10 ⁸ | 6.10×10 ⁻⁵ | 5.99×10 ⁻⁵ | 6.04×10 ⁻⁵ |
| 120 | 1.69×10 ⁸ | 1.52×10 ⁸ | 3.11×10 ⁻⁵ | 4.53×10 ⁻⁵ | 3.82×10 ⁻⁵ |
| 180 | 2.87×10 ⁸ | 2.14×10 ⁸ | 1.83×10 ⁻⁵ | 3.22×10 ⁻⁵ | 2.53×10 ⁻⁵ |
| 240 | 4.94×10 ⁸ | 2.91×10 ⁸ | 1.07×10 ⁻⁵ | 2.37×10 ⁻⁵ | 1.72×10 ⁻⁵ |
| 420 | 1.35×10 ⁹ | 4.47×10 ⁸ | 3.90×10 ⁻⁶ | 1.54×10 ⁻⁵ | 9.65×10 ⁻⁶ |
| 1440 | 1.81×10 ⁹ | 1.00×10 ⁹ | 2.91×10 ⁻⁶ | 6.89×10 ⁻⁶ | 4.90×10 ⁻⁶ |
| 2880 | 4.03×10 ⁹ | 1.84×10 ⁹ | 1.31×10 ⁻⁶ | 3.74×10 ⁻⁶ | 2.52×10 ⁻⁶ |

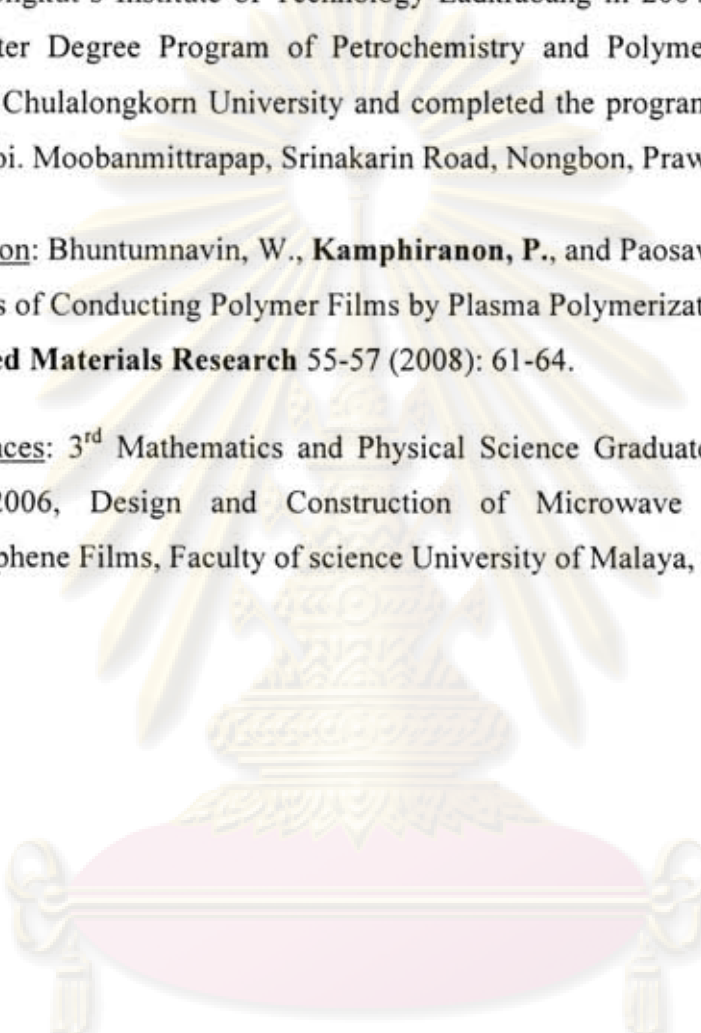
จุฬาลงกรณ์มหาวิทยาลัย

VITAE

Miss Phensupa Kamphiranon was born on March 1, 1983 in Bangkok, Thailand. She obtained the Bachelor Degree of Science in Industrial Chemistry from King Mongkut's Institute of Technology Ladkrabang in 2004. She was admitted to the Master Degree Program of Petrochemistry and Polymer Science, Faculty of Science, Chulalongkorn University and completed the program in 2008. Her address is 56/4 soi. Moobanmittrapap, Srinakarin Road, Nongbon, Prawet, Bangkok 10250.

Publication: Bhuntumnavin, W., **Kamphiranon, P.**, and Paosawatyanong, B.
Synthesis of Conducting Polymer Films by Plasma Polymerization Process.
Advanced Materials Research 55-57 (2008): 61-64.

Conferences: 3rd Mathematics and Physical Science Graduate Congress, December 12-14 2006, Design and Construction of Microwave Plasma Reactor for Polythiophene Films, Faculty of science University of Malaya, Malaysia.



ศูนย์วิทยทรัพยากร
จุฬาลงกรณ์มหาวิทยาลัย